Green Chemistry

ROYAL SOCIETY OF CHEMISTRY

CRITICAL REVIEW

View Article Online
View Journal | View Issue

Cite this: *Green Chem.*, 2025, **27**, 8710

Sustainable approaches in vat photopolymerization: advancements, limitations, and future opportunities†

Mirko Maturi, *[a] Erica Locatelli, [b] Alberto Sanz de Leon, [a] Mauro Comes Franchini [b] and Sergio Ignacio Molina [a]

Vat photopolymerization (VP) is reshaping advanced manufacturing, yet its dependence on petrochemical-derived resins poses significant sustainability challenges. This review critically evaluates conventional photocurable formulations, highlighting the limitations of standard metrics such as the biobased carbon content (BCC%), and introduces the sustainable formulation score (SFS) as a comprehensive alternative. By integrating factors like atom economy, hazardous reagent usage, solvent selection, and end-of-life considerations, SFS offers a more holistic measure of environmental impact. The analysis encompasses diverse resin systems, including (meth)acrylated vegetable oil derivatives, biobased small molecules from lignin and other renewable sources, non-isocyanate urethanes, and thiol–ene formulations. For vegetable oil-based systems, a key trade-off is observed between achieving high biobased content and maintaining optimal mechanical properties, driven by variations in the degree of acrylation and processing conditions. In contrast, the synthesis of small biobased molecules often involves toxic reagents and less favorable atom economies, reducing their overall green appeal. Moreover, non-isocyanate urethanes and thiol–ene systems emerge as promising routes for improving sustainability while preserving performance. Overall, this review underscores the need for unified green metrics and optimized synthesis strategies to bridge the gap between environmental sustainability and material performance in photopolymer formulations, paving the way for more responsible and efficient additive manufacturing technologies.

Received 8th May 2025,
Accepted 1st July 2025

DOI: 10.1039/d5gc02299a

rsc.li/greenchem

Green foundation

1. The review introduces the sustainable formulation score (SFS), a new comprehensive metric that integrates atom economy, synthetic hazards, solvent selection, and end-of-life properties to assess the sustainability of photocurable resins, offering a more complete picture of sustainability. Advances include the development of bio-based resin components from vegetable oils, lignin derivatives, terpene derivatives, and non-isocyanate urethanes, highlighting trade-offs between green credentials and material performance.
2. This field addresses urgent environmental concerns tied to plastic waste and fossil-derived materials. Vat photopolymerization is central to multiple high-impact sectors (healthcare, automotive, and electronics) and greener formulations align with growing regulatory and consumer pressures. The interdisciplinary nature of this work also fosters innovation across chemistry, materials science, and engineering.
3. The SFS framework will help standardize sustainability assessments and guide formulation design. Future directions include replacing hazardous reagents, improving recyclability, and achieving high performance without compromising environmental goals.

Introduction

In recent years, additive manufacturing has emerged as a transformative technology, offering unprecedented precision and design freedom across various industries.[1–4] Among the different additive manufacturing techniques, vat photopolymerization (VP) methods, including stereolithography (SLA) and digital light processing (DLP), have gained significant traction due to their ability to produce highly detailed and mechanically robust components.[5,6] VP has experienced remarkable growth, driven by advancements in light-based

[a]*Departamento de Ciencia de los Materiales, I. M. y Q. I., IMEYMAT, Facultad de Ciencias, Universidad de Cádiz, Campus Río San Pedro, s/n, 11510 Puerto Real, Cádiz, Spain*
[b]*Department of Industrial Chemistry "Toso Montanari", University of Bologna, Bologna 40136, Italy*

† Electronic supplementary information (ESI) available. See DOI: https://doi.org/10.1039/d5gc02299a

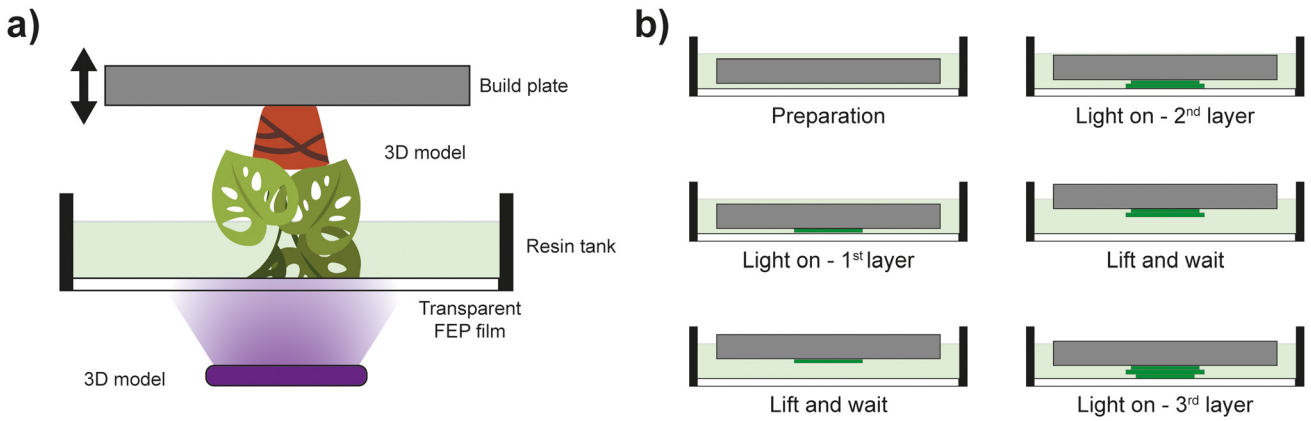

Fig. 1 Vat photopolymerization process. (a) Overview of the VP setup and (b) steps for the layer-by-layer manufacturing of 3D objects by photopolymerization.

curing mechanisms, resin formulations, and processing techniques. SLA and DLP have become dominant in industries such as healthcare, automotive, aerospace, and consumer goods, enabling rapid prototyping and production of complex geometries with high resolution and excellent surface finish. The increasing accessibility of VP systems, coupled with ongoing material innovations, has led to a proliferation of applications ranging from dental implants and medical devices to microfluidics and customized electronics.[7–9]

VP relies on the selective curing of liquid photopolymer resins by a light source that initiates polymerization. The process starts with a vat of resin containing a photocurable liquid mixture. In SLA, a laser cures the resin point by point, while in DLP, a digital projector cures entire cross-sections simultaneously, layer by layer. After each layer, the build platform moves to expose fresh resin, repeating until the object is complete (Fig. 1). Post-processing steps, such as washing, additional UV curing, and support removal, are usually required to improve the printed part's mechanical and structural properties.[10]

As VP technologies continue to evolve and expand, so do the concerns regarding their environmental footprint. The reliance on petrochemical-derived resins raises critical sustainability challenges, necessitating a shift toward greener alternatives to ensure the long-term viability of VP-based manufacturing. Despite these technological breakthroughs, the environmental impact of photopolymer-based materials remains a significant concern, calling for the development of more sustainable solutions.

Conventional photopolymer resins are predominantly formulated using fossil-derived acrylates, methacrylates, and epoxides, many of which pose environmental and health risks due to their limited biodegradability and potential toxicity. Furthermore, the production and disposal of these materials contribute to carbon emissions and plastic waste accumulation, exacerbating global ecological challenges.[11,12] Regulatory pressures and consumer demand for eco-friendly products are driving the transition toward greener photopolymer technologies. Ultimately, the sustainability imperative in

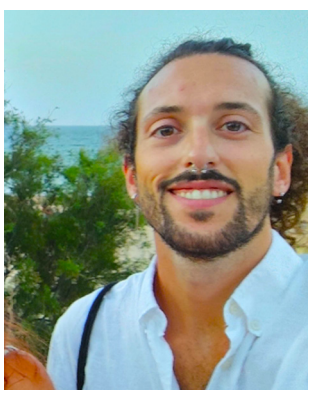

Mirko Maturi

Mirko Maturi, PhD, is a postdoctoral researcher at the University of Cádiz (Spain), where he develops sustainable resin systems and functional nanocomposites for vat photopolymerization-based 3D printing. With a background in materials science and polymer chemistry, his research focuses on the synthesis of biobased photocurable formulations, surface-functionalization of nanomaterials, and the development of sustainable and functional polymer (nano)composites for additive manufacturing. He earned his PhD at the University of Bologna (Italy) working on hybrid nanomaterials for theranostics, organic electronics, and additive manufacturing.

Erica Locatelli

Prof. Erica Locatelli is an associate professor of organic chemistry at the University of Bologna, at the Department of Industrial Chemistry "Toso Montanari". After earning her master's degree in industrial chemistry in 2010 and PhD in chemical sciences in 2014, she worked as a research fellow in the field of nanoscience and nanotechnology for materials science and biomedical applications. Since 2024, she continues her career and research by applying the principle of organic chemistry and nanotechnology towards the obtainment of sustainable, bio-based complex functional materials.

VP underscores the need for continued innovation in materials science, ensuring that the benefits of additive manufacturing are aligned with environmental responsibility. To address these issues, researchers and industry stakeholders are actively exploring bio-based, recyclable, and degradable photopolymers as potential substitutes for traditional resin formulations.[13–15] The integration of renewable monomers, along with the development of recyclable resin systems, represents a promising avenue toward reducing the environmental burden of VP-based manufacturing.

Sustainability assessments of photopolymer resins often rely on metrics that provide valuable information about the proportion of renewable content in a formulation but fail to capture the full sustainability profile of a material. For instance, a resin with a high bioderived content may still involve energy-intensive synthesis routes or generate hazardous by-products. Additionally, these metrics do not account for end-of-life considerations, such as recyclability, degradation behaviour, or toxicity of degradation products, which are crucial for holistic sustainability assessments. The environmental footprint of photopolymer resins is not solely determined by their raw material sources but also by the chemical processes involved in their synthesis. Many bio-based resins require complex chemical modifications that involve hazardous reagents, high energy consumption, and the generation of unwanted by-products. These factors can offset the sustainability benefits of using renewable feedstocks. Additionally, certain functionalization steps necessary to impart photopolymerization reactivity may introduce non-biodegradable or toxic moieties, further complicating the environmental profile of the final material. Given the limitations of conventional sustainability assessments, there is a need for a more comprehensive metric that accounts for both the production and disposal phases of photopolymer resins.

The sustainable formulation score (SFS) is herein proposed as an integrative metric that evaluates the sustainability of a photopolymer formulation based on multiple factors, including atom economy, synthesis parameters, and end-of-life considerations. Unlike traditional metrics that focus solely on bio-based content, SFS incorporates (i) atom economy, which accounts for the efficiency of chemical reactions in minimizing waste, (ii) synthesis parameters, based on the eventual use of hazardous reagents, energy consumption, and emissions, (iii) End-of-Life factors, which considers recyclability, biodegradability, and toxicity of degradation products. By incorporating these elements, SFS provides a more holistic evaluation of resin sustainability. This metric ensures that formulations with a high renewable content are not undermined by energy-intensive or hazardous synthesis routes. Additionally, SFS helps manufacturers and researchers prioritize formulations that balance performance with environmental responsibility, facilitating the transition toward truly sustainable photopolymer materials.

The primary goal of this review is to critically assess current sustainable resin strategies in VP, highlighting their strengths, limitations, and potential for improvement. By analysing the existing approaches to bio-based, recyclable, and degradable photopolymer formulations, this review aims to provide a comprehensive overview of the progress made in developing greener alternatives. Furthermore, it seeks to identify knowledge gaps and future research directions that could accelerate the transition toward truly sustainable VP resins. The discussion will emphasize the need for improved sustainability metrics, such as the proposed Sustainable Formulation Score, and explore novel material design strategies that balance environmental considerations with the functional requirements of advanced manufacturing applications.

Sustainability formulation score (SFS)

In the recent scientific literature, the sustainability of photocurable formulations for VP is often asserted in a qualitative and arbitrary manner. Claims of sustainability are frequently

Alberto Sanz de Leon

Prof. Alberto Sanz de León is an Associate Professor in the field of Materials Science at the University of Cádiz. He received his PhD in polymer chemistry at the Institute of Polymer Science and Technology of the Spanish National Research Council (2015). In 2016–2018 he worked at the Max Planck Institute of Colloids and Interfaces in the rational design of biomimetic biomaterials. His current research focuses on the development of new functional and bio-based polymers and nanocomposites for additive manufacturing.

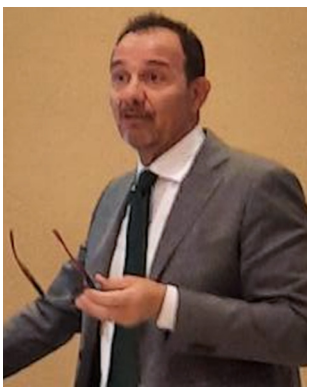

Mauro Comes Franchini

Prof. Mauro Comes Franchini, is Full Professor of Material Organic Chemistry at the Department of Industrial Chemistry "Toso Montanari, University of Bologna. His interests are in the field of innovative processing techniques with the aim of developing new organic materials for applications. Fields of interests are the organic electronics, the nanomedicine and the industrial applications in particular in the field of the Additive Manufacturing (3D-Printing) through the synthesis of new materials starting from natural pool sources.

based on the mere presence of bio-derived components, the incorporation of some sustainable building blocks, or the partial or complete recyclability of the material, without a comprehensive assessment of the formulation's overall environmental impact.[16,17] Only a limited number of studies quantitatively assess the sustainability of their approaches using green metrics, primarily focusing on biobased mass content (BMC%, eqn (1)).[18–20] For a formulation including n components i, each with its own weight fraction w_i:

$$\mathrm{BMC}\% = \sum_{i=1}^{n} w_i \cdot \frac{\mathrm{MW}_{\mathrm{BB},i}}{\mathrm{MW}_i} \quad (1)$$

where MW_i is the molecular weight of component i and $\mathrm{MW}_{\mathrm{BB},i}$ is the molecular weight of the biobased portion of its molecules. Even though BMC% gives good indications on the biobased content of each formulation, and it can be easily calculated knowing the molecular structure of each component of the formulation, the definition of $\mathrm{MW}_{\mathrm{BB}}$ is not always trivial, especially during the condensation of small molecules. For example, during the formation of acrylate esters with biobased diols, the ester oxygen atom is arbitrarily assigned either to the biobased diol portion or to the non-biobased acrylate residue, causing significant oscillations in the BMC% value, especially for small molecules or heavily acrylated ones. Furthermore, this parameter is impossible to assess if the composition of the formulation and the chemical structure of its components are unknown. To overcome this, BMC has been replaced with the biobased carbon content (BCC%) defined according to eqn (2).[18,19,21] For a formulation including n components i, each with its own weight fraction w_i:

$$\mathrm{BCC}\% = \frac{\text{total biobased carbon mass}}{\text{total carbon mass}} = \frac{\sum_{i=1}^{n} w_i C_{\%,i} \frac{n_{\mathrm{BC},i}}{n_{\mathrm{C},i}}}{\sum_{i=1}^{n} w_i C_{\%,i}} \quad (2)$$

Sergio Ignacio Molina

Prof. Sergio I. Molina is Full Professor at the University of Cadiz in the field of Materials Science and Engineering. He is the leader of the research Group INNANOMAT. He has been a visiting researcher at the Universities of Cambridge, Liverpool and Sheffield, in U. K., and in the EPFL of Lausanne, in Switzerland, and a visiting professor in ORNL, USA. He is the Scientific Director of the Additive Manufacturing Division in the University of Cadiz. His research is currently dedicated to materials for additive manufacturing techniques and to the development and advanced characterization of functional nanomaterials.

where $C_{\%,i}$ is the total carbon content of each component i, $n_{\mathrm{BC},i}$ is the number of biobased carbon atoms in its molecular structure and $n_{\mathrm{C},i}$ is the total number of carbon atoms in the molecules of component i. With this approach, it is much easier to define the biobased portions of each molecule, but relating the sustainability of a formulation only to its carbon content leads to significant deviations from BMC% when the formulation is rich in heteroatoms, which are not accounted for in this definition. Nonetheless, the definition of BCC% was introduced with ASTM D6866,[22] as it can be fully determined and verified by combining ^{14}C-radiocarbon analysis with the determination of the total carbon content of the formulation, with no *a priori* knowledge of the materials' composition.[23–25]

However, the use of BMC and BCC as the only sustainability parameters for a photocurable formulation is not satisfactory, since the environmental impact of the synthesis of each component is not taken into account. This is particularly important in photocurable formulations, as many partially biobased monomers and reactive diluents are prepared by reacting volatile, toxic and polluting (meth)acrylic acid derivatives such as acryloyl chloride in environmental unfriendly halogenated solvents. Moreover, excess of reagents or the formation of high amounts of sub-products are neglected by both BMC% and BCC%, but their effect on the sustainability of each synthetic procedure can be evaluated using atom economy (AE), defined in eqn (3).[26,27] For each component i of a formulation:

$$\mathrm{AE}_i = \frac{\mathrm{MW}_i}{\sum_j (n_j \cdot \mathrm{MW}_j)} \quad (3)$$

where MW_i is the molecular weight of component i and $\sum_j (n_j \cdot \mathrm{MW}_j)$ is the sum over all reagents j used in the synthesis of component i of their molecular weight MW_j multiplied by n_j, the number of equivalents of reagent j used for the synthesis of 1 equivalent of component i. Additional green metrics such as the E-factor,[28–30] process mass intensity,[31,32] energy efficiency,[33] and eco-scale[34,35] might be introduced, but their evaluation require a quantitative assessment and analysis of process parameters such as the amount of produces waste, the energy consumption for synthesis and workup, amongst others. The lack of a unified parameter integrating multiple aspects of sustainability, such as atom economy, biobased content, and the impact of component synthesis, complicates direct comparisons across different processes and materials. Developing a new green metric capable of encompassing these factors in a single value would provide a more holistic and adaptable sustainability assessment, facilitating decision-making in diverse industrial and research scenarios.[36]

To address this issue, herein we define a new green metric, denoted as the Sustainable Formulation Score (SFS), defined according to eqn (3). For a formulation including n components i, each with its own weight fraction w_i:

$$\mathrm{SFS} = 100 \cdot F_{\mathrm{EoL}} \cdot \sum_{i=1}^{n} (w_i \cdot \mathrm{BCC}_i \cdot F_{\mathrm{syn},i}) \quad (4)$$

where F_{EoL} is defined as the end-of-life factor, and $\sum_{i=1}^{n}(w_i \cdot BCC_i \cdot F_{syn,i})$ is the weighted sum of the synthetic factors F_{syn} of each component multiplied by the corresponding biobased carbon content, calculated for each component according to eqn (2). The end-of-life factor F_{EoL} is included to account for the possible biodegradability, recyclability and/or reprocessability of the 3D printed formulation, while the synthetic factor F_{syn} relates to green chemistry aspects of the synthesis of each component of the formulation.

In particular, F_{syn} is, for each component, defined by the combination of several sub-factors, each one representing different aspects of the sustainability of the synthetic procedure which assign a penalty or bonus based on predefined criteria, according to eqn (4):

$$F_{syn} = f_{haz} \cdot f_{sol} \cdot f_{T+t} \cdot AE \quad (5)$$

where f_{haz} relates to the use of hazardous chemicals; f_{solv} relates to the sustainability of the employed solvents; f_{T+t} is defined as the temperature–time factor, defined according to eqn (6) for the synthesis of each component i of the formulation:

$$f_{T+t} = f_T{}^{1/f_t} \quad (6)$$

where f_T relates to reaction temperature and f_t to reaction time. This definition allows for increasing the impact of the time factor as the temperature factor decreases, but time has no impact on the overall sustainability if the temperature factor is equal to 1 (room temperature synthesis); AE is to the atom economy of the synthetic process, according to eqn (3).

When syntheses are performed in consecutive steps, the sub-factors used to calculate the synthetic factor (F_{syn}) correspond to the lowest value in each sub-factor category across all steps. With this approach, sub-factors equal to 1 have no effect on the SFS, subfactors below 1 act as penalties, and subfactors higher than 1 act as bonuses. Furthermore, components of the formulation characterized by BCC_i = 0 will not contribute to SFS, regardless of their synthesis conditions. The criteria used to assign values to each parameter considered in this review are summarised in Table 1.

To ensure a consistent and meaningful application of the SFS, each factor in the formula must be evaluated systematically according to a defined benchmark:

• Hazard factor (f_{haz}): penalty and reward values ranging from 0.5 to 1.2 are assigned based on hazard classifications from the Globally Harmonized System (GHS).[37] Substances with severe health risks (*e.g.*, carcinogens) are penalized with a value of 0.5, while inherently safe or biobased reagents are rewarded with a value of 1.2. This range reflects a deliberate compromise: it imposes a significant penalty for hazardous chemicals without adding undue complexity or distorting scores with arbitrarily low values. Each formulation component is assigned an f_{haz} value based on the most hazardous reagent used (excluding catalysts).

• Solvent factor (f_{sol}): evaluated using the CHEM21 solvent selection guide,[38] where halogenated solvents receive the lowest score (0.5), and solvent-free protocols the highest (1.2). Each formulation is assigned the f_{sol} value corresponding to the most hazardous solvent used.

• Temperature–time factor (f_{T+t}): this factor is computed from reaction temperature and time using eqn (6). For multi-step reactions, the overall reaction time and average temperature are considered. This formulation balances energy efficiency with practical feasibility in synthetic design.

• End-of-life factor (F_{EoL}): values range from 0.5 to 2, rewarding fully biodegradable or circular systems.

All thresholds were carefully tuned to prevent any single factor from disproportionately influencing the overall Sustainability Formulation Score. The SFS thus offers a multi-dimensional assessment framework, encompassing hazardous reagent use, solvent selection, reaction conditions, atom economy, and end-of-life attributes. Each formulation component contributes to the final score according to its weight fraction in the resin, biobased carbon content, and environmental impacts associated with its synthesis.

To further clarify how the SFS accounts for the mass of hazardous reagents used in a formulation, it is important to note that the amount of each reagent is inherently reflected through the atom economy (AE) parameter, which penalizes reactions requiring large stoichiometric excesses. In this framework, formulations involving high quantities of reagents, regardless of their hazard level, will display lower AE values and thus contribute to a reduced SFS. Simultaneously, the hazard factor (f_{haz}) ensures that the intrinsic toxicity of individual substances is considered independently of their quantity. This dual approach allows the SFS to capture both the material inefficiency of a synthesis and the associated health and environmental risks. Moreover, although solvents are not accounted for in AE calculations due to potential recovery and recycling in industrial settings, the solvent factor (f_{sol}) imposes penalties for the use of toxic or environmentally persistent solvents, regardless of quantity.

The scoring criteria (Table 1) assign equal weight to the main synthesis-related parameters, namely hazardous reagent use, solvent selection, and reaction conditions. However, the end-of-life factor (F_{EoL}) is intentionally assigned a broader range of values (0.5 to 2) than the other factors. This reflects its overarching importance for long-term environmental performance, as it captures sustainability dimensions, such as biodegradability, recyclability, and alignment with circular economy strategies, that are often excluded from conventional green chemistry metrics focused solely on synthetic efficiency.

This design choice ensures that formulations offering improved disposal, reprocessing, or material recovery are strongly incentivized within the SFS framework. Nevertheless, we recognize that this weighting may, in some cases, cause F_{EoL} to exert a larger influence on the overall score, particularly when compared to synthesis-level factors. This is a deliberate trade-off to foreground end-of-life considerations, but it also highlights the need for flexibility.

Table 1 Values assigned to the different sustainability factors that define the SFS based on experimental conditions employed for their preparation and their end-of-life properties

Factor	Value	Criteria
f_{haz}	1.2	Negligible hazard (safe for routine use) Chemicals with little to no known health or environmental risks under normal use conditions. No H-statements or only extremely mild warnings
	1.0	Low hazard (minimal health risks but still require safe handling) Mildly hazardous substances with temporary or minor effects but still requiring safe handling and disposal. H320: Causes eye irritation H303: May be harmful if swallowed H313: May be harmful in contact with skin H333: May be harmful if inhaled
	0.9	Moderate hazard (irritants, flammables, and short-term risks) Chemicals that can cause moderate harm to humans or the environment, including strong irritants, flammables, and oxidizers. H315: Causes skin irritation H319: Causes serious eye irritation H225: Highly flammable liquid and vapor H270: May cause or intensify fire; oxidizer H412: Harmful to aquatic life with long-lasting effects
	0.7	High hazard (severe health or environmental damage) Highly toxic, corrosive, or reactive substances that can cause serious health or environmental harm but are not immediately fatal in small doses. H301: Toxic if swallowed H311: Toxic in contact with skin H331: Toxic if inhaled H314: Causes severe skin burns and eye damage H318: Causes serious eye damage H400: Very toxic to aquatic life
	0.5	Extreme hazard (life-threatening & irreversible damage) Severe toxicity, carcinogenicity, mutagenicity, reproductive toxicity, or fatal effects in small amounts. Includes highly persistent environmental toxins. H300: Fatal if swallowed H310: Fatal in contact with skin H330: Fatal if inhaled H340: May cause genetic defects H350: May cause cancer H360: May damage fertility or the unborn child H370: Causes damage to organs H372: Causes damage to organs through prolonged exposure
f_{sol}	1.2	No solvent
	1.0	Use of recommended solvents (*e.g.*, water, alcohols, acetone, anisole, ethyl acetate)
	0.8	Use of problematic solvents (*e.g.*, toluene, tetrahydrofuran, heptane, dimethylsulfoxide)
	0.7	Use of hazardous solvents (*e.g.*, dichloromethane, dimethyl formamide, *N*-methyl pyrrolidone)
	0.5	Use of highly hazardous solvents (*e.g.*, diethyl ether, benzene, chloroform)
f_T	1.0	Room temperature
	0.9	Mild heating or cooling (5–15 °C or 35–79 °C).
	0.8	Significant heating or cooling (−10 to 5 °C or 80–150 °C)
	0.7	Extreme conditions (<−10 °C or >150 °C)
f_t	1.2	≤30 min
	1.0	30 min < time ≤ 6 hours
	0.9	6 hours < time ≤ 12 hours
	0.8	12 hours < time ≤ 24 hours
	0.7	>24 hours
F_{EoL}	2	Fully recyclable and biodegradable
	1.7	Either highly recyclable or biodegradable (but not both).
	1.5	Partially recyclable or compostable, with minor waste generation
	1.2	Limited recyclability, requiring specialized processing (*e.g.*, mechanical grinding or dissolution in organic solvents). Healable
	1.0	Non-recyclable but with low environmental persistence
	0.8	Non-recyclable, generating long-term waste but no hazardous degradation products
	0.5	Non-recyclable and producing hazardous waste upon degradation (*e.g.*, halogenated polymers).

To maintain broad applicability, the SFS is designed to be comparative, modular and adaptable. Users may recalibrate the relative weightings of F_{EoL} or other sub-factors to align the metric with specific application domains, regulatory environments, or sustainability goals. This flexibility ensures that the SFS remains a robust yet context-sensitive tool for assessing and guiding the development of environmentally responsible materials.

Although the SFS remains a semi-quantitative tool, it is intended to support meaningful comparisons between formulations and guide the development of more sustainable alternatives. Importantly, it is not intended to provide an absolute metric of sustainability, but rather a flexible framework that can be adapted by adjusting the weighting of individual sub-factors to prioritise specific sustainability goals (*e.g.*, reducing energy consumption or maximising end-of-life compatibility). For the purpose of this review, we adopt a balanced implementation of the SFS, in which all critical sustainability dimensions relevant to the preparation and use of photocurable formulations are equally considered. This approach aims to support a more rational and comprehensive sustainability assessment, consistent with the principles of green chemistry and the development of environmentally responsible materials for advanced manufacturing technologies. The SFS is conceived as a comparative, formulation-level metric to evaluate the relative sustainability of photopolymer resin formulations, both conventional and emerging, based on synthesis and end-of-life considerations. It is not intended as an absolute indicator of "green" status. To aid interpretation, we classified the reviewed formulations into

five color-coded sustainability categories based on their observed SFS distribution (Table 2). This system enables a rapid assessment of relative greenness and provides a benchmarking tool for positioning new formulations within the current state of the art.

One limitation of the current SFS framework is that it does not incorporate the durability or functional lifetime of the final printed materials. While such attributes are crucial for comprehensive sustainability assessment, especially when comparing short-lived biodegradable products with durable, non-degradable alternatives, they are seldom reported in the VP resin literature. Most studies lack data on aging, fatigue resistance, or end-use performance, making it difficult to include these factors systematically. In such cases, the SFS should be complemented by life cycle assessments, particularly when use-phase impacts are significant.

The SFS is derived from data typically reported in laboratory-scale studies, which facilitates broad applicability but also imposes limitations. It does not account for process-level improvements that may arise during industrial scale-up, such as solvent recovery, reagent recycling, or energy efficiency. Similarly, upstream impacts related to feedstock extraction and

Table 2 Classification of VP resin formulations by sustainability formulation score (SFS) based on the observed distribution in the literature. The table defines five sustainability categories, each associated with a colour code, SFS range, and a generic example of typical formulation characteristics. The number of articles in each class is calculated from the full dataset, providing a data-driven benchmark for interpreting and comparing the sustainability of new formulations

SFS range	Sustainability	Number of reviewed formulations	Description	Examples
0–14	Very low	43	Predominantly petrochemical origin, little or no use of green chemistry principles, high environmental impact	Most commercial formulations, primarily based on fossil-derived monomers or heavily modified biobased molecules, synthesized using hazardous reagents and solvents, with poor atom economy and high energy requirements. The final material is non-biodegradable, non-recyclable, and poses significant environmental and health risks at end-of-life, essentially representative of conventional, non-sustainable photopolymer resins
15–29	Low	61	Some initial adoption of renewable content or greener synthesis, but significant improvements needed	A resin that uses a mix of biobased and fossil-derived components, with significant chemical processing involving hazardous chemicals, low atom economy, and/or high energy consumption. End-of-life options are poor or limited to incineration or landfill, and the overall environmental impact is only modestly improved compared to conventional resins
30–44	Moderate	38	Noticeable integration of biobased materials and/or green processes, with partial attention to end-of-life aspects	A formulation with a high proportion of biobased content, but requiring more extensive chemical modification (*e.g.*, acrylation or methacrylation of natural oils or small molecules) that involves hazardous reagents, non-green solvents, or moderate energy input. End-of-life options may be limited (*e.g.*, partial biodegradability or recyclability), and atom economy is moderate
45–59	Good	13	High biobased content, greener synthesis, and clear end-of-life or recyclability strategies	A resin formulation in which the main components are minimally modified biobased macromolecules (such as lightly functionalized natural polymers or oils) using mild, low-hazard chemistry and sustainable solvents. The synthesis is energy-efficient and avoids toxic byproducts. The final material is designed for biodegradability or easy recycling, though some minor synthetic steps or additives may be present
≥ 60	High	6	Leading-edge, fully or nearly fully biobased, circular, or recyclable systems with minimal synthesis penalties and advanced end-of-life design	A formulation composed entirely of unmodified, naturally occurring biopolymers or small molecules (*e.g.*, vegetable oils, polysaccharides) that are directly photocurable, requiring no chemical modification, hazardous reagents, or solvents. All synthesis is performed at room temperature with perfect atom economy, and the final material is fully biodegradable and/or recyclable. This represents the ideal, maximum sustainability scenario

purification are excluded due to the lack of consistent reporting. A more refined, process-aware SFS could be developed in the future to capture these aspects and better reflect formulations optimized for industrial application. However, within the current boundaries of available data, the SFS provides a pragmatic and consistent comparative framework.

For commercially available, partially biobased (meth)acrylated components for which the synthesis process is unknown, the synthesis sustainability factors have been estimated using the most common synthetic pathways used in common industrial practice. In particular, acrylate and methacrylate esters are assumed to be synthetized by the reaction of 1.5 eq. of the alcohol with 1 eq. of acrylic or methacrylic acid under acid catalysis for 5 h at 100 °C in solventless conditions.[39–41] For hydroxyethyl acrylate and methacrylate, the common industrial synthetic pathways includes the reaction of 1 eq. of acrylic or methacrylic acid with 1.5 eq. of ethylene oxide (at 100 °C for 2 h), while glycidyl methacrylate is prepared by reacting 1 eq. of methacrylic acid with 1.5 eq. of epichlorohydrin (at 100 °C for 3 h).[42,43] Co-reagents employed at concentrations below 1 wt% are not included in the calculation of atom economy for simplicity, due to their negligible contribution. Natural products used without any chemical modification were assigned with the highest values for each sub-factor while, if chemical modification is required for their production, each sub-factor is assigned the value of 1. Inorganic solid fillers such as silica are not considered in the resin's composition for the calculation of the SFS. With respect to the end-of-life parameter F_{EoL}, for formulations where neither recyclability nor biodegradability were evaluated, the standard value of 0.8 was assigned. Only in the case of resins composed of biomacromolecules (see the "functionalized natural polymers" section) and reactive diluents below 10 wt%, the biodegradability of the 3D printed materials is assumed, and F_{EoL} was set equal to 1.7. For water-based formulations such as 3D printable hydrogels, the resin composition is calculated on its dry mass. When evaluating the biobased carbon content of surface-functionalized nanomaterials such as nanocellulose, as the functionalities are only introduced on the surface, their contribution is considered negligible, and the biobased content of the nanomaterial and its molecular weight are considered unchanged during functionalization. According to the provided definition, SFS can range from 0 for a non-biobased formulation to a maximum value of 345 for a theoretical fully biobased, recyclable and biodegradable formulation whose components are produced without the use of toxic compounds, at room temperature, and with perfect atom economy. A spreadsheet file containing the composition of all the resins discussed in this review, the calculation of their SFS together with the details on the values assigned to each sustainability subfactor, is provided as ESI.†

Sustainable resin systems

In the quest to develop greener alternatives for VP, photocurable components can be broadly classified into three main categories, each characterized by distinct structural features, synthetic strategies, and sustainability trade-offs (Fig. 2). The first category encompasses (meth)acrylated small molecules, comprising low-molecular-weight monomers and reactive diluents derived from renewable feedstocks (*e.g.*, lignin-derived phenols, itaconic acid derivatives), which are valued for their tuneable properties and printability, but whose sustainability is often compromised by the use of hazardous reagents and solvents in their synthesis. The second class includes photocurable macromolecules, such as functionalized biopolymers, which typically exhibit high biobased carbon content and enable solvent-free formulations, though they often require functionalization steps that impact mechanical performance and crosslinking efficiency. The third and most forward-looking category comprises recyclable and reprocessable

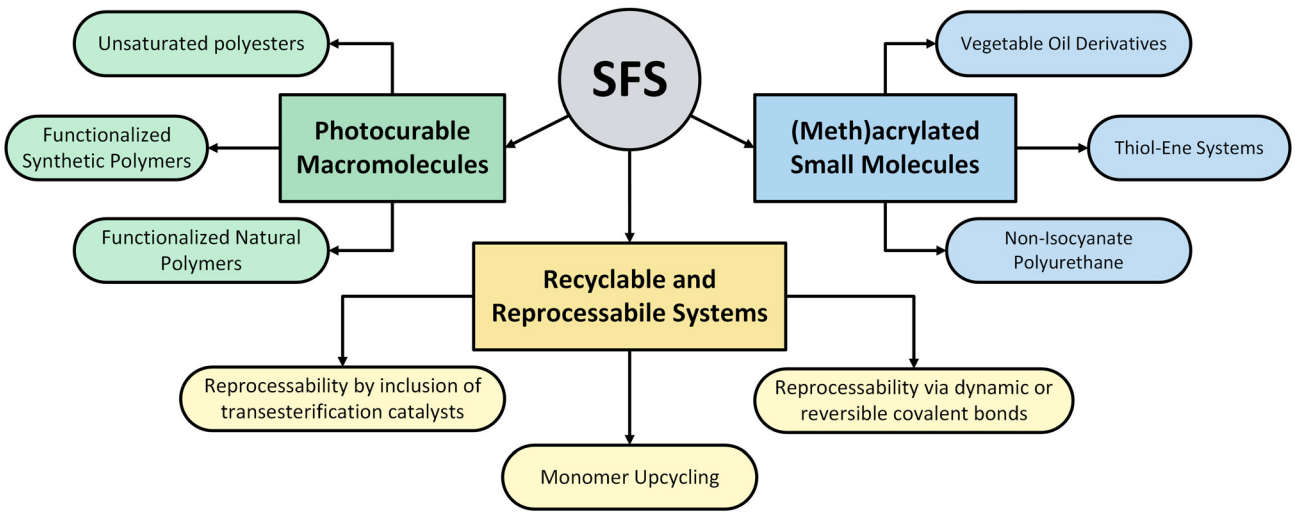

Fig. 2 Classification of sustainable components of photocurable formulations for VP reviewed in this work, in the SFS framework.

systems, which aim to improve the end-of-life profile of VP materials by enabling chemical recycling, reshaping, or degradation under mild conditions.

(Meth)acrylated small molecules

(Meth)acrylated small molecules play a crucial role in photopolymerization-based 3D printing, particularly in VP techniques such as stereolithography (SLA) and digital light processing (DLP). These molecules serve as reactive monomers or oligomers that undergo photopolymerization upon exposure to UV or visible light, forming crosslinked polymer networks that define the final properties of the printed structures. Acrylates generally exhibit faster polymerization kinetics due to their higher double-bond reactivity, while methacrylates offer greater thermal and mechanical stability due to the steric hindrance of the methyl group.[44] In photopolymerization-based 3D printing, (meth)acrylated small molecules function as primary monomers or reactive diluents in resin formulations. They reduce viscosity, improving printability and resin flow, while also influencing the degree of crosslinking and final mechanical properties. The choice of (meth)acrylated small molecules directly affects critical performance aspects such as mechanical strength, toughness, chemical resistance, and biocompatibility. Highly crosslinked systems exhibit superior mechanical and thermal stability but may suffer from brittleness, whereas monomers with flexible linkages improve toughness and elongation at break. Despite their advantages, (meth) acrylated small molecules also present important challenges. The polymerization process can lead to shrinkage, residual stress, and oxygen inhibition, affecting print resolution and mechanical integrity. Moreover, many commercial (meth)acrylated resins exhibit cytotoxicity due to unreacted monomers, limiting their direct use in biomedical applications.[45] Furthermore, they are derived from petrochemical sources, contributing to resource depletion and greenhouse gas emissions. These monomers are often toxic, with potential carcinogenic, mutagenic, and irritant effects on human health and the environment.[46,47] Research efforts focus on developing bio-based alternatives and low-toxicity monomers to enhance sustainability and performance.

Vegetable oil derivatives. Vegetable oils are naturally occurring triglycerides extracted from plant seeds, nuts, or fruits. They serve as essential dietary components, industrial feedstocks, and renewable resources for bio-based materials and chemicals. Beyond food applications, vegetable oils play a crucial role in industrial and technological fields.[48] They are key raw materials for biofuels, including biodiesel, which is produced through the transesterification of triglycerides with alcohols while, in the chemical industry, they serve as renewable feedstocks for biopolymers, lubricants, surfactants, and coatings.[49,50] Epoxidized vegetable oils (EVOs) are derivatives of vegetable oils in which the C=C double bonds of unsaturated fatty acids have been converted into epoxide groups through an oxidation process, typically carried out using peracids such as peracetic or performic acid, or *via* metal-catalyzed hydrogen peroxide oxidation (Scheme 1a).[51,52] However,

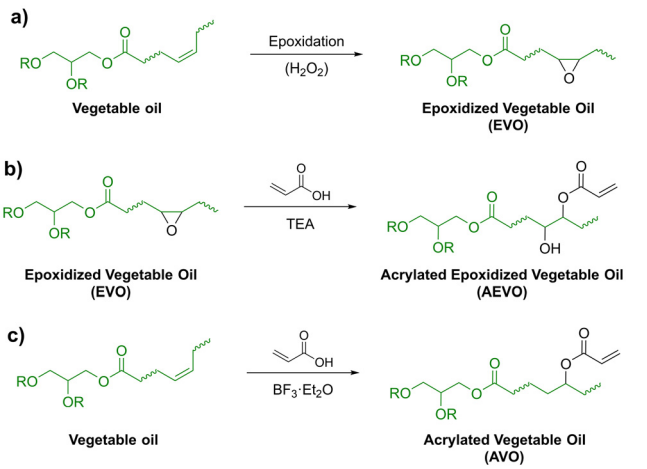

Scheme 1 Acrylation reaction on vegetable oils. (a) Epoxidation reaction, (b) Acrylation of epoxidized vegetable oils (TEA = triethylamine), and (c) direct acrylation of vegetable oils. The bioderived portion of each structure is depicted in green.

increasing concerns regarding the sustainability of the epoxidation process have led the research community to explore more environmentally friendly alternatives, such as chemoenzymatic oxidation and the use of acid ion-exchange resins.[53–55] Common epoxidized vegetable oils include soybean oil (ESO), linseed oil (ELO), sunflower oil (ESFO), and castor oil (ECO). Due to differences in fatty acid composition, the choice of oil affects the degree of epoxidation and, consequently, the reactivity of the final product. EVOs are widely used as bio-based plasticizers and stabilizers in PVC formulations, enhancing flexibility and thermal stability.[56] Their renewable nature makes them attractive for sustainable material development, including bio-based adhesives, coatings, and composites.[57–60] The epoxide functionality in EVOs is susceptible to nucleophilic attack, allowing for further reaction with acrylic and methacrylic acids to graft the corresponding acrylate α-hydroxy esters onto the fatty acid chains. The (meth)acrylation reaction is typically performed in the presence of Lewis bases such as triethylamine (Scheme 1b), which deprotonates the carboxylic acid and facilitates the nucleophilic ring-opening of the epoxide by the resulting carboxylate ion, or Lewis acids, which protonate the oxirane oxygen atom weakening the epoxide ring.[61] More efficient modifications have been achieved using acyl chlorides, but their high volatility, toxicity, and environmental impact raise significant concerns.[62] Alternative strategies involve the direct acrylation of vegetable oils with acrylic acid, using boron trifluoride diethyl etherate ($BF_3{\cdot}Et_2O$) as a Lewis acid catalyst.[63,64] In this process, $BF_3{\cdot}Et_2O$ activates the double bonds of the fatty acid chains, making them more susceptible to attack by carboxylic acids. However, this method requires overstoichiometric amounts of $BF_3{\cdot}Et_2O$, which is highly unstable, volatile, toxic, and corrosive, and a large excess of acrylic acid. Additionally, the resulting acrylated vegetable oils lack hydroxyl groups on the fatty acid chains, leading to thermosetting materials with lower mechanical properties

due to the absence of hydrogen bonding interactions between the acrylated monomers (Scheme 1c).

It is indeed remarkable that acrylated EVOs (AEVOs) can be 3D printed in most cases without the addition of reactive diluents, thus leading to photocurable formulations with BCC% above 85%, but the assessment of their SFS allows for a more comprehensive evaluation of their sustainability as photocurable components for VP 3D printing. In 2023, Mendes-Felipe *et al.* compared the properties of 3D printed acrylated epoxidized soybean oil (AESO) and acrylated soybean oil (ASO), revealing that the two step epoxidation-acrylation strategy allowed for obtaining thermosets with significantly higher Young's modulus and tensile strength than those of the $BF_3{\cdot}Et_2O$-catalyzed one-step approach.[65] This was thought to be related to a lower crosslinking density in ASO-based resins, together with a lower degree of intramolecular H-bonding, and supported by the acrylation degree data extracted from NMR analysis which corresponded to 2.46 and 1.44 acrylates per triglyceride molecule in AESO and ASO, respectively.

Significant variability in acrylation efficiency has been detected amongst different works employing similar substrates with similar synthetic approaches. In fact, in 2021 Vazquez-Martel *et al.* described the direct acylation of vegetable oils using acrylic acid and BF_3 etherate for 3D printing applications, comparing the obtained products in terms of the number of acrylate groups introduced per oil molecule.[66] They reported consistent conversions of double bonds into acrylate groups amongst different vegetable oils (59–68%), but the obtained acrylation degrees (2.34 for ASO) differ significantly from other works (1.44 from Mendes-Felipe *et al.*,[65] for example). Analogously, Wu *et al.* produced a sustainable photocurable 3D printable formulation by direct BF_3-catalyzed acrylation of waste cooking oil collected from a local McDonald's restaurant.[67] It this case, an acrylation degree of 2.01 was achieved, but the used mixture of oils was characterized by approximately 3.3 double bonds per triglyceride, lower than what has been reported for soybean oil (around 4.18). Perez *et al.* reported acrylation degrees of 1.6–2.5 using similar direct acrylation approaches, while Zhang described acrylation efficiencies up to 3.09 acrylate groups per triglyceride.[63,68] Finally, many authors employed commercial AESO, which is declared to be characterized by 2 acrylate moieties per triglyceride,[69,70] but some authors employed NMR analysis to assess its acrylation degree achieving results ranging from 2.7 to 3.5.[71,72] By comparing the SFSs calculated for each of the described formulations (Table 3), AVO-based resins (SFS ~ 22) are generally less sustainable than AEVO-based ones (SFS > 40) with comparable $BCC_{\%}$, as the direct acrylation reaction is often performed with harsher experimental conditions and with lower atom economy. In this context, Pezzana *et al.* recently developed a photocurable resin for vat photopolymerization based solely on epoxidized soybean and linseed oils (ESO and ELO), without the use of acrylates or reactive diluents.[73] The formulation employed SbF_6^--based organic salts as photoinitiators to trigger the cationic polymerization of epoxides. This innovative acrylate-free strategy enabled the production of 3D printed materials with exceptional biomass carbon content (BCC%) and among the highest static flexural strength (SFS) values reported in this section, 97% and 43, respectively. However, the epoxidation *via* hydrogen peroxide restricted the synthetic factor (F_{syn}) to approximately 0.5. Moreover, the cationic polymerization required elevated printing temperatures (up to 100 °C), necessitating specialized VP equipment and increasing the energy demand, thus limiting the resin's broader applicability. The resulting printed parts were mechanically soft, with Young's

Table 3 Acrylation degree, sustainability indexes and mechanical properties of AEVOs, AVOs, and EVOs employed in reactive diluent-free vegetable oil-based formulations for VP 3D printing

Triglyceride derivative	Molecular Weight[a] (g mol^{-1})	Number of acrylate groups per triglyceride	BCC%	SFS		Elastic modulus (MPa)	Elongation at break (%)	Tensile strength (MPa)	Ref.
AESO2.46	1136	2.46	88.5%	42.8		1.433 ± 0.370	3.44 ± 0.46	3.46 ± 0.25	65
ASO1.44	1097	1.44	93.0%	34.1		0.085 ± 0.007	11.04 ± 1.31	0.43 ± 0.07	
ACO2.57	1062	2.57	88.4%	21.8		13 ± 0.42	—	—	66
ASuO2.5	1067	2.5	88.5%	21.9		10 ± 0.37	—	—	
ASO2.34	1088	2.34	89.0%	22.1		10 ± 0.44	—	—	
ASeO2.25	1036	2.25	89.4%	21.6		8 ± 0.23	—	—	
AOO1.85	1004	1.85	91.0%	21.3		6 ± 0.15	—	—	
AESO2	1096	2[b]	90.5%	47.2		—	—	—	69–70, 74 and 76
						44.5 ± 5.5	15.5 ± 2.5	3.61 ± 1.04	78
						101.9 ± 7.1	11.4 ± 1.7	6.60 ± 1.40	79
ESO	—	—	97.5%	41.0		0.27 ± 0.02	5.9 ± 1.3	1.1 ± 0.3	73
ELO	—	—	97.4%	42.5		3.3 ± 1.3	3.3 ± 1.3	10.0 ± 0.3	

[a] Calculated as the sum of the average MW of the triglyceride (920 g mol^{-1} for soybean oil, 877 g mol^{-1} for canola oil, 887 g mol^{-1} for sunflower oil, 874 g mol^{-1} for sesame oil and 871 g mol^{-1} for olive oil) and the mass of acrylate moieties (71 g mol^{-1}) multiplied by the number of acrylate groups per triglyceride. In the case of AEVOs, an additional 17 g mol^{-1} are added per acrylate group to account for the OH group generated by the epoxide ring opening. In the case of AVOs, an additional 1 g mol^{-1} is added per acrylate group to account for the added proton in the same position. [b] Declared by the manufacturer.

moduli ranging from 0.3 to 3 MPa depending on the type of vegetable oil used.

From this overview, it appears clear that, when talking about AEVOs and AVOs, the scientific literature refers to a great variety of acrylated triglycerides from different sources, with different sustainability indexes and with different acrylation degrees, which lead to 3D printed materials characterized by a wide range of mechanical properties. Due to their low acrylic acid content, when printing AEVOs and AVOs as the only component of photocurable formulation the achieved mechanical properties are usually very low, with tensile strengths that hardly surpass a few MPa, far from the 50 MPa that are typical of most commercial formulations. Therefore, when aiming at proposing materials possessing actual mechanical stability that can really compete with commercial non-sustainable photocurable resins, AEVOs and AVOs need to be formulated with appropriate reactive diluents that are, in most cases, the acrylate or methacrylate esters of green and bioderived building blocks. Such (meth)acrylated building blocks are often characterized by high biobased carbon contents (BBC_i), but the experimental conditions required for their synthesis significantly impact on their synthetic factor $F_{syn,i}$ (especially for acrylate esters) thus limiting significantly their contribution to the sustainability of the overall formulations. The sustainability indexes and mechanical properties of said formulations are collected in Table 4.

In 2021, Barkane *et al.* compared the properties of 3D printed AESO with its formulation prepared by mixing it at 63 wt% with 1,6-hexanediol diacrylate (HDDA) and trimethylolpropane triacrylate (TMPTA), to study the effect of the photoinitiator concentration on the curing degree and kinetics of the system during 3D printing.[74] Unfortunately, the authors did not experimentally measured the acrylation degree of the employed AESO nor the mechanical properties of the 3D printed formulations, but from the presented data it is possible to assess the use of HDDA and TMPTA has significantly affected the sustainability of the proposed approach, thus limiting and SFS to 36, compared to the score above 47 usually achieved when printing AESOs with no reactive diluent.

Lublin *et al.* formulated AESO (with known acrylation degree of 3.5) with isobornyl methacrylate (IBOMA) in different ratios, analysing the micro- and nanoscale stiffness of 3D printed materials by quasi-static nanoindentation and comparing these finding with tensile testing data.[75] As IBOMA

Table 4 Sustainability indexes and mechanical properties of 3D printed photocurable formulations including AEVOs and partially sustainable reactive diluents

Formulation	Triglyceride acrylation degree	BCC%	SFS		Elastic modulus (MPa)	Elongation at break (%)	Tensile strength (MPa)	Ref.
AESO 65% HDDA 30%	2[a]	72.3%	36.0	🟡	—	—	—	74
AESO 70% IBOMA 30%	3.5	79.3%	39.4	🟡	~700–900	~14–17	~15–23	75
AESO 40% IBOMA 60%		75.4%	33.9	🟡	~1600–1850	~4–13	~30–41	
AESO 80% IBOA 20%	2[a]	85.9%	44.1	🟡	—	—	—	76 and 77
AESO 50% IBOA 50%		83.5%	38.1	🟡	—	—	—	
AESO 80% LA 20%	2[a]	86.7%	45.5	🟢	16.9 ± 2.4	20.3 ± 1.9	2.37 ± 0.25	78
AESO 50% LA 50%		84.9%	41.4	🟡	1.4 ± 0.2	8.2 ± 2.0	0.22 ± 0.20	
AESO 80% LA 20%	2[a]	86.7%	45.5	🟢	21.8 ± 0.5	23.1 ± 2.9	4.02 ± 0.42	79
AESO 50% LA 50%		84.9%	41.4	🟡	10.0 ± 0.7	9.8 ± 2.3	0.87 ± 0.25	
AESO 80% LMA 20%		85.4%	44.0	🟡	32.1 ± 2.5	17.1 ± 4.6	3.75 ± 0.86	
AESO 50% LMA 50%		82.6%	38.0	🟡	12.5 ± 0.2	17.7 ± 1.4	1.77 ± 0.13	
AESO 80% IBOA 20%		85.9%	44.1	🟡	50.4 ± 8.6	44.6 ± 3.4	10.13 ± 0.58	
AESO 50% IBOA 50%		83.5%	38.1	🟡	508.3 ± 17.4	8.0 ± 0.2	21.57 ± 0.22	
AESO 80% IBOMA 20%		84.5%	43.8	🟡	140.9 ± 3.5	35.6 ± 4.3	13.59 ± 1.13	
AESO 50% IBOMA 50%		80.9%	37.4	🟡	531.4 ± 20.0	9.3 ± 0.5	26.57 ± 1.93	
AESO 63% HDDA 29% TMPTA 5%	2[a]	72.3%	36.0	🟡	125	4.5	4.4	80

[a] Declared by the manufacturer.

is characterized by $BCC_{\%}$ and $F_{syn,i}$ (71% and 0.47, respectively), quite significant for a commercial methacrylate, when its concentration was increased from 30 wt% to 60 wt%, a moderate improvement was observed for all mechanical properties, both at the macroscopic and microscopic scale, without affecting severely the sustainability of the formulations. In fact, such increase in the IBOMA content only led to a reduction of SFS from 39 to 34.

Parallelly, isobornyl acrylate (IBOA) has a higher BCC% (77%) since the lighter acrylate residue have less impact on the carbon atom count, but an almost identical $F_{syn,i}$ of 0.46. This reactive diluents was used in two similar works from the same authors, Bergoglio *et al.*, which describe the preparation of AESO/IBOA-based photocurable resins including up to 30 wt% of bioactive glass for possible future applications in tissue engineering.[76,77] As the IBOA concentration was increased from 20 to 50 wt%, the biobased content of the formulations decreased slightly from 85.9% to 83.5%, but a more significant difference can be detected using SFS, which decreased from 44 to 38.

An additional sustainable reactive diluent was employed by Bodor *et al.* in 2024, who formulated AESO with increasing amounts of lauryl acrylate (LA).[78] Due to the long fatty acid-derived aliphatic chain, LA possesses $BCC_{\%}$ (80%), but the need for the acrylation reaction has an impact on its F_{syn} (0.55). Furthermore, the use of acrylated reactive diluent with high biobased contents is inherently accompanied by a low concentration of photoreactive groups in their formulations, leading to low crosslinking densities in the 3D printed photopolymer, and therefore poor mechanical properties. In fact, unlike IBOMA and ACMO, when LA is added to AESO at increasing concentrations, the mechanical properties of the 3D printed material decrease consistently, with tensile strengths that fall below 1 MPa when LA concentration is 40 wt%, accompanied by a reduction of the SFS to 41. These findings suggest once again that the use of acrylated and methacrylated building blocks for the formulation of resins for VP is not often the optimal strategy for achieving both high sustainability and state-of-the-art mechanical properties, as good mechanical properties are achieved with high density of (meth)acrylate groups, which often lead to significant reduction in their overall bioderived contents.

Similar findings were reported the same year by Porcarello *et al.*, who studied the effect of increasing concentrations of LA, IBOA, IBOMA and lauryl methacrylate (LMA) in AESO-based photocurable formulations on the mechanical properties of the corresponding 3D printed materials.[79] In this work, it has been demonstrated how reactive diluents characterized by a long aliphatic chain such as LA and LMA have negative effects on the mechanical performances of AESO-based resins, while IBOA and IBOMA led to significant increases in elastic modulus and tensile strength when their concentration was increased. These findings suggest that, when targeting improvements in mechanical properties in 3D printed photopolymer, the crosslinking density is not the only determining factor, but intermolecular weak forces play a fundamental role. While IBOA and LMA are characterized by comparable biobased carbon contents (77% and 75%, respectively), and therefore comparable proportion of photocurable with respect to their molecular mass, their effect on the mechanical properties of AESO-based 3D printed formulations is opposite.

An alternative strategy has been followed by Jurinovs *et al.*, who formulated AESO with HDDA and trimethylolpropane triacrylate (TMPTA) using low concentrations of surface modified nanocellulose (<0.1 wt%) as a reinforcement filler.[80] Thanks to this approach, the reported resin was characterized by good sustainability indexes (BCC% = 72% and SFS = 36) and good mechanical properties, ensured by a covalent interaction between the surface of nanocellulose and the AESO-based polymer matrix.

Epoxidized soybean oil has been also reacted with different carboxylic acids, producing the corresponding ester bound to the fatty acid backbone. A summary of the differently functionalized epoxidized vegetable oils and their formulations, together with the corresponding sustainability indexes and the mechanical properties of their 3D printed materials is provided in Table 5. A first example has been reported by Guit *et al.* in 2020, who described the synthesis of methacrylated epoxidized 40.

Soybean oil (MAESO) by reacting methacrylic acid with epoxidized soybean oil using triphenylphosphine as the Lewis base catalyst.[81] By adjusting the reaction conditions and the molar ratios between the reagents, the authors of this work have been able to produce MAESOs with different acylation degrees (2.3 and 3.0), which have been formulated at 60 wt% with IBOMA as the reactive diluent. The presented results show clearly that, despite having the same functionalization degree, resins formulated with $MAESO_3$ were characterized by higher stiffness and tensile strength compared to $AESO_3$, and when the acylation degree of the epoxidized vegetable oil was increased from 2.3 to 3.0 the printed material display higher elastic modulus and lower elongation at break. The type of modification of the triglyceride did not affect significantly the sustainability of their formulations, as they were all characterized by a BBC% in the 77–79% range and SFS around An original approach has been subsequently reported by Zhu *et al.*, who developed a partially-biobased photocurable gallic acid derivative to be employed for the epoxide ring-opening reaction in epoxidized soybean oil.[82] By reacting a slight excess of methacrylic anhydride with biobased gallic acid, they have been able to produce a mixture of gallic acid trimethacrylate (GATA) and methacrylic acid that was employed for the functionalization of ESO in the same pot (Scheme 2a). The obtained modified triglycerides, named GMAESO, were characterized by pendant methacrylate and GATA moieties with an overall methacrylate content of 3.29 per triglyceride molecule. However, the number of gallate groups per triglyceride was not determined, thus hindering the possibility for a quantitative assessment of the sustainability indexes that characterize the macromer. If we assume that GATA and methacrylic acid possess similar reactivity towards the epoxide ring opening,

Table 5 Sustainability indexes and mechanical properties of 3D printed photocurable formulations including functionalized EVOs

Formulation	Triglyceride functionalization degree	BCC%	SFS		Elastic modulus (MPa)	Elongation at break (%)	Tensile strength (MPa)	Ref.
$MAESO_2$ 60% IBOMA 40%	2.3	79.1%	35.6	🟡	870 ± 44	18 ± 3	36.4 ± 0.4	81
$MAESO_3$ 60% IBOMA 40%	3	77.0%	34.6	🟡	1007 ± 30	10 ± 2	43.7 ± 0.3	
$AESO_3$ 60% IBOMA 40%	3	79.1%	38.2	🟡	727 ± 12	24 ± 3	28.3 ± 0.3	
GMAESO 80% HEMA 20%	3.29	73.4%	34.0	🟡	350.0 ± 33.2	4.4 ± 0.6	15.5 ± 0.8	82
GMAESO 60% HEMA 40%		64.7%	28.7	🟠	442.9 ± 18.1	8.4 ± 1.2	32.1 ± 0.6	
GMAESO 40% HEMA 60%		55.1%	23.4	🟠	601.1 ± 27.2	9.7 ± 1.1	44.1 ± 1.1	
IPESO 80% TMPTA 20%	3.5	47.2%	14.8	🔴	269.72 ± 22.65	8.30 ± 0.55	25.01 ± 0.71	83
IPESO 50% TMPTA 50%		29.6%	9.3	🔴	521.09 ± 29.76	9.03 ± 0.73	47.40 ± 1.58	
ESO_HEA 100%	4.2	82.3%	25.5	🟠	—	—	0.14	84
ESO_HEA 80% TMPTA 20%		66.4%	20.4	🟠	—	—	1.13	
ESO_HEMA 100%		78.2%	25.3	🟠	—	—	0.51	
ESO_HEMA 80% TMPTA 20%		63.2%	20.2	🟠	—	—	2.44	
MBSS 42% HHDA 7.4% BPAEDA 49.4%	—	44.2%	15.1	🟠	1700	1	17	85
DMSS 42% HHDA 7.4% BPAEDA 49.4%	—	40.6%	13.8	🔴	600	3	13	
AESS 42% HHDA 7.4% BPAEDA 49.4%	—	46.1%	20.0	🟠	450	6	8	

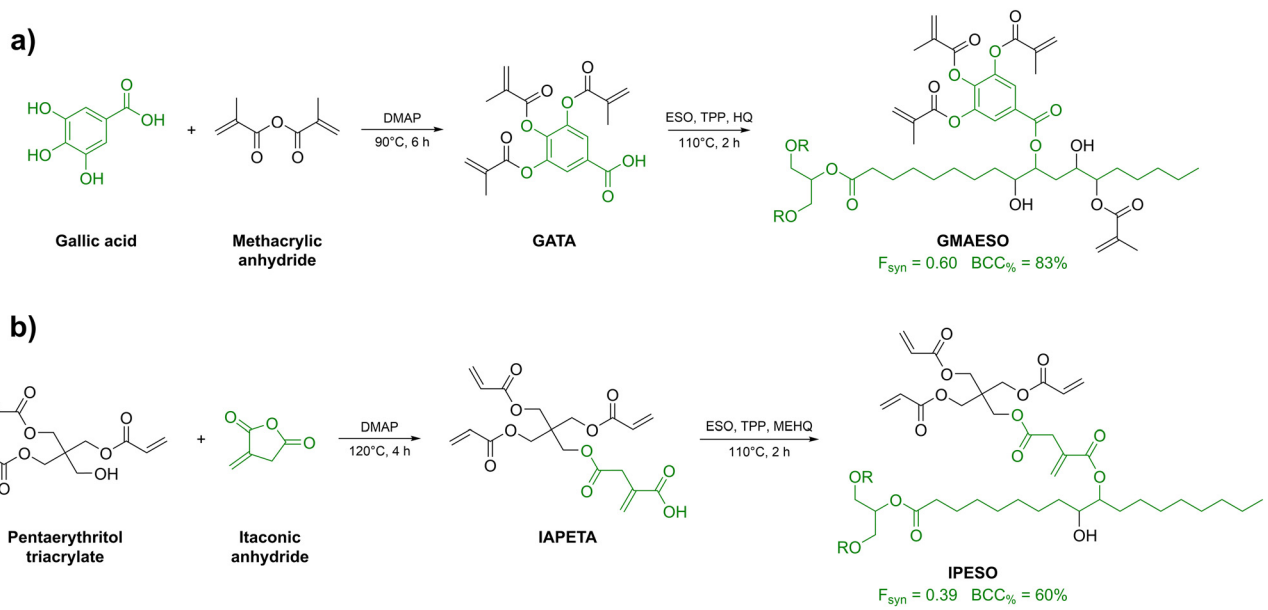

Scheme 2 Functionalization of epoxidized soybean oil (ESO) using partially biobased polyacrylated carboxylic acids. DMAP = 4-dimethylaminopyridine, TPP = triphenylphosphine, HQ = hydroquinone, MEHQ = methyl hydroquinone. The bioderived portion of each structure is depicted in green. Re-drawn from ref. 82 and 83.

the BCC_i and F_{syn} of GMAESO can be estimated to be around 83% and 0.60, respectively. Therefore, the use of GATA compared to methacrylic acid has allowed for a slight increase in the achievable acrylation degree of the triglyceride, but the sustainability of the overall macromer has not been significantly improved. Furthermore, GMAESO was formulated with 2-hydroxyethyl methacrylate (HEMA), which has low BCC_i, leading to formulations printed into materials that indeed possess good mechanical properties, but with limited SFS (23 to 34, depending on the composition).

Similarly, it has been recently reported by Lin and co-workers the analogous production of an itaconic acid-based triacrylate derivative, to be employed for the epoxide ring opening of ESO.[83] By reacting itaconic anhydride with the free OH group of pentaerythritol triacrylate, the triacrylate itaconic acid ester IAPETA was synthesized and grafted to the epoxidized fatty acid chains of soybean oil producing the photocurable triglyceride named IPESO (Scheme 2b). In this case, the acrylate moieties were quantified to be equal to 14 per triglyceride, including the acrylic C=C functionality of itaconic acid, representing an acrylation degree higher than those previously reported in the literature. However, as the grafted IAPETA moiety has a low bioderived mass content, the extensive functionalization of the fatty acid chains causes a severe reduction of BCC_i, which fall to 60%. Furthermore, the synthesis of IPESO involves the use of dichloromethane as the solvent, which causes a reduction of its F_{syn} to 0.39. IPESO was then formulated at different concentrations with non-bioderived TMPTA, causing a further reduction in the sustainability of the formulations (SFS < 15, depending on the composition) with no significant improvements in terms of achieved mechanical properties.

Finally, Bodhak *et al.* recently reported a different strategy for the acrylation of epoxidized soybean oil employing 2-hydroxyethyl acrylate and methacrylate (HEA and HEMA) for the epoxide ring-opening reaction using hydrogen tetrafluoroborate as the catalyst.[84] Even though the authors did not calculate the actual degree of acrylation of the macromolecule, they employed ESO characterized by 7.33 g of epoxide oxygen per 100 g of oil, corresponding to a total of around 4.2 epoxide groups per triglyceride. By assuming that all epoxide groups have reacted with HEA and HEMA, as it is claimed in the work, this number also corresponds to the degree of functionalization, and it allows us to calculate their BCC_i, and F_{syn} (84% and 0.38 for ESO_HEA and 80% and 0.40 for ESO_HEMA, respectively). Despite the high functionalization degrees achieved, this approach led to 3D printed materials with very low tensile strength values, able to slightly surpass 1 MPa only when formulated with 20 wt% of non-renewable TMPTA. Nonetheless, the harsh experimental conditions and the low biobased mass of HEA and HEMA residues led to SFSs below 26.

A different epoxidized substrate was employed by Silbert *et al.* in 2020, who employed epoxidized sucrose soyate (ESS) in a similar way.[85] EES is composed by a sucrose core functionalized on all its hydroxylic sites with soybean oil-derived fatty acids, which is then epoxidized similarly to what has been described for vegetable oils. LCA applied to the ESS recently confirmed its potential for lower carbon footprint and improved circularity.[86]

In this work, ESS was functionalized with one acrylic acid molecule per epoxide (AESS), two methacrylic acid groups per epoxide (DMESS) or one acrylic and one butyric acid group per epoxide (MBESS) and formulated with around 50 wt% of bisphenol A ethoxylate diacrylate (BPAEDA) (Scheme 3). Due to the high amount of non-biobased crosslinker used, the sustainability of the proposed formulations is indeed low (BCC% ranging from 40% to 46% and SFS from 14 to 20), but this work suggests the potential of functionalized ESS as a biobased building block for photocurable 3D printable formulations, thanks to its good F_{syn} (0.5–0.6) and high biobased carbon content (above 70%).

In conclusion, the use of vegetable oil-derived photocurable components, such as AEVOs and AVOs, enhances the sustainability of VP formulations due to their high bioderived mass. However, their inherently low degree of functionalization limits photocrosslinking, which increases the biobased content but compromises mechanical performance, often requiring the addition of (meth)acrylate-based diluents that reduce the overall SFS. The (meth)acrylation process itself results in varying functionalization degrees, complicating comparisons across studies—a factor often overlooked in the literature. While epoxidation routes have been more successfully optimized, direct acrylation and epoxide ring-opening methods still rely on hazardous chemicals, elevated temperatures, and long reaction times, all of which negatively impact the overall sustainability profile.[87] Moreover, the continued reliance on acrylic and methacrylic acid derivatives generally restricts SFS values.

(Meth)acrylated monomers. Green chemistry offers a wide range of biobased building blocks that display functionalities exploitable for chemical modification with photopolymerizable moieties. Among these, lignin-derived phenolic compounds such as eugenol[88,89] guaiacol,[90] syringol,[91] gallic acid,[92,93] and vanillin[94,95] have emerged as promising candidates for the synthesis of (meth)acrylated monomers. These compounds are naturally occurring or derived from lignin depolymerization, offering renewable alternatives to conventional petrochemical-based monomers while retaining reactive functional groups that facilitate chemical modification.[96,97]

By leveraging these lignin-derived phenolic building blocks, researchers have designed sustainable photopolymerizable materials with reduced environmental impact while maintaining excellent mechanical properties and functional versatility. However, when compared to other strategies developed to improve resins sustainability, the use of (meth)acrylated molecules usually leads to lower sustainability indicators, as the introduced (meth)acrylic groups occupy a higher proportion of the molecular weight of these molecules. Furthermore, (meth) acrylation is often performed using acyl chlorides in halogenated solvents, furtherly impacting their sustainability. A summary of the formulations presented in this section, together with the corresponding sustainability indexes and the mechanical properties of 3D printed materials is provided in Table 6.

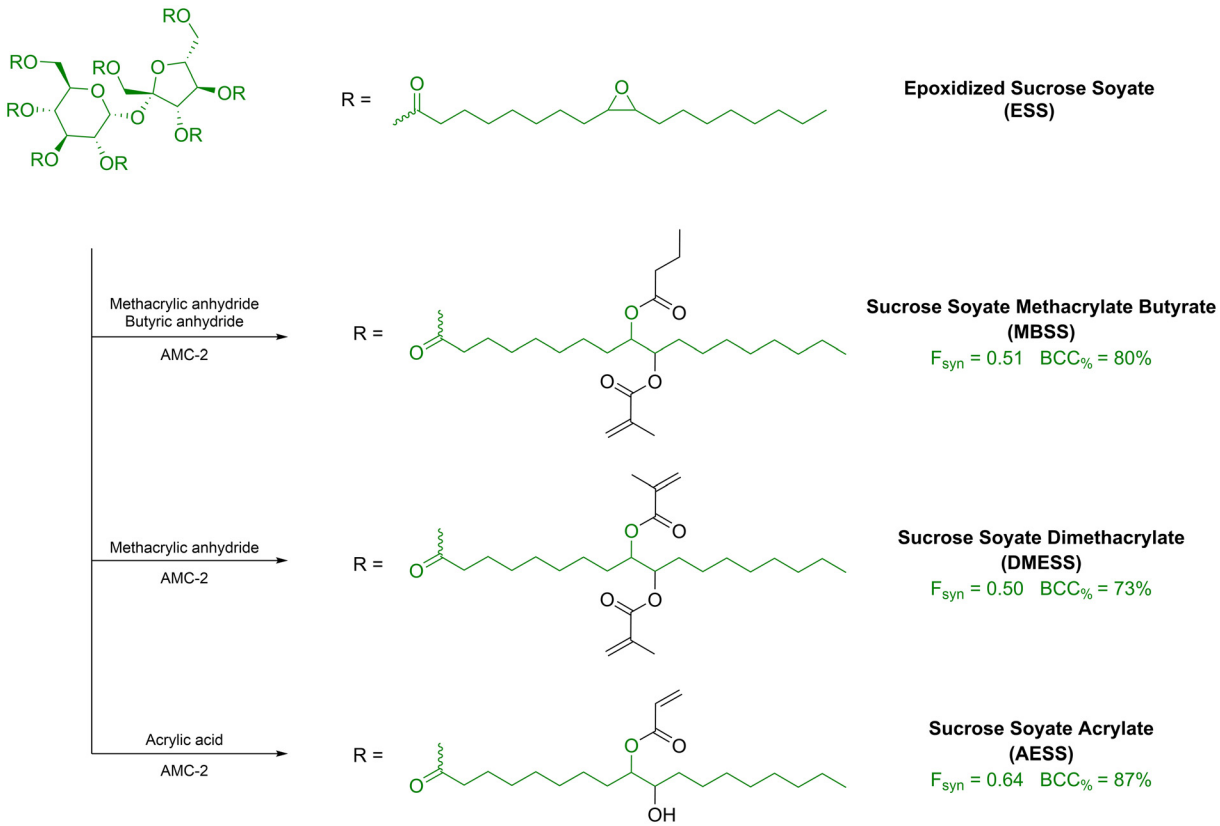

Scheme 3 Photocurable epoxidied sucrose soyate derivatives used in photocurable formulations for VP. The bioderived portion of each structure is depicted in green. Re-drawn from ref. 85.

Table 6 Sustainability indexes and mechanical properties of 3D printed photocurable formulations including (meth)acrylated phenolic compounds from lignin and glycidyl methacrylate derivatives

Formulation (wt%)	BCC%	SFS		Elastic modulus (GPa)	Elongation at break (%)	Tensile strength (MPa)	Ref.
4pGA 50% LA 50%	78.3%	46.7	🟢	—	1700 ± 100	0.20 ± 0.06	98
4pGA 60% LA 10% SA 30%	75.9%	30.9	🟡	—	4.7 ± 0.9	20 ± 2	
SMA 100%	66.5%	24.0	🟠	—	2.4 ± 0.4	30 ± 9	
SMA 50% LMA 50%	71.0%	38.3	🟡	—	3 ± 1	1.9 ± 0.6	
Eu-BzMA 98%	48.9%	8.1	🔴	2.71 ± 0.59[b]	—	43.5 ± 3.40[b]	99
Gu-BzMA 98%	40.2%	6.4	🔴	1.91 ± 0.01[b]	—	36.2 ± 0.63[b]	
MGA 99%	36.4%	7.5	🔴	—	—	—	100
GuM 20% EA 60% VDM 20%	58.8%	17.3	🟠	1.02 ± 0.02[a]	6.9 ± 1.1[a]	44.6 ± 1.8[a]	105
GuM 40% EA 40% VDM 20%	59.1%	18.5	🟠	1.09 ± 0.02[a]	7.6 ± 1.6[a]	49.7 ± 2.8[a]	
GuM 60% EA 20% VDM 20%	59.4%	19.8	🟠	1.23 ± 0.07[a]	8.9 ± 1.6[a]	61.7 ± 5.1[a]	
VM 48% GDM 50%	46.6%	26.4	🟠	4.903 ± 0.120	0.27 ± 0.05	12.49 ± 1.63	106
BHMP2 99%	54.8%	29.6	🟠	1.563	3.42	31.1	108
BHMP3 99%	57.1%	30.8	🟡	4.480	0.84	45.2	
DAS 43% PEGDA 55%	17.7%	3.7	🔴	0.106 ± 0.013	6.7 ± 0.9	5.8 ± 0.7	110

[a] Assessed on bulk-photocured resins, not on 3D printed samples. [b] Tested under flexural conditions.

As a first example, Chin *et al.* have recently described the synthesis of (meth)acrylated derivatives of 4-propylguaiacol and syringol by acylation of the corresponding sustainable phenols with (meth)acryloyl chloride.[98] The produced 4-propylguaiacol acrylate (4pGA), syringyl acrylate (SA) and syringyl methacrylate (SMA) were then formulated in different proportions with LA (for 4pGA and SA) or LMA (for SMA) to produce photocurable resins which were efficiently 3D printed by means of a custom-made VP system using no multifunctional crosslinker. The reported syntheses involved the use of acyl chlorides and halogenated solvents, as well as equimolar amounts of triethylamine, leading to low f_{haz}, f_{solv} and AE, which led to F_{syn} factors below 0.3. Interestingly, the absence of crosslinking allowed the photopolymers to be soluble in organic solvents, allowing for the recovery of the 3D printed materials by dissolution in organic solvents and their reforming by solvent-casting. This fact is considered in the evaluation of F_{EoL}, which compensated for the low sustainability of the synthetic steps leading to SFS values as high as 47. Furthermore, this crosslinker-free approach allowed for the obtainment of very soft thermoplastic elastomeric 3D printed materials, with elongations at break as high as 1700%, but very low tensile strengths.

A different strategy was followed by Zhou *et al.*, who exploited the phenolic moieties of guaiacol and eugenol to transform them into the corresponding benzoxazine upon reaction with formaldehyde and a 2-(2-aminoethoxy) ethanol, followed by methacrylation (Scheme 4).[99] The prepared monomers, Eu-BzMA and Gu-BzMA, had sufficiently low viscosity to be formulated and processed *via* VP with no added reactive diluent, leading to 3D printed materials BCC% that resembles those of their monomers (49% for Eu-BzMA, and 40% for Gu-BzMA, respectively). However, as the syntheses were conducted using chloroform, acyl chlorides, high temperatures and prolonged times, the corresponding SFSs are very low in both cases (8.1 for Eu-BzMA, and 6.4 for Gu-BzMA, respectively). Interestingly, as the benzoxazine ring is notoriously able to undergo ring-opening polymerization upon heating above 200 °C, thermally cured 3D printed materials displayed very high elastic moduli with no need for the presence of multifunctional crosslinkers, but with limited biobased contents.

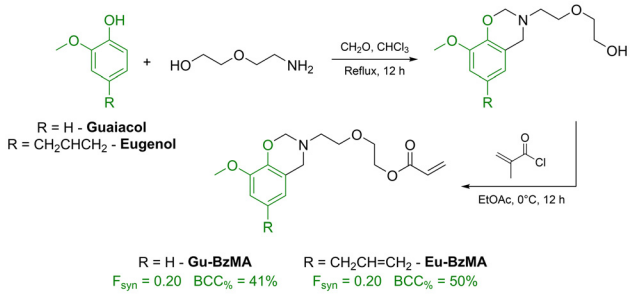

Scheme 4 Synthesis of guaiacol and eugenol-derived acrylate benzoxazines. The bioderived portion of each structure is depicted in green. Re-drawn from ref. 99.

This effect is even more pronounced for Eu-BzMA, as its pending allylic group provides an additional crosslinking site during thermally induced polymerization.

The same year, Sesia *et al.* reported the microwave-assisted synthesis of methacrylated gallic acid (MGA) using biobased gallic acid and methacrylic anhydride.[100] Even though the use of acid anhydrides is indeed more sustainable than acid chlorides, especially if no catalyst or solvent is used as in this case, concerns must be raised in terms of atom economy, as one methacrylic acid molecule is wasted per molecule of methacrylic anhydride reacted.[101] In fact, the AE of 0.37 caused a significant reduction of the corresponding F_{syn}, widely compensating for the sustainability bonuses introduced by the solventless microwave-assisted approach. Furthermore, the presence of three methacrylic acid residues per gallic acid molecule have a tremendous effect on the BCC% of MGA, which is only 37%. When formulated with the appropriate photoinitiator, MGA was able to produce high-resolution 3D printed objects with SFS as low as 7.5, and mechanical properties of the 3D printed material were not evaluated.

Vanillin is a very versatile green building block for the development of reactive monomers and advanced sustainable materials thank to the presence of an aldehyde group in addition to its phenolic nature.[102] This functionality can be reacted with (meth)acrylated amines to form the corresponding photocurable imines,[103] which have been widely exploited for the production of self-healing and recyclable photocurable resins. This approach will be presented in more detail in the section dedicated to recyclable and reusable resins. Upon reaction with mild reducing agents, vanillin can be converted into vanillyl alcohol, which can be employed as a diol for the synthesis of sustainable polyesters or further acetylated with carboxylic acids of interest.[104] For example, in 2019 Ding *et al.* employed vanillin dimethacrylate (VDM) as the reactive diluent for photocurable resins based on guaiacyl methacrylate (GuM) and 3,6-dioxa-1,8-octanedithiol eugenol acrylate (DOEA), obtained by thiol–ene addition of eugenol on both sides of 3,6-dioxa-1,8-octanedithiol, followed by acrylation with acryloyl chloride.[105] A series of formulation with different proportions between the monomers were 3D printed and tested, allowing the authors to achieve Young's moduli as high as 1.23 GPa. However, the use of a non-sustainable long-chain dithiol had a severe impact on the maximum achieved sustainable mass content (BCC% = 59%), and the use of acryloyl chloride heavily impacts on their sustainability claims (SFS < 20).

An atom-economic approach has been subsequently reported by Bassett *et al.* in 2020, who employed a one pot, two-step approach to synthesise a photocurable resin composed of equimolar amounts of vanillin methacrylate (VM) and glycerol 1,3-dimethacrylate (GDM).[106] This has been achieved by reacting vanillin with methacrylic anhydride, leading to a mixture of VM and methacrylic acid, followed by the addition of a stoichiometric amount of glycidyl methacrylate (GMA), which reacted with methacrylic acid to quantitatively form GDM (Scheme 5). The formulation for VP was simply prepared by adding the photoinitiator to the VD/GDM

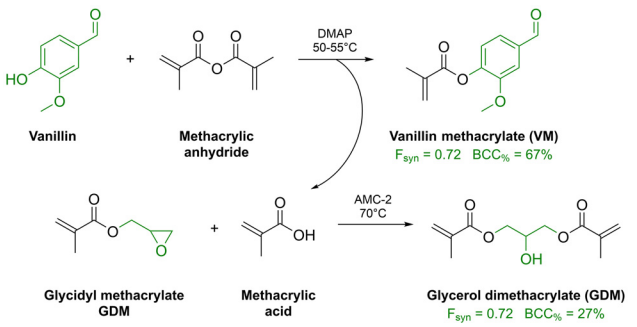

Scheme 5 One-pot two-step synthesis of an equimolar mixture of vanillin methacrylate and glycerol dimethacrylate. The bioderived portion of each structure is depicted in green. Re-drawn from ref. 106.

mixture, leading to the obtainment of a very rigid and brittle photopolymer, characterized by a biobased carbon content below 50%. Nonetheless, the atom economy and solventless nature of the one-pot two-step synthetic strategy employed are considered in the calculated SFS, which is as high as 26.4.

Thanks to its reactivity towards carboxylic acid, GMA has also found application for the methacrylation of biobased acids and diacids to produce reactive diluents, but its sustainability is closely tied to the environmental impact of its key precursor, epichlorohydrin (ECH). Traditionally, ECH is synthesized from petrochemical-based propylene, a process that generates significant carbon emissions and toxic byproducts. However, a more sustainable alternative has been implemented at the industrial scale, to produce ECH from glycerol, a renewable byproduct of biodiesel production, significantly reducing reliance on fossil resources and lowering greenhouse gas emissions.[107,108] By incorporating bio-based ECH into GMA synthesis, the overall sustainability of GMA-derived reactive diluents can be improved, making them more environmentally friendly while maintaining their high performance in photopolymerization applications.

In 2020, Miao *et al.* described the synthesis of bis(2-hydroxy-3-(methacryloyloxy) propyl) succinate (BHMP2) and bis(2-hydroxy-3-(methacryloyloxy) propyl) itaconate (BHMP3) by reacting GMA with succinic and itaconic acid, respectively, using triphenylphosphine as the catalyst (Scheme 6).[109] The syntheses were performed in sustainable conditions and with good atom economies, leading to F_{syn} of 0.67 for both reactive diluents. As the obtained esters were liquid at room temperature, it was possible to mix them with the appropriate photoinitiator without the need for additional reactive diluents, leading to a photocurable formulation with higher BCC% (55% for BHMP2 and 57% for BHMP3) and SFS (30 for BHMP2 and 31 for BHMP3) than previous MA biobased systems. The 3D printing of such difunctional monomers allowed to achieve photopolymers with high elastic moduli (1.5–4.5 GPa) and tensile strengths (31–45 MPa), especially in the case of BHMP3, where the acrylate functionality of itaconic acid was able to participate in the photopolymerization process.

It is worth mentioning the recent work of Hodasova *et al.*, who reported a photocurable formulation for VP 3D printing using allylic esters instead of the more conventional acrylic acid derivatives.[110] In this work, succinic acid was reacted with allyl bromide to produce the corresponding diallyl succinate (DAS), which was formulated with an excess of poly(ethyleneglycol) diacrylate (PEGDA) and a photoinitiator to be 3D printed into partially biodegradable materials. Although the sustainability of the reported approach is very low (SFS = 3.7), this is mainly due to the use of toxic and volatile allyl bromide in the synthesis (F_{syn} = 0.27) and the high content of non-renewable PEGDA in the formulation. Nevertheless, the introduction of common C=C moieties into photocurable systems for VP paves the way for the incorporation of new unsaturated green building blocks, such as terpenes, into these applications. The scientific literature clearly shows that the incorporation of (meth)acrylated green molecules in photocurable formulation for VP present several advantages, including a wide range of mechanical properties achievable, often without

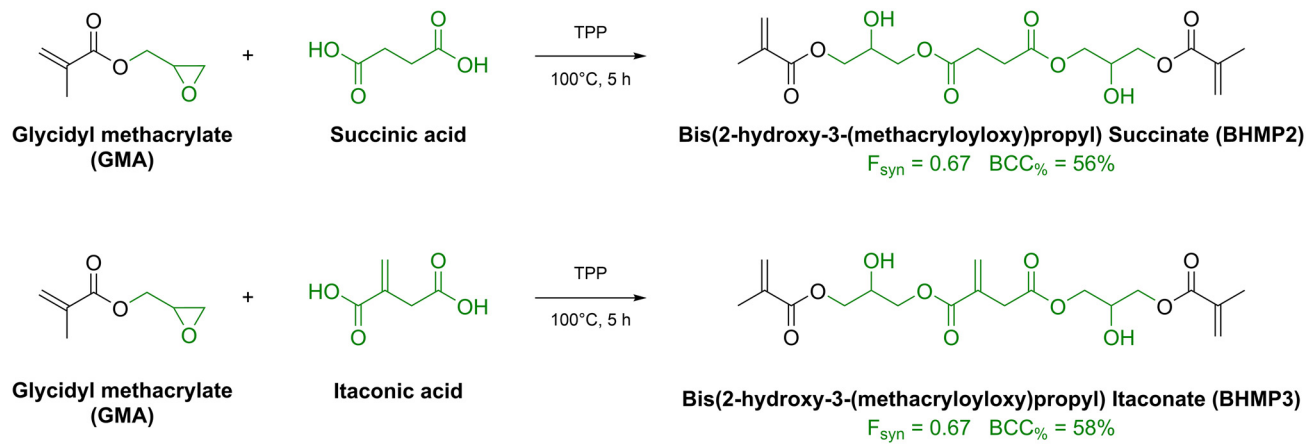

Scheme 6 Synthesis of itaconic and succinic acid-based reactive diluents proposed by Miao *et al.* The bioderived portion of each structure is depicted in green. Re-drawn from ref. 109.

the addition of reactive diluents. The chemical versatility of such building blocks allows for the development of new and original chemical modification strategies that could allow to expand further the range of materials properties, but their overall sustainability is still low, from a green chemistry perspective. To date, the chemical modification of these compounds frequently relies on toxic reagents, hazardous solvents, and energy-intensive conditions involving prolonged reaction times and elevated temperatures, factors that significantly undermine their sustainability. Addressing these limitations is essential for advancing greener photocurable formulations, with a promising first step being the replacement of acrylic and methacrylic acid by fully biobased alternatives, such as itaconic acid.

Photocurable non-isocyanate urethanes. Photocurable urethanes are widely used in vat photopolymerization-based 3D printing due to their exceptional mechanical properties, chemical resistance, and versatility in formulation. These materials are typically based on urethane acrylates or urethane methacrylates, which undergo rapid crosslinking upon exposure to UV or visible light, forming highly durable polymer networks. Compared to purely acrylate-based photopolymers, urethane-based resins offer improved toughness and reduced brittleness, making them particularly attractive for applications demanding mechanical resilience.[111–113] Despite their advantages, the synthesis of photocurable urethanes presents significant sustainability challenges, primarily due to their reliance on petroleum-derived raw materials and the environmental impact of their production processes. These materials are synthesized through the reaction of polyols with isocyanates to form the urethane backbone, followed by functionalization with acrylate or methacrylate groups to enable photopolymerization. The isocyanates used in the formation of the urethane linkage further exacerbate sustainability concerns. Compounds such as toluene diisocyanate (TDI) and methylene diphenyl diisocyanate (MDI) are produced using highly hazardous reagents, most notably phosgene, a toxic gas that requires strict handling and containment measures.[114] The synthesis of isocyanates also generates byproducts that contribute to atmospheric pollution and require extensive purification, increasing both the energy consumption and environmental footprint of these materials. Furthermore, the reactive nature of isocyanates poses occupational health risks, necessitating strict safety protocols during production and handling.[115,116] To address these issues, non-isocyanate urethanes have emerged as a promising alternative to conventional isocyanate-based systems. These materials eliminate the use of toxic isocyanates in their synthesis, relying instead on alternative chemistries such as the reaction between cyclic carbonates and amines to form urethane linkages.[117–119] Additionally, non-isocyanate urethanes can be synthesized from biobased sources, such as CO_2-derived carbonates and bio-based diamines, further enhancing their environmental profile. Details on the sustainability and mechanical properties of the isocyanate-free urethanes and reactive diluents discussed in this section are summarized in Table 7. In the context of VP 3D printing, this approach was first introduced by Schimpf *et al.* in 2019, who reported the synthesis of partially biobased hydroxyurethane dimethacrylates (HUDMs) by reacting a series of aliphatic diamines, including biobased 1,5-pentanediamine (cadaverine), with glycerol carbonate methacrylate (GCM).[120] (Scheme 7). Glycerol carbonate is a promising highly sustainable building block, as it is commonly produced by reaction of glycerol with CO_2 in the presence of a catalyst, and it can be quantitatively transformed into hydroxyurethanes upon reaction with aliphatic amines.[121] Nonetheless, direct synthesis of GCM from CO_2 has been performed using GMA under catalytic conditions, leading to partially renewable methacrylated urethanes for 3D printing. Furthermore, as aliphatic amines can react with methacrylates *via* aza-Michael addition, the use of a slight excess of diamine has allowed for partial oligomerization *via* the formation of secondary amine bonds. The authors showed, as a proof-of-concept the printability of one of the synthesized HUDM, which was prepared with a non-biobased diamine (4,9-dioxa-1,12-dodecanediamine). Such HUDM, named DODA12-G, was mixed with ACMO and VP 3D printed into solid materials that displayed very good elastic modulus and tensile strength, even though the use of non-renewable ACMO and a non-renewable diamine negatively affected the sustainability of the formulation, which was characterized by a BCC% of 16.1% and a SFS of 8.2. Beyond the formation of the urethane backbone, the functionalization of these materials with photoreactive acrylate or methacrylate

Table 7 Sustainability indexes and mechanical properties of 3D printed photocurable formulations including photocurable non-isocyanate urethanes

Formulation	$BCC_{\%}$	SFS	Elastic modulus (GPa)	Elongation at break (%)	Tensile strength (MPa)	Ref.
DODA12-G 60% ACMO 40%	16.1%	8.2	3.16 ± 0.04	4.2 ± 1.4	81 ± 7	120
UDO_3-I 50% GPT 20% GDM 20%	63.5%	15.3	0.685 ± 0.044	1.60 ± 0.3	10.6 ± 1.9	20
UDO_3-I 50% GPT 5% GDM 5% I_2B_1 30%	88.1%	30.5	0.910 ± 0.025	4.0 ± 0.4	30.9 ± 2.7	

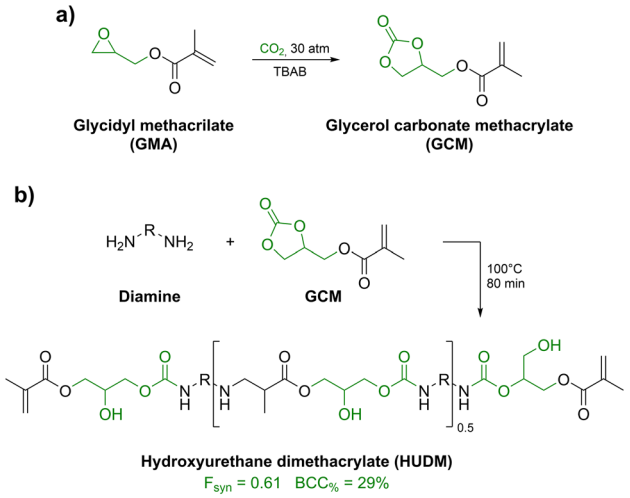

Scheme 7 Sustainable synthesis of glycerol carbonate methacrylate (a) and hydroxyurethanes dimethacrylate. The bioderived portion of each structure is depicted in green. TBAB = tetrabutylammonium bromide. Re-drawn from ref. 120.

groups introduces additional challenges. This issue can be addressed by replacing (meth)acrylic acid with sustainable itaconic acid. Itaconic acid, also known as 2-methylenesuccinic acid, is a photocurable dicarboxylic acid that was traditionally derived from the distillation of citric acid but is now produced through biomass fermentation.[122,123] Additionally, itaconic acid was recently recognized by the US Department of Energy as one of the top 12 building block chemicals due to its sustainable production process, low toxicity, and wide range of potential applications.[124,125] Similar to (meth)acrylates, itaconic acid can react with alcohols, including non-isocyanate urethanes to form liquid homodiesters or heterodiesters, which are suitable for efficient 3D printing.

In 2024, Carmenini *et al.* reported the synthesis of a fully biobased liquid urethanediol diitaconate (UDO_3-I), obtained by reacting biobased putrescine with CO_2-derived propylene carbonate, followed by the functionalization of the derived diurethanediol with monomethyl itaconoyl chloride.[20] The obtained UDO_3-I was successfully formulated with glycerol-derived acrylated reactive diluents (glycerol dimethacrylate, GDM, and glycerol propoxylate triacrylate, GPT) and a liquid itaconic acid bifunctional diester (1,4-butanediol bis(methyl-itaconate), I_2B_1). With this approach, and including 7.2 wt% of a castor oil-derived plasticizer in all formulations, the authors have been able to achieve elastic moduli as high as 1 GPa with very high $BCC_{\%}$, almost touching 90%. It is worth to point out that the use of itaconic acid chloride for the synthesis of UDO_3-I (F_{syn} = 0.18) indeed impacts on the sustainability of its synthetic process, but I_2B_1 (F_{syn} = 0.71) was instead prepared by tin-catalyzed solventless transesterification of dimethyl itaconate with 1,4-butanediol, suggesting how the sustainability of itaconic acid-based formulations could be further improved by exploiting the reactivity of both its carboxylic acid residues.

Thiol–ene systems. In thiol–ene photopolymerization, thiols and electron-rich alkenes undergo rapid addition polymerization *via* a radical-mediated step-growth mechanism, where photogenerated radicals initiate a sequence of alternating thiol–ene additions.[126,127] Unlike conventional free-radical (acrylate) polymerization, which is prone to oxygen inhibition and uncontrolled propagation, thiol–ene polymerization remains highly efficient even in the presence of oxygen, as thiyl radicals can readily regenerate.[128–130] Due to its distinct polymerization pathway, thiol–ene photopolymerization offers several advantages over traditional acrylate-based systems in terms of reactivity, network homogeneity, and sustainability. The step-growth nature of thiol–ene polymerization leads to uniform network formation with near-stoichiometric consumption of functional groups, significantly reducing shrinkage and improving mechanical stability. Additionally, thiol–ene systems exhibit rapid polymerization kinetics, often achieving full conversion within seconds under UV or visible-light irradiation, making them highly suitable for high-speed manufacturing processes. Beyond improved processing characteristics, thiol–ene photopolymerization also offers notable sustainability benefits.[131,132] Especially for application in photocurable resins for VP, where liquid formulations are required, sustainable alkenes are often selected amongst terpenes and terpenoids. Terpenes and terpenoids are a large and diverse class of naturally occurring organic compounds derived from isoprene units. They are widely found in plants, particularly in essential oils, resins, and secondary metabolites, and are responsible for many characteristic aromas and flavors.[133–135] These compounds play crucial roles in plant physiology and have extensive applications in pharmaceuticals, materials science, and sustainable chemistry.[136] Terpenes are hydrocarbons composed solely of carbon and hydrogen, whereas terpenoids, also known as isoprenoids, often contain additional functional groups such as hydroxyl, carbonyl, or ester groups, which enhance their chemical diversity and biological activity. Industrially, terpenes and terpenoids are used as bio-based solvents, adhesives or coatings and chemical modifications strategies are being explored to enhance their functionality for various industrial and biomedical applications, including photopolymerization-based 3D printing.[137] A summary of the formulations presented in this section, together with their sustainability indexes and mechanical properties is provided in Table 8.

A first example of this approach has been reported in 2019 by Weems *et al.*, who described the preparation of thiol–ene photocurable resins for VP using pure terpenes like limonene, geraniol, nerol or linalool as the alkenes and stoichiometric amounts of pentaerythritol tetrakis(3-mercapropropionate) (PETMP) as the crosslinking thiol.[138] Interestingly, the formulation included 1.5 wt% of carotenoids extracted from paprika (mainly capsanthin) as the radical stabilizer. The photocurable mixtures have demonstrated to be able to easily harden under UV irradiation, leading to solid 3D objects with mechanical properties strictly related to the nature of the used alkene. Limonene led to soft and highly deformable materials with

Table 8 Sustainability indexes and mechanical properties of 3D printed photocurable formulations including thiol–ene systems

Thiol	Ene	BCC%	SFS		Elastic modulus (MPa)	Elongation at break (%)	Tensile strength (MPa)	Ref.
PETMP 62%	Limonene 35%	54.2%	41.9		43.8	180	24.4	138
PETMP 59%	Linalool/Geraniol/Nerol 38%	54.3%	45.3		0.4/0.5/0.4	107/93/111	2.8/2.4/2.4	
PETMP 71%	Polymyrcene	44.7%	8.3		—	120%	2.6	140
PETMP 48%	PLcoM 41%	58.8%	21.4		~25[a]	~95[a]	~10[a]	141
					~250[b]	~20[b]	~22[b]	
	TTT 8.2%				~700[c]	~5[c]	~37[c]	
					>1000[d]	~2[d]	~53[d]	
PETMP 49%	Linalool 30%	61.7%	51.5		0.3 ± 0.3	118 ± 24	4.4 ± 1.5	142
PETMP 52%	Allyl-Lin 27%	49.4%	22.8		1.3 ± 0.7	84 ± 14	0.8 ± 0.1	
PETMP 40%	HDI-Lin 39%	54.0%	27.9		125 ± 34	16.5 ± 18	15.7 ± 7.4	
PETMP 38%	IPDI-Lin 41%	50.7%	25.7		77.5 ± 12.7	70 ± 10	9.6 ± 1.2	
PETMP 37%	MDI-Lin 42%	48.5%	25.4		12.6 ± 1.9	113 ± 15	3.0 ± 1.2	
TMPTMP 59%	PerIt 23% Limonene 12%	48.2%	27.7		56.9 ± 4.5[e]	220 ± 3[e]	10.6 ± 0.4[e]	143
TMPTMP 58%	PerIt 23% Linalool 13%	48.2%	29.1		6.3 ± 1.0[e]	158 ± 3[e]	3.3 ± 0.3[e]	
TMPTMP 58%	PerIt 23% Perillyl alcohol 13%	48.2%	29.0		5.0 ± 0.9[e]	101 ± 4[e]	2.7 ± 0.5[e]	
Thiocure 332 68%	TALG 28%	12.7%	1.6		8.92 ± 0.12	24.4 ± 5.1	2.06 ± 0.38	145
PETMP 46%	LGO.M1 53%	26.1%	7.7		12.3 ± 1.0	143 ± 5	8.2 ± 0.6	146
PETMP 43%	LGO.M2 55%	24.0%	7.2		7.4 ± 1.0	110 ± 9	5.0 ± 0.4	
PETMP 3.2%	AESO2 87% VDM 7.6%	80.9%	43.4		—	—	—	147
PETMP 57%	Allyl PAEL 5% TTT 38%	2.7%	0.5		1800 ± 30	3 ± 1.6	28.1 ± 3.1	148
PETMP 54%	Allyl PAEL 10% TTT 36%	5.4%	0.9		1100 ± 20	8 ± 1.6	21.4 ± 1.1	
PETMP 54% ISMP 5%	Allyl PAEL 5% TTT 36%	5.0%	1.3		1400 ± 40	6 ± 1.5	25.0 ± 4.2	
PETMP 52% ISMP 5%	Allyl PAEL 10% TTT 33%	7.7%	1.8		1000 ± 10	10 ± 1	19.1 ± 2.2	

[a] PLcoM made using 10% limonene and 90% myrcene. [b] PLcoM made using 25% limonene and 75% myrcene. [c] PLcoM made using 35% limonene and 65% myrcene. [d] PLcoM made using 100% limonene and 0% myrcene. [e] Not determined on 3D printed materials, but on photocured 2D films.

good tensile strength, while the thiol–ene polymerization of terpenoids proved to be less effective due to the presence of OH groups that stabilize radical species.[139] With respect to the sustainability indexes, the use of a large amounts of non-sustainable PETMP had a severe effect on the overall BCC% (54%). Nonetheless, the use of unmodified natural products in the formulations led to significantly high SFSs, which reached 42 and 45 for terpene- and terpenoid-based formulations, respectively.

The following year, the same group reported a second strategy following a similar approach, and using myrcene as the alkene and PETMP as the thiol.[140] In this work, the authors pre-polymerized myrcene by radical or anionic polymerization to afford polymyrcene, which was then formulated with the thiol and 3D printed into solid materials that displayed high elongation at break but low tensile strength. As thiol–ene resins require an accurate balancing of the stoichiometry between the thiol and the ene to achieve effective polymerization, the use of highly unsaturated hydrocarbons such as myrcene requires low mass fractions compared to the thiol, affecting the sustainability of the formulation. In fact, stoichiometric proportions were achieved using only 28 wt% of bio-based polymyrcene, and the harsh experimental conditions required for its synthesis (*e.g.* the use of strong oxidizers such as H_2O_2 or pyrophoric reagents such as *n*-BuLi) negatively impacted on its F_{syn}, leading to an overall SFS as low as 8.3. A similar strategy was once again proposed by the same group in 2022, who studied the effect of the ratio between myrcene and limonene in their polyolefinic copolymers on the properties of the 3D printed materials obtained upon their formulation with PTMPTA and 1,3,5-triallyl-1,3,5-triazine-2,4,6(1*H*,3*H*,5*H*)-trione (TTT).[141] Since myrcene and limonene are isomers, their relative content did not affect the SFS of the formulations, which was assessed to be around 21 for all formulations. Nonetheless, the authors demonstrated that increasing limonene content in the prepolymer can cause a significant improvement in mechanical properties, achieving tensile strengths as high as 50 MPa, apparently overcoming what was previously believed to be a limitation in the mechanical properties achievable with thiol–ene photocurable systems.

The same authors reported one more approach to thiol–ene-based photocurable resins for VP, by formulating PETMP

with linalool-derived diurethanes, compared to pristine linalool and Allyl-Lin, its allylic ether (Scheme 8).[142]

Diurethanes were prepared by reaction of 2 equivalents of linalool with either 1,6-hexanediisocyanate (HDI-Lin), isophorone diisocyanate (IPDI-Lin) or methylene diphenyl diisocyanate (MDI-Lin) under DBU catalysis. All formulations were composed of equimolar amounts of SH groups and C=C double bonds, and 20 wt% sustainable propylene carbonate was added as non-reactive diluent. By analysing the proposed syntheses for the linalool-based reactive diluents, it appears clear that the proposed linalool-derived components have reduced sustainability, either because of the use of allyl bromide (for Allyl-Lin) or because of isocyanates. However, SFS > 20 have been achieved for all formulations, mostly because of the presence of a significant amount of sustainable propylene carbonate, which contributes with a net of 16 SFS units in each formulation. The use of a non-reactive diluent severely affected the mechanical properties of the 3D printed materials, which are generally quite low and with a significant error that is symptomatic of high variability in the mechanical behaviour of the prepared materials. A very sustainable approach was reported recently by Chiaradia *et al.*, who synthesize the monoester of itaconic acid with perillyl alcohol (PerIt) *via* enzyme catalysis to produce a fully biobased trifunctional component for thiol–ene photoresins.[143] Interestingly, itaconic acid had previously demonstrated to be able to react both with thiols and with another itaconic acid residue, leading to double thiol–ene and polyitaconate networks during radical polymerization processes.[144] PerIt was then formulated with trimethylolpropane tris(3-mercaptopropionate) (TMPTMP) and either perillyl alcohol, linalool or limonene as reactive diluents to achieve solid materials upon photopolymerization during 3D printing. The mechanical properties of the obtained materials are in line with previously presented data, with limonene-containing formulations displaying better mechanical properties due to the absence of the free OH group of linalool and perillyl alcohol that interferes with the formation of radical species. Furthermore, the presented approach displays high sustainability indexes, with SFSs around 30 even though their BCC% is limited to below 50% due to the required presence of equimolar amounts of the non-biobased thiol.

In addition to terpenes, which naturally carry the unsaturations required for thiol–ene photopolymerization, many authors explored the possibility of functionalizing hydroxylated biobased building blocks with allyl bromide, forming their corresponding allyl ethers. This has been demonstrated, for example, by Porwal *et al.* in 2023, who described the allylation of cellulose-derived levoglucosan into triallyl levoglucosan (TALG).[145] The prepared TALG was then formulated with a stoichiometric amount of ethoxylated trimethylolpropane tris(3-mercaptopropionate) (Thiocure 332) and 13 wt% fumed silica as a rheology modifier, and 3D printed using a custom UV-assisted direct ink writing setup. The 3D printed materials displayed hydrogel-like mechanical properties with low elastic modulus and tensile strength, but they were able to fully degrade in 1 M NaOH solution in less than 48 hours due to alkaline hydrolysis of the ester bonds of the thiol crosslinker.

This was taken into account for the evaluation of the F_{EoI} of the formulation, but the harsh conditions required for the synthesis of TALG, the low atom economy of its production and the limited biobased content of the formulation (BCC% = 12.7%) reveal the poor sustainability of the presented approach (SFS = 1.6). The following year, Pezzana *et al.* reported the esterification of (1*R*,2*S*,5*R*)-6,8-dioxabicyclo[3.2.1]

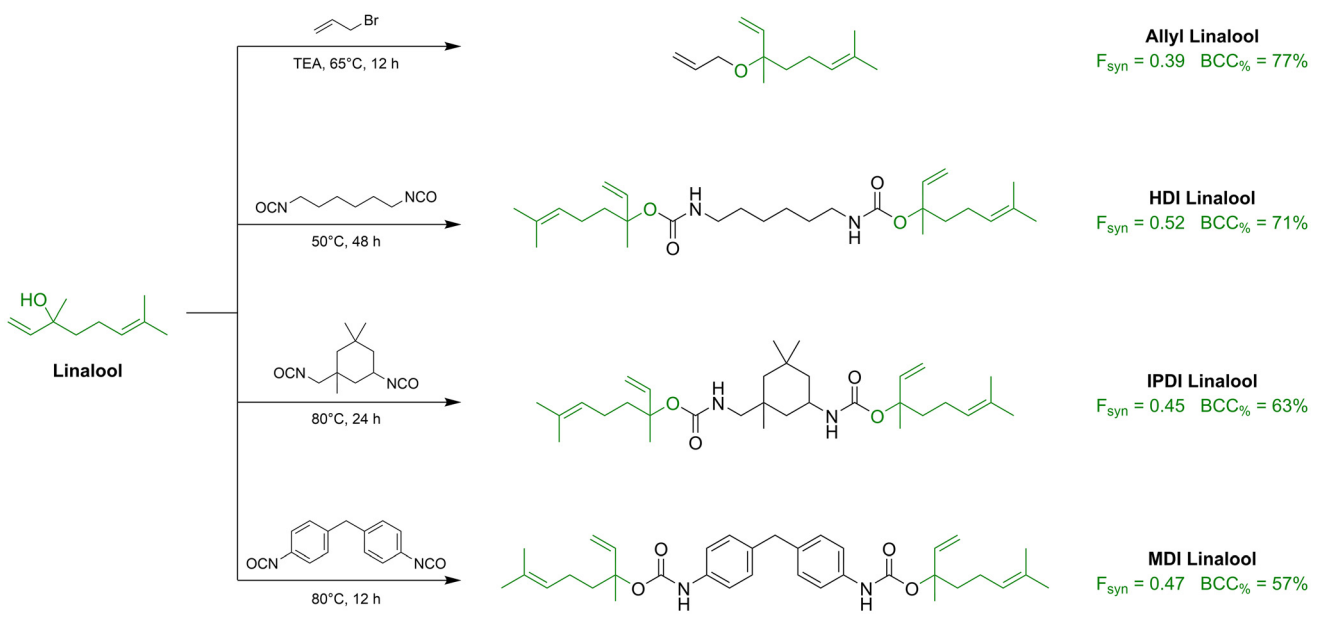

Scheme 8 Synthesis of linalool-based allyl ether and diurethanes. The bioderived portion of each structure is depicted in green. Re-drawn from ref. 142.

octane-2,4-diol (LGOL-OH), obtained from levoglucosenone prepared by cellulose pyrolysis, with either 3-butenoic or 4-pentanoic acid (named LGO.M1 and LGO.M2, respectively).[146] These partially biobased alkenes were then formulated with PETMP and 3D printed to afford once again solid photopolymers degradable in alkaline environments. Nonetheless, the low atom economy of the employed Steglich esterification combined with the use of halogenated solvents for the synthesis of LGO.M1 and LGO.M2, and their low biobased carbon contents, led to the obtainment of resins with low sustainability indexes (BMC% = 26% and 24%, SFS = 7.7 and 7.2 for LGO.M1 and LGO.M2, respectively). As it is common for thiol–ene formulations, soft 3D printed materials with low elastic moduli and high deformation at break were obtained with this approach (12.3 and 7.4 MPa, respectively).

A mixed acrylate/thiol–ene approach has been reported by Sereikaite in 2022, who described the formulation of acrylated epoxidized soybean oil (AESO) with vanillin dimethacrylate (VDM) and PETMP.[147] However, in the reported approach a very small amount of thiol was used (3.2 wt%), leading to material properties and sustainability indexes that are comparable to those of previously described vegetable oil-based approaches (BCC% = 81%, SFS = 43), rather than those of thiol–ene systems. Furthermore, mechanical properties of 3D printed materials were not evaluated.

Finally, Pal *et al.* recently released a work where they reported the synthesis of acryloyl ethyl lactate and acryloyl allyl lactate copolymers (allyl PAEL) and thiolated isosorbide (ISMP), which were formulated with TTT and PETMP to achieve photocurable formulations for VP that were easily degradable by alkaline hydrolysis (Scheme 9).[148] However, due to the high number of synthetic steps required for the preparation of the partially biobased thiol (ISMP) and ene (allyl PAEL), their synthetic factor F_{syn} is quite low (0.35 and 0.20, respectively), even if their biobased carbon content is around 50% for both compounds. Moreover, very small amounts of partially biobased monomers have been used in the formulations, which were mainly composed of TTT and PETMP, which granted the good mechanical properties measured by the authors. For this reason, all formulations were characterized by SFS below 2 and BCC% below 10%, making the sustainability of the proposed approach almost negligible. However, this work represents an interesting use of non-photocurable biobased ethyl lactate into photoreactive components, opening for the possibility to adapt the proposed strategy in more sustainable fashions.

To summarize, the analysis of the recent literature of thiol–ene networks demonstrated that good sustainability indexes can be achieved using unmodified terpenes, but also that the mechanical performances of thiol–ene 3D printed photopolymers are still far from those of acrylate-based systems. However, when targeting soft materials with high deformability, thiol–ene systems have proven great potential. Nonetheless, the sustainability of such formulations could be greatly improved by developing sustainable and biobased thiol crosslinkers which have proven to be able to efficiently crosslink under photoradical conditions, such as cysteine derivatives.[149–151]

Photocurable macromolecules

Photocurable macromolecules in liquid formulations for VP 3D printing represent an advanced class of materials designed to overcome the limitations of conventional low-molecular-weight acrylate or thiol–ene systems. Unlike small monomers, these pre-polymerized macromolecules incorporate photocurable moieties along their polymer backbone, allowing for controlled crosslinking upon exposure to light. Their inclusion in resin formulations significantly influences rheological behaviour, curing kinetics, and final material properties. One of the primary advantages of using pre-polymerized macromolecules is the ability to tailor viscosity while maintaining a high degree of reactivity. Since VP 3D printing relies on precise light penetration and rapid curing, the balance between resin flowability and polymerization rate is critical. For this reason, macromolecular building blocks used in VP formulations are typically designed with relatively low molecular weights, often in the range of several hundred to a few thousand g mol^{-1}, to ensure the viscosity remains compatible with high-resolution layer-by-layer processing. Excessively high molecular weight polymers increase resin viscosity beyond practical limits, hindering recoating, light penetration, and layer fidelity.[152] Additionally, lower molecular weight macromers provide a higher density of reactive functionalities per unit mass, enhancing crosslinking efficiency and mechanical homogeneity in

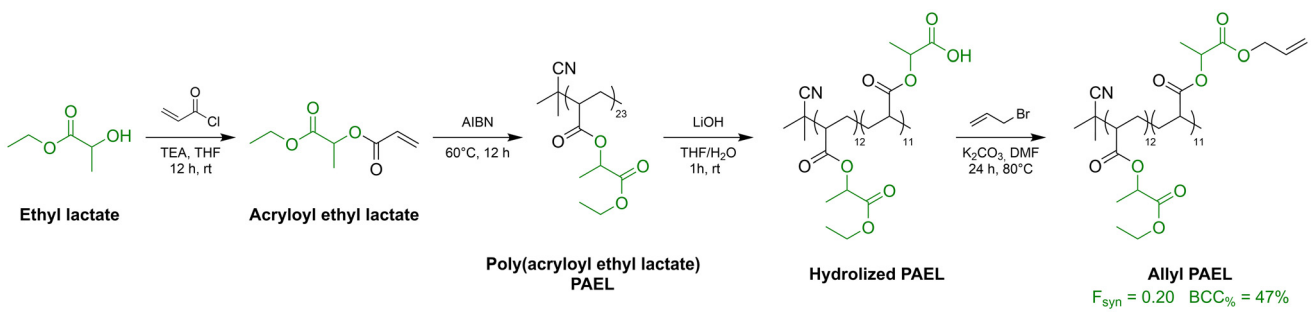

Scheme 9 Synthesis of acryloyl ethyl lactate and acryloyl allyl lactate copolymer Allyl PAEL. The bioderived portion of each structure is depicted in green. Re-drawn from ref. 148.

the printed object. Low-viscosity monomers often lead to brittle networks with high volumetric shrinkage, whereas macromolecular precursors enable the formulation of resins with reduced shrinkage, improved toughness, and enhanced mechanical stability.[153] This is particularly relevant for applications requiring structural integrity, such as biomedical implants or functional components in engineering.[154] Moreover, their reduced volatility and lower toxicity contribute to safer handling and processing conditions.

Unsaturated polyesters. Unsaturated polyesters (UPs) are emerging as promising components for VP formulations due to their versatile structural properties, photopolymerizability, and potential for incorporating biobased components. These polyesters are synthesized through the polycondensation of unsaturated dicarboxylic acids, such as itaconic acid, with biobased diols like ethylene glycol or 1,4-butanediol, amongst others. The presence of unsaturated bonds in their backbone enables radical crosslinking under UV or visible light exposure, forming durable polymer networks suitable for 3D printing applications. In particular, the double carboxylic acid functionalities of itaconic acid have allowed for its polymerization with biobased diols, to produce fully biobased liquid UPs able to form a secondary polymeric network by photoradical polymerization during 3D printing. However, their relatively high viscosity can hinder printability, requiring the addition of reactive diluents to achieve optimal flow properties. Whit this approach, when highly biobased reactive diluents are selected, resin formulations with very high sustainability indexes can be achieved. A summary of the formulations presented in this section, together with their sustainability indexes and mechanical properties is provided in Table 9.

A first example of this approach was reported in 2020 by Maturi *et al.*, who reported the synthesis of poly(propanediyl-*co*-glyceryl itaconate-*co*-vanillate), PPGIV, by thermal polycondensation of itaconic acid with vanillic acid, 1,3-propanediol and glycerol.[155] The obtained polyester was then formulated with HEMA-esters of itaconic and citric acid (named BHI and THC), and 3D printed into high resolution 3D objects with good sustainability indexes (BCC% = 72% and SFS = 39). This approach opened for the possibility of the development of new biobased diols and diacids to be polymerized with itaconic acid introducing additional chemical functionalities, with the aim of improving the processability of the resins and the mechanical properties of their 3D printed materials. For example, itaconic acid was polymerized with sustainable diamidodiols prepared by ring-opening ε-caprolactone on both sides of putrescine, a sustainable aliphatic diamine, leading to the obtainment of a fully biobased poly(ester amide), PEA.[156] A similar formulation approach based on BHI and THC has allowed to achieve 3D printed materials with significantly higher deformation at break, thanks to the presence of intermolecular interaction amongst the amide linkages in the UP structure. This approach allowed to achieve substantially high sustainability indexes, with an SFS close to 47. In a further work, partially biobased thioether-polyols have been synthetized by thiol–ene addition of 2-mercaptoethanol to the unsaturations of naturally occurring terpenes (such as limonene, linalool and geraniol), which have been once again polymerized with itaconic acid with or without the addition of biobased linear diols (Scheme 10).[19]

The obtained poly(ester thioether)s were then formulated with the itaconic acid-based bifunctional reactive diluent I_2B_1, leading to the obtainment of the fist (meth)acrylate-free formulation for VP, characterized by biobased carbon contents surpassing 85% and SFSs above 41. Finally, the same authors reported the synthesis of a sustainable diester by Diels–Alder cycloaddition of dimethyl itaconate on the conjugated unsaturation of myrcene, which was polymerized with dimethyl itaconate and biobased 1,4-butanediol to achieve, once again, fully biobased UPs for VP applications (named IBM).[18] By tailoring the macromolecular features IBM (such as molecular weight and ratio between the different monomers) and its for-

Table 9 Sustainability indexes and mechanical properties of 3D printed photocurable formulations including unsaturated polyesters

Unsaturated polyester	Reactive diluents	BCC%	SFS		Elastic modulus (MPa)	Elongation at break (%)	Tensile strength (MPa)	Ref.
PPGIV 48.5%	BHI 24% THC 24%	72.2%	38.9	🟡	62 ± 5	18.0 ± 2.9	5.4 ± 0.7	155
PEA 48.5%	BHI 25% THC 8% HEMA 7.5%	77.1%	46.8	🟢	84.7 ± 5.9	34.2 ± 2.4	5.4 ± 0.6	156
IA-Lim 60%	I_2B_1 28.7%	85.7%	41.8	🟡	218 ± 26	6.9 ± 0.8	10.2 ± 0.5	19
IA-Lin 60%	I_2B_1 28.7%	85.9%	42.0	🟡	122 ± 10	7.3 ± 1.3	6.2 ± 0.6	
IA-Ger 60%	I_2B_1 28.7%	91.5%	43.6	🟡	171 ± 11	7.2 ± 0.9	9.0 ± 0.6	
IBM 70%	BHDD 17% L-HEMA 10%	79.1%	35.2	🟡	19.7 ± 1.0	17.3 ± 2.1	2.78 ± 0.41	18
IBM 50%	I_2B_1 20% iPr-MONO 20%	96.5%	43.4	🟡	370 ± 35	6.36 ± 0.87	18.7 ± 1.9	
PE-SebA 50%	ACMO 47%	50.9%	16.6	🟠	22.3 ± 6.1	59.2 ± 3.7	4.6 ± 0.4	157
PE-FDCA-DoDO 50%	IBOMA 47%	82.4%	29.7	🟠	137 ± 19	24.8 ± 3.8	7.3 ± 1.3	
PE-SA-DoDO 50%	IBOMA 47%	82.4%	29.5	🟠	71 ± 7	25.2 ± 1.2	1.8 ± 0.2	
MASAPA 60%	PEGDA 40%	15.9%	4.2	🔴	—	20[a]	0.44[a]	161

[a] From compressive testing.

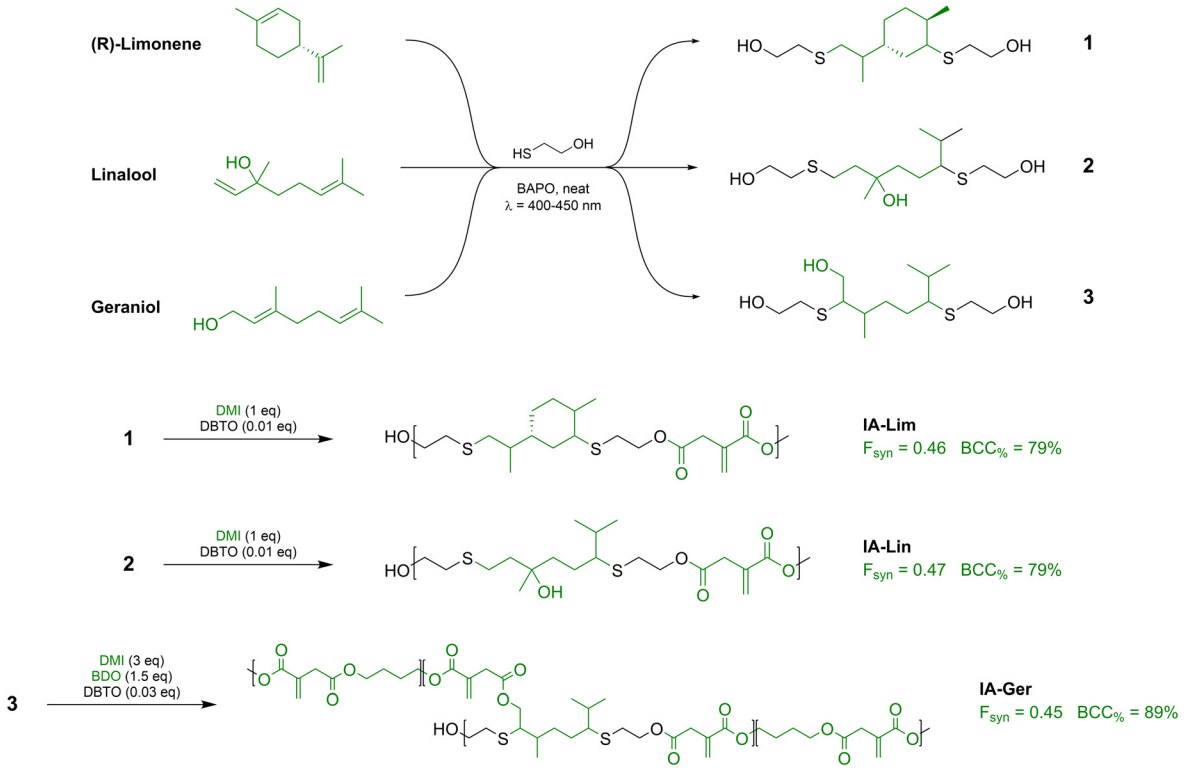

Scheme 10 Synthesis of thioether polyols by thiol–ene photoradical addition of 2-mercaptoethanol on the unsaturation of terpenes (top) and their polymerization with itaconic acid to achieve photocurable poly(ester thioether)s. The bioderived portion of each structure is depicted in green. DMI = dimethyl itaconate, DBTO = dibutyltin(IV) oxide, BDO = 1,4-butanediol. Re-drawn from ref. 19.

mulation with sustainable reactive diluents, a wide range of mechanical properties were achieved, with elastic moduli ranging from 6.8 to 504 MPa. Furthermore, many of the presented resins were characterized by the highest $BCC_{\%}$ ever reported so far (96.5%), as all the resins components were fully biobased, except for the photoinitiating system.

Similar approaches have been recently reported in a series of works from Papadopoulos *et al.*, who analysed the effects of the inclusion of different secondary acids in itaconic acid-based polyesters on the properties of their 3D printed formulations with (meth)acrylate-based reactive diluents.[157–160] However, this strategy led to materials with lower sustainability (SFS = 17–30) and poorer mechanical performances.

As an alternative strategy, Barker *et al.*, introduced fumaric acid as a new photocurable diester for applications in VP formulations.[161] Due to its unsaturated dicarboxylate structure, fumaric acid can participate in free-radical polymerization, even though it has lower reactivity compared to acrylic, methacrylic and itaconic acid due to steric and electronic effects.[162–164] With this concept in mind, the authors of this work prepared a copolyester of maleic acid, phthalic acid and succinic acid with diethyleneglycol using the corresponding cyclic anhydrides (MASAPA), followed by amine-catalysed isomerization of the maleic acid units into fumaric acid. The polyester was then formulated with PEGDA and 3D printed into solid high-resolution structures. Even though the sustainability of the presented approach is low due to the use of non-biobased co-monomers in the polyester chain and of non-biobased PEGDA as the reactive diluent (BCC% = 16%, SFS = 4), this work suggests the potential of biobased fumaric acid as photocurable building block in sustainable formulations for VP.

Itaconic acid polyesters have also been recently grafted onto graphene oxide surface to produce 3D printed photopolymer composites, improving its dispersibility and mechanical matrix-to-filler stress transfer through a sustainable photocurable polymeric coating.[165]

Overall, biobased unsaturated polyesters, mainly represented by itaconic acid polyesters, signify a versatile approach to produce 3D-printable formulations with high biobased contents (BCC% up to 96.5%) and high overall sustainability (SFS up to 46). Nonetheless, their syntheses conditions are indeed improvable, as they commonly require long reaction times and high temperatures, affecting the sustainability of their formulations due to high energy consumption. Moreover, their high viscosity prevents them from being formulated at concentrations above 50–60 wt%, thus limiting the achievable sustainability when formulated with (meth)acrylated reactive diluents, and the achieved mechanical properties are generally good but not outstanding.

Functionalized synthetic polymers. Terminal or lateral chemical functionalities of synthetic polymers have been often exploited to introduce photocurable groups in their structures,

with the aim of performing a secondary radical crosslinking. This is usually done to achieve photocurable formulations that can lead to VP 3D printed materials that possess the mechanical, thermal or functional properties of the functionalized synthetic polymer they contain. One of these polymers is indeed polycaprolactone (PCL). PCL is a biodegradable, semicrystalline aliphatic polyester known for its good mechanical properties, biocompatibility, and ease of chemical modification.[166,167] Its hydroxyl end-groups provide reactive sites for functionalization, allowing the incorporation of photocurable moieties that enable its use in VP, where it can be processed into high-resolution structures with tunable mechanical properties and degradation rates. Its slow hydrolytic degradation under physiological conditions makes it particularly attractive for biomedical applications, including tissue engineering scaffolds and controlled drug delivery systems.[168] Furthermore, it is synthesized by ring-opening polymerization of ε-caprolactone (CL), whose sustainable synthesis from biobased 6-hydroxyhexanoic acid is well consolidated in the scientific literature and is currently being implemented at the industrial scale.[169,170]

A summary of the formulations presented in this section, together with their sustainability indexes and mechanical properties is provided in Table 10.

A first example of its use for 3D-printable photocurable resins dates back to 2011, when Elomaa and co-workers reported the synthesis of low molecular weight three-armed polycaprolactone which was further functionalized at its chain termini with methacrylic acid using methacrylic anhydride and triethylamine in DCM.[171] Interestingly, no reactive diluents were used, and the obtained PCL-MA_3 macromers (M_n = 1.5–6 kDa) were only added to the photoinitiating system and heated to around 45 °C to ensure the rheology required for 3D printing.

The use of PCL as the only photocurable component led to fully biocompatible 3D printed materials, able to host fibroblasts due to its interconnected pore structure. Nonetheless, the synthetic strategy involved using halogenated solvents and hazardous compounds, thus reducing the F_{syn} of the macromer to 0.34. However, the biodegradability of the 3D printed material was taken into account in the evaluation of F_{EoL}, which led to an SFS of 45. A few years later, the same authors reported an analogous strategy, where CL was instead copolymerized with an L-alanine-derived depsipeptide (3-methylmorpholine,2-5-dione, MMD), leading to three-armed poly(depsipeptide-*co*-caprolactone) copolymers, named PDPCL (Scheme 11).[172]

By adjusting the relative amount of MMD to CL, the authors were able to prepare different copolymers with 0%, 5%, and 10% molar depsipeptide content, named PCL, PDP5CL, and PDP10CL. Analogously to their previous work, the so obtained poly(ester amide)s were functionalized at their chain ends with methacrylic acid units, leading to PCL-MA_3, PDP5CL-MA_3, and PDP10CL-MA_3 photocurable copolymers. As before, the photocurable macromers were formulated with the photoinitiator with no additional reactive diluents. Compared

Table 10 Sustainability indexes and mechanical properties of 3D printed photocurable formulations including functionalized synthetic polymers

Synthetic polymer	Reactive diluents	BCC%	SFS		Elastic modulus (MPa)	Elongation at break (%)	Tensile strength (MPa)	Ref.
PCL-MA_3 95%	—	75.8%	44.7		15.4 ± 0.7	19.3 ± 0.5	2.55 ± 0.12	171
PCL-MA_3 97%	—	76.2%	60.2		60	21[a]	25[a]	172
PDP5CL-MA_3 97%	—	75.7%	11.1		75	23[a]	40[a]	
PDP10CL-MA_3 97%	—	74.4%	10.6		110	40[a]	95[a]	
PCL-OCON-MA 96%	—	94.0%	44.4		100–230[b]	70–160[b]	—	173
Allyl-PCL-Allyl 38%	PETMP 1.2%	38.6%	8.7		148 ± 24	483 ± 118	11.1 ± 2.8	174
PCL-$Allyl_3$ 48%	PETMP 2.2%	46.6%	10.6		78 ± 15	238 ± 68	6.9 ± 0.9	
PCL-$Allyl_4$ 47%	PETMP 3.0%	45.8%	10.3		46 ± 18	76 ± 36	4.6 ± 1.4	
SH(PCI) 40%	Me-MONO 20% I2B1 20% PETA 10%	86.6%	33.2		157 ± 4	10.8 ± 1.1	10.7 ± 0.5	176
SH(PCI) 50%	DOIT 20% OligoPDI 20%	96.6%	36.7		22.1 ± 2.0	20.0 ± 2.9	3.6 ± 0.4	
SH(PCI) 72%	GPT 9% GDM 9%	82.8%	23.6		41.9 ± 1.7	18.4 ± 2.4	5.2 ± 0.5	
PCTAc 69%	EOEOEA 30%	26.5%	4.0		1.2 ± 0.0	78.2 ± 10.4	0.7 ± 0.1	177
PCL-MMA 1 : 1 99%	—	47.1%	12.6		—	—	107 ± 3[c]	180
PCL-MMA 2 : 1 99%	—	56.5%	16.4		—	—	100[c]	
PCL-MMA 3 : 199%	—	62.1%	19.0		—	—	90[c]	
PCL-MMA 4 : 1 99%	—	71.1%	23.6		—	—	83 ± 3[c]	
PvCHC-PDL-PvCHC 67%	TMPTMP 3%	82.0%	40.4		0.120 ± 0.049	113 ± 10	0.145 ± 0.015	181
PvCHC-PDL-PvCHC 66%	TMPE3TMP 5%	80.4%	39.5		0.093 ± 0.009	115 ± 12	0.139 ± 0.006	
PvCHC-PDL-PvCHC 63%	TMPE7TMP 9%	77.4%	37.8		0.069 ± 0.028	115 ± 12	0.127 ± 0.016	

[a] Determined at yield, not at break. [b] Varies in the reported range depending on the methacrylation degree of the PCL macromer. [c] Flexural strength.

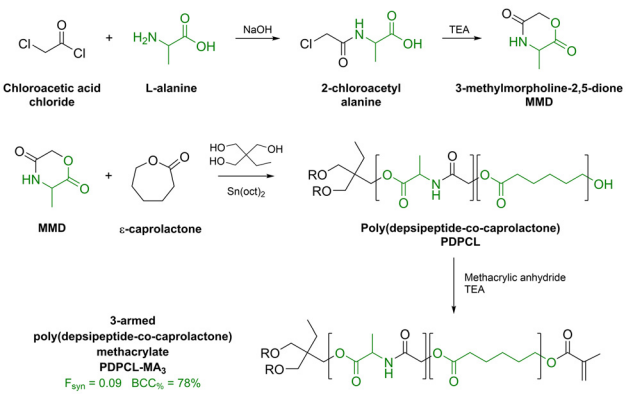

Scheme 11 Synthesis of photocurable PDPCL-MA3. The bioderived portion of each structure is depicted in green. TEA = triethylamine, Sn (oct)2 = tin(II) bis(2-ethylhexanoate). Re-drawn from ref. 172.

to their previous work, the macromers were characterized by lower molecular weight (around 700 Da), and they could be printed at room temperature, leading to fully biocompatible materials with mechanical properties enhanced relative to depsipeptide-free analogues also thanks to the higher density of methacrylate groups that derives from the lower molecular weight of the macromers. Nonetheless, the use of hazardous solvents and reagents in the preparation of the MMD monomer as well as the low atom economy of such chemical reactions severely affected the synthetic factor F_{syn} of the macromers, which was as low as 0.09 in both depsipeptide-containing polymers.

A similar reactive diluent-free approach was presented in 2016 by Zarek *et al.*, who functionalized PCL with higher molecular weight (around 10 kDa) using isocyanatoethyl methacrylate, to achieve a photocurable macromer for the 3D printing of shape-memory materials.[173] Once again, PCL was formulated with the photoinitiator and printed with no added reactive diluent, but the high molecular weight employed required higher printing temperatures, around 90 °C. The non-biobased nature of the photocurable pending group became negligible when measured in proportion to the long biobased PCL chain, but its chemical modification conditions, involving dioxane and isocyanates, severely impacted on its F_{syn}. Nonetheless, this approach allowed to produce functional PCL-based photocured materials with very high biobased mass (BCC% = 94%) and good sustainability index (SFS = 44), mostly increased by their biodegradability. However, the complexity of the system required for its 3D printing should be also considered when evaluating the overall sustainability of this approach.

A different approach was recently reported by Quaak *et al.*, who prepared telechelic and star-shaped PCL which were functionalized at their chain ends with allyl isocyanate, with the aim of introducing the unsaturations required for thiol–ene photopolymerization.[174] Due to the high molecular weight of the synthetized PCLs (around 8 kDa), the formulation required very low amounts of thiol for its photocrosslinking, but the formulations contained high amount of non-sustainable and non-reactive *N*-methyl pyrrolidone (NMP) to dissolve the polymer, thus enabling 3D printing at room temperature. This, together with the negative impact of the isocyanate-based PCL modification strategy and the absence of biodegradability studies, heavily affected the sustainability of the formulations, which displayed $BCC_{\%}$ in the 36%–48% range and SFSs from 8 to 11. Nonetheless, the materials with tensile strength up to 10.7 MPa and elongation of 20%, exceeding benchmarks for similar systems. The same year, the authors of this work reported a further application of said formulations for volumetric 3D printing.[175]

A further functionalization approach for PCL has been reported by Spanu *et al.*, who designed the ring-opening polymerization of CL on biobased sorbitol, and the following one-pot functionalization of the hydroxylated chain termini with itaconic acid to produce fully biobased sorbitol hexa(pentacaprolactone) methylitaconate, SH(PCI).[176] In addition, new itaconic acid based reactive diluents have been presented in this work, including methyl (4-hydroxybutyl) itaconate (Me-MONO), dodecyl methyl itaconate (DOIT) and oligo(dodecanedioyl itaconate) (Oligo PDI). The itaconic acid-based macromer was a liquid at room temperature and could be formulated and 3D printed with itaconated and (meth)acrylated reactive diluents at loadings of up to 72 wt%. Despite achieving high biobased content values (BCC% up to 97%), the use of monomethyl itaconoyl chloride, prepared by chlorination of the corresponding carboxylic acid with oxalyl chloride, significantly reduced the synthetic factor F_{syn} (0.30), thereby limiting the overall SFS of the formulations to below 40. Nonetheless, SH(PCI) has proven to be an efficient biobased macromer for acrylate-based formulations, enhancing their sustainability while yielding softer and more deformable materials.

In a further work, CL was co-polymerized with trimethylene carbonate (TMC) using diethylene glycol as the initiator, leading to poly(caprolactone-*co*-trimethylene carbonate) random copolymer diols (PCT) that were further functionalized on both sides with acrylated L-lysine isocyanate, leading to photocurable acrylated PCT (PCTAc).[177] From the sustainability perspective, TMC is not considered biobased since its synthesis requires stoichiometric amounts of hazardous and oil-based ethyl chloroformate, even though its production from biobased 1,3-propanediol has been reported,. Another synthetic strategy involves the reaction of CO_2 with oxetane, but these processes are still far from being considered sustainable and biobased.[178,179] Once formulated with 30 wt% of 2-(2-ethoxy-ethoxy) ethyl acrylate (EOEOEA), PCTAc led to 3D printable formulations with generally low sustainability (BCC% = 27% and SFS = 4), due to the use of a non-sustainable reactive diluent and to the low sustainability of the synthetic steps required for the synthesis of the photocurable polymer, which involved the use of acrylates, isocyanates and halogenated solvents. Nonetheless, the prepared materials displayed remarkable biocompatibility, but the reported mechanical properties (Young's modulus of 1.2 MPa and tensile strength of 0.7 MPa) are far from being competitive.

A different yet fascinating strategy for including sustainable polymers in photocurable resins for VP has been recently

reported by Figalla *et al.*[180] The authors of this work efficiently depolymerized poly(lactic acid) waste using varying amounts of propylene glycol (PG) under titanium(IV) butoxide catalysis, and the obtained diols were efficiently methacrylated using methacrylic anhydride, and 3D printed after the addition of the photoinitiator only (Scheme 12). When analysing the sustainability of this approach, it appears clear that when the PLA-to-PG ratio is increased from 1 : 1 to 1 : 4, the sustainability increases too, since less methacrylate groups are required per gram of PLA. However, the harsh experimental conditions required for PLA depolymerization, as well as the use of methacrylic anhydride which affects the atom economy of the preparation, prevented F_{syn} to grow significantly, leading to overall sustainability scores ranging from 13 to 24.

Nonetheless, the materials displayed good mechanical performances, as it is suggested by the presented flexural strength data. In all the examples discussed up to this point, photocurable groups were introduced at the chain termini of synthetic polymers. However, in some cases photopolymerization can take place by exploiting pending functionalities that can react with the opportune reactive diluents to achieve crosslinked photopolymer systems during the 3D printing process. This strategy has been exploited by Poon *et al.* in 2024, who reported the block copolymerization of biobased poly(ε-decalactone) with vinylcyclohexene oxide and CO_2, leading to linear poly(ester-*co*-carbonate) with pending vinyl groups (PvCHC-PDL-PvCHC) that were exploited for thiol–ene photopolymerization.[181] After formulation with stoichiometric amounts of trifunctional thiols such as TMPTMP and its ethoxylated variants $TMPE_3TMP$ and $TMPE_7TMP$ (with 3 and 7 ethylene glycol units, respectively) and the addition of 30 wt% of ethyl acetate, the authors were able to achieve 3D printable formulations with high sustainability indexes (BCC% from 77% to 83% and SFS from 37 to 41). However, a high contribution to the resins' sustainability is given by the addition of biobased ethyl acetate in high concentrations, whose evaporation after 3D printing led to materials with extremely low tensile strengths and elastic moduli (around 100 kPa in all cases).

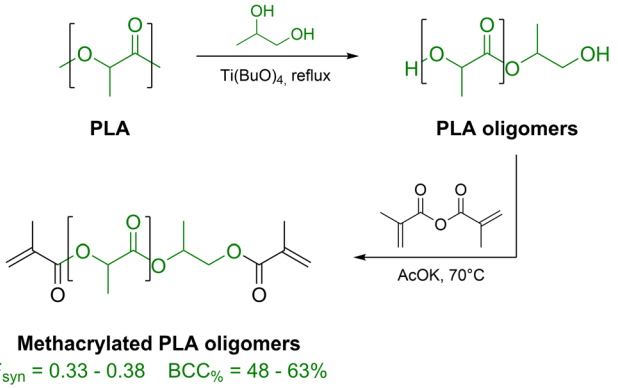

Scheme 12 Alcoholysis of waste PLA and functionalization with methacrylic acid residues, for applications in VP. The bioderived portion of each structure is depicted in green. Re-drawn from ref. 180.

To summarize, the recent literature has shown that the functionalization of synthetic polymers such as PCL with photocurable functionalities allows for the fabrication of biodegradable and biocompatible materials *via* VP 3D printing, which generally leads to non-biodegradable polyacrylate networks. This is mainly due to low concentration of photocurable groups in their resins, which causes the final photopolymers to mostly resemble the physical–chemical properties of the synthetic polymers formulated in the photocurable mixture. Nonetheless, the lower concentration of photocurable groups often reflects in poorer mechanical properties or the requirement of harsh conditions during the printing process if the use of reactive diluents is avoided.

Functionalized natural polymers. Natural polymers, including polysaccharides, polypeptides and polyphenols, have emerged as promising candidates in materials science due to their intrinsic biocompatibility, biodegradability, and sustainable sourcing.[182–184] However, their direct use in advanced manufacturing techniques like vat photopolymerization (VP) 3D printing is often hindered by their lack of photocurable functionalities and poor solubility in conventional resin systems. To overcome these limitations, chemical modification strategies have been employed to introduce photoreactive groups, such as (meth)acrylates and vinyl groups, by leveraging their abundant hydroxyl, amine, and carboxyl functional groups. These modifications enhance their processability while retaining their unique physicochemical properties, such as hydrophilicity, bioactivity, and mechanical tunability. Functionalized natural polymers have been widely explored for biomedical applications, including tissue engineering scaffolds, drug delivery systems, and bioinks for 3D bioprinting.[185,186] Beyond biomedical applications, their use in sustainable photopolymer formulations aligns with the growing demand for greener alternatives in additive manufacturing, enabling the development of high-performance, renewable-based materials. Many works describe the modification of biomacromolecules to use them in low concentration (below 10 wt%) as reinforcement filler for acrylate-based photopolymer composites.[187,188]. It must be noted that, due to the rheological requirements of liquid resins for VP 3D printing, many natural polymer-containing formulations reported in the literature cannot be processed with this technology and require different 3D printing strategies such as direct ink writing (DIW). These studies will not be included in this review, as we will only focus on formulations for VP 3D printing where the biopolymers participate substantially in the formation of the photopolymer, in concentrations of at least 10% of the total resin dry mass (thus excluding water in the case of 3D printed hydrogels). A summary of the formulations presented in this section, together with their sustainability indexes and mechanical properties is provided in Table 11.

As the most common biopolymer on earth, cellulose and its chemically modified variants have been widely used for producing sustainable and biocompatible 3D printable formulations for VP. Cellulose in its native form is highly crystalline and insoluble in most organic mixtures, and its mechanical strength has been widely exploited to produce reinforced

Table 11 Sustainability indexes and mechanical properties of 3D printed photocurable formulations and hydrogels including functionalized natural polymers

Natural Polymer	Reactive diluents	BCC%	SFS	Elastic modulus (MPa)	Elongation at break (%)	Tensile strength (MPa)	Ref.
Polysaccharides							
F-MCC 5%	AESO2 46.5% HEA 46.5%	70.5%	30.3	39.64	—	4.56	191
F-MCC 13%	AESO2 42.5% HEA 42.5%	70.8%	28.9	76.35	—	5.94	
F-MCC 20%	AESO2 39% HEA 39%	71.0%	27.6	298.24	—	10.30	
mCMC 98%	—	64.7%	37.0	—	—	0.044	195
mCMC 65.8% mNC 32.9%	—	76.1%	50.8	—	—	0.038	
CHI-MA 50%	PEGDA 50%	40.4%	15.3	0.049 ± 0.005	—	—	196
Pul-NB 89.3%	DTT 9.8%	63.7%	42.7	0.0013[a]	—	0.005[a]	197
Nor-HA_{CA} 84.4%	DTT 8.4%	67.5%	19.2	0.06[a]	—	—	198
SA-CSA 49.5% SA-NOR 49.5%	—	89.7%	26.5	0.044 ± 0.003[a]	27	0.019	199
GGMMA 97.5%	—	89.5%	47.8	—	90	0.090	200
Polypeptides							
Silk-GMA 99.8%	—	89.6%	18.0	0.015 ± 0.003	124.2 ± 41	0.075 ± 0.008	201
MA-BSA 75%	PEGDA 25%	67.1%	24.8	473[a]	75[a]	130[a]	203
Gel-NB 46.7%	PEG-SH4 46.7% PEG-NB4 3.9%	21.0%	9.0	—	—	—	204
Lignins							
Lignin-M 15%	SR494 34% Ebecryl 8210 34% Genomer 1122 17%	12.5%	6.2	370 ± 20	7.6 ± 1	15 ± 8	206
UALS 35%	ACMO 51% ACC 12%	31%	4.3	1.53 ± 0.05	47.1 ± 4.7	0.65 ± 0.057	208

[a] Maximum strength determined by compression testing.

nanocomposites.[189,190] A first example of its use in VP 3D printing in high concentrations has been recently reported by Parikh *et al.*, who described the synthesis of methacrylated microcrystalline cellulose (F-MCC) and its formulations at concentrations up to 20 wt% with a mixture of AESO and HEA, describing the first example of cellulose-bases VP-printed thermoset material.[191] From the perspective of printability and mechanical properties, increasing concentration of F-MCC in the photocurable resin has allowed for a remarkable increase in its mechanical properties, demonstrated by a 10-fold increase in elastic modulus and a 3.5-fold increase in tensile strength when the composite with 20 wt% F-MCC is compared to the polymer matrix with no cellulose added. However, from the sustainability point of view, the use of methacrylic anhydride and DMF for the functionalization of MCC affected importantly its synthetic factor F_{syn}. This, and the fact that highly sustainable AESO was employed as reactive diluent in high concentrations, had as a consequence a slight reduction in the SFS of the formulations (from 30 to 28) with increasing F-MCC content. Nonetheless, this issue could be easily solved by developing more sustainable cellulose functionalization approaches such as, for example, surface oxidation or Lewis acid-catalysed esterification.[192–194]

This path was followed in some way by Cafiso *et al.*, who reported in 2022 the functionalization of nanocellulose (NC) with 2-(methacryloyloxy)propyl trimethoxysilane (MTEOS) and its formulation in hydrogels of methacrylated carboxymethyl cellulose (mCMC) containing water-soluble photoinitiators, to achieve a 3D printable hydrogels fully based on cellulose derivatives.[195] Since the silanization of NC is limited to its surface, its biobased carbon content is not affected by the functionalization reaction, unlike its atom economy, which reduced the synthetic factor F_{syn} to 0.56. Once again, the extensive functionalization of carboxymethyl cellulose with methacrylic anhydride led to lower biobased carbon content and F_{syn}, but the assumed biodegradability of the material (which was not tested by the authors but considered due to its cellulosic nature) boosted their SFSs up to 50. As it could be expected, higher sustainability indexes are achieved with higher methacrylated NC (mNC) contents.

A similar strategy was described by Zanon *et al.*, who described the preparation of methacrylated chitosan (CHI-MA) for its 3D printing with potential applications in tissue engineering.[196] Prepared by reaction of chitosan acetate with methacrylic anhydride under microwave irradiation, CHI-MA with a methacrylation degree of 24 mol% was dissolved in water together with methacrylated quinizarin dyes and the photoinitiator to achieve biocompatible 3D printed hydrogels. The addition of photocurable dyes affected positively the printing speed and resolution, and the sustainable conditions for the synthesis of CHI-MA would allow to reach good SFS values, but the presence of non-renewable PEGDA in high concentrations prevent us from assuming the biodegradability of the 3D printed hydrogel, leading to an overall SFS of 15.

In addition to cellulose and chitosan, other polysaccharides have been functionalized with photocurable groups for applications in VP 3D printing, often exploiting thiol–ene chemistry in place of acrylate radical polymerization. A popular strategy involves the functionalization of the biomacromolecule of choice with norbornene units, which bear a C=C unsaturation susceptible to attack by photogenerated thiyl radicals (Scheme 13).

A fist example of this strategy has been recently reported by Feng *et al.*, who described the functionalization of pullulan, a polysaccharide produced from starch by the fungus *Aureobasidium pullulans*, with carbic anhydride, leading to the corresponding ester (Pul-NB).[197] The functionalized polysaccharide was then dissolved in water with dithiothreitol (DTT), a water-soluble dithiol, and the appropriate photoinitiator and 3D printed into 3-dimensional hydrogel structure. Due to hydrogel nature of the material, its mechanical properties are indeed very low, but the high porosity and cytocompatibility of the prepared formulation open for their application in 3D bioprinting. Nonetheless, the use of a large excess of carbic anhydride, which is hazardous and non-biobased, and the extensive functionalization degree (30 mol%) required for efficient hydrogelation during 3D printing affected the SFS of its formulation, but this was greatly compensated by the biodegradability of the material, accounted for in the evaluation of the end-of-life factor F_{EoL}. In fact, the proposed approach led to materials with SFS = 43 with BCC% = 64%.

A very similar strategy was presented the same year by Galarraga *et al.*, who used DTT to photocrosslink hyaluronic acid (HA) during VP 3D printing.[198] With a synthetic protocol analogous to the one just described, the authors produced norbornene-functionalized HA ($NorHA_{CA}$) using carbic anhydride in water. Aqueous mixtures were prepared including norbornene-modified HA with a functionalization degree of 40 mol%, DTT, and a water-soluble photoinitiator, to achieve VP 3D printable and biodegradable hydrogels. In this case, a huge excess of carbic anhydride has been used for the synthesis, and the corresponding low AE prevented this formulation from reaching a significant sustainability score.

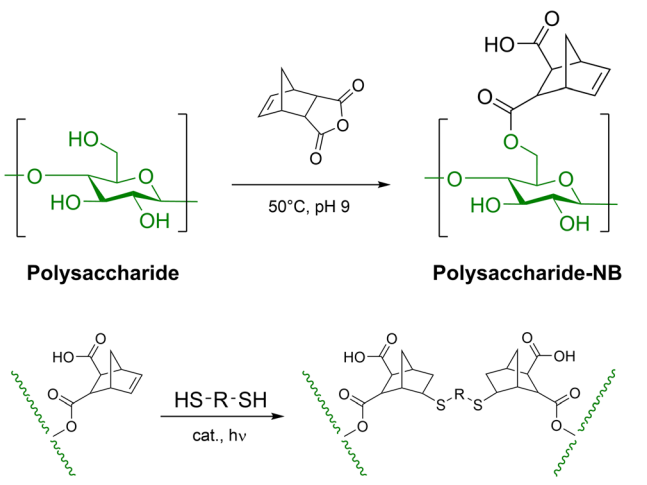

Scheme 13 Functionalization of polysaccharides with carbic anhydride and following thiol–ene crosslinking.

Instead of using a small molecule thiol such as DTT, thiolated biomacromolecules can be exploited to achieve efficient crosslinking without the need for small molecular weight additives. This was the case in the study reported by Zanon *et al.* in 2023, who separately produced norbornene-functionalized and cysteamine-functionalized alginate (SA-NOR and SA-CSA, respectively) with the objective of coupling them *via* thiol–ene photopolymerization during 3D printing, without the addition of any reactive co-monomer.[199] With this approach, they have been able to achieve biocompatible hydrogels with good mechanical properties and high biobased carbon contents (BCC% = 90%). However, the carbodiimide-mediated amidation performed for both modifications of sodium alginate involved the use of large excess of reagents, and the waste of many equivalents of carbodiimide, which affected significantly the atom economy of the two synthetic processes (AE = 0.13 and 0.27 for SA-CSA and SA-NOR, respectively), leading to an overall sustainability score slightly above 26. Analogously, in 2022 Wang *et al.* produced methacrylated *O*-acetyl galactoglucomannan (GGMMA) with methacrylic anhydride, and they employed it as the sole photocurable components of VP 3D printed hydrogels.[200] With this approach, and thanks to the low methacrylation degree of 0.25 which preserved most of the biobased carbon content of the biopolymer, highly sustainable soft hydrogels (SFS = 48 and BCC% = 90%) with antimicrobial properties were efficiently prepared, and 3D printed with high spatial accuracy.

In addition to polysaccharides, polypeptide and proteins offer many functional groups for their functionalization, and their good solubility in water allow for their use for the preparation of water-based photocurable hydrogels. As the aminoacidic composition of natural polypeptides may vary depending on their sources, a detailed evaluation of the biobased carbon content after chemical modification is difficult to perform if the degree of functionalization of the macromolecule is not carefully evaluated by the authors of each work. In any case, for the purposes of this review, we have made a few assumptions that will allow us to estimate the sustainability of polypeptide-based formulations: (1) the biobased carbon content (BCC%) is assumed that functionalized polypeptides retain 90% biobased carbon content when functionalization is performed using non-biobased molecules. This reflects the dominance of the polypeptide backbone, which remains biogenic, while accounting for a moderate reduction due to the incorporation of fossil-derived functional groups; (2) the total carbon content of the polypeptides is approximated to 53%, corresponding to the average carbon content of the most abundant naturally occurring amino acids. This assumption simplifies the analysis by avoiding the need for detailed compositional analysis for each specific polypeptide; (3) the atom economy is calculated as the ratio of the mass of polypeptide successfully functionalized to the total mass of all reagents employed in the functionalization reaction. This approach pro-

vides a first-order approximation of the synthetic efficiency in terms of material usage.

A first example has been reported by Kim *et al.*, who has been able to efficiently VP 3D bioprint solutions of glycidyl methacrylated silk fibroin (Silk-GMA) with living cells for cartilage tissue engineering.[201,202] GDM was reacted with the pending amino groups of abundant lysine residues, leading to extensively methacrylated Silk-GMA which was formulated in water with a photoinitiator and 3D printed. With this approach, thanks to the assumed biodegradability of polypeptides and to the absence of reactive diluents, the calculated SFS would reach outstanding values; however, the dissolution of silk fibroin for chemical modification required huge amounts of LiBr (around 4 times the mass of silk fibroin) which must be taken into account in the evaluation of the AE. Therefore, notwithstanding the great biocompatibility and mechanical properties demonstrated by this approach, Silk-GMA-based hydrogels are still far from being considered highly sustainable solutions (SFS = 18).

In addition to silk fibroin, also bovine serum albumin (BSA) has been functionalized with methacrylic acid residues and formulated in water-based photocurable mixtures for achieving 3D hydrogels *via* VP. This has been reported by Smith *et al.*, who efficiently functionalized BSA with methacrylic anhydride to produce methacrylated BSA (MA-BSA).[203] Compared to the methacrylation with GDM reported by Kim *et al.*,[201] the authors of this work managed to achieve methacrylated BSA by using only a slight excess of methacrylic anhydride, allowing to maintain good atom economy for the functionalization of the biomacromolecule. MA-BSA was then formulated with PEGDA in aqueous solution, and 3D printed into biocompatible hydrogels. Interestingly, when water was removed from the hydrogels, the obtained bioplastics displayed high compressive modulus (up to 638 MPa), especially after a thermal curing that enabled the formation of intermolecular interactions between the BSA chains. Regardless for the presence of 25 wt% of non-renewable PEGDA, good sustainability indexes were achieved, with an SFS of 25 for a BCC% of 67%.

Gelatine is another protein of interest for the preparation of photocurable formulations. In 2023, Duong *et al.* reported its functionalization with carbic anhydride to produce norbornene-functionalized gelatine (Gel-NB) which was then formulated with a four-armed thiol-terminating PEG (PEG-SH_4. 10 kDa) and four-armed norbornene-terminating PEG (PEG-NB_4) and 3D-printed by VP.[204] As previously discussed with polysaccharides, the modification with carbic anhydride is usually accompanied by low atom economy, which ultimately affects the sustainability of the overall formulation. In fact, due to the use of high concentrations of PEG-SH_4, the reported approach was possessed a low sustainability score of 9, accompanied by a total biobased carbon content as low as 21%. In addition to polysaccharides and polypeptides, another widely used biomacromolecule that display plenty of functional groups for chemical modification is indeed lignin. We have already discussed the synthesis of reactive diluent from lignin-derived small molecules, but lignin itself can represent the central core of a new set of photocurable macromolecules. However, when lignin is formulated for VP applications, its chemical modification should involve the vast majority of its phenolic OH groups, to prevent it from trapping the photogenerated radical species thanks to its well-described radical scavenger capacity.[205,206] Due to the high heterogeneity of lignin structure, which heavily depends on the source and the extraction processes, the same assumptions made for polypeptides regarding the calculation of the sustainability indexes are applied here. A first lignin methacrylation approach was reported by Sutton in 2018, who extracted lignin from pulp-grade wood chips of hybrid poplar and proceeded with its methacrylation using methacrylic anhydride in the presence of DMAP.[207] The obtained methacrylated lignin (Lignin-M) was efficiently VP 3D printed after its formulation at concentrations up to 15 wt% with non-renewable high performance reactive diluents, leading to photocurable formulations with good mechanical properties but very low sustainability. In fact, the calculated SFS was limited to a value of 6 due to the high amount of non-biobased reactive diluents, but the good F_{syn} value for methacrylated lignin (0.56), together with its high biobased carbon content (90%), make it a promising candidate for the development of highly sustainable formulations. In a recent work by Yang *et al.*, a more complex chemical modification of lignin has been performed with analogous purposes. In this work, the authors functionalized lignosulfonate, usually obtained as lignin-based byproduct of wood pulp production, with a difunctional isocyanate (hexamethylene diisocyanate, HDI) followed by a further functionalization with 2-hydroxyethyl acrylate, to introduce the photocurable moieties required for photopolymerization, producing lignosulfonate urethane acrylate (UALS) (Scheme 14).[208] Compared to the work of Sutton *et al.* previously described, this approach allowed lignin to be formulated at higher concentrations (up to 35 wt%) including ACMO as the main component and aqueous acrylated choline chloride (ACC, 80% in water) as reactive diluent. However, the higher lignin-derived content of the formulations is widely compensated by the extensive functionalization with toxic isocyanates, leading to even lower sustainability scores. In fact, the calculated SFS is only 4 for the formulation with the highest lignin content, and the total biobased content is as low as 31%. Furthermore, the prepared materials displayed very low tensile strengths, hardly reaching 1 MPa.

To summarize, this analysis has shown that functionalized natural polymers are still far from representing valuable sustainable components for the preparation of liquid formulations for VP aiming at the production of solid objects with good mechanical properties, but it demonstrated success in achieving printability and hydrogel formation suitable for biomedical applications.

Recyclable and reprocessable systems

Thus far, this review has provided a comprehensive assessment of sustainable partially biobased resin systems, empha-

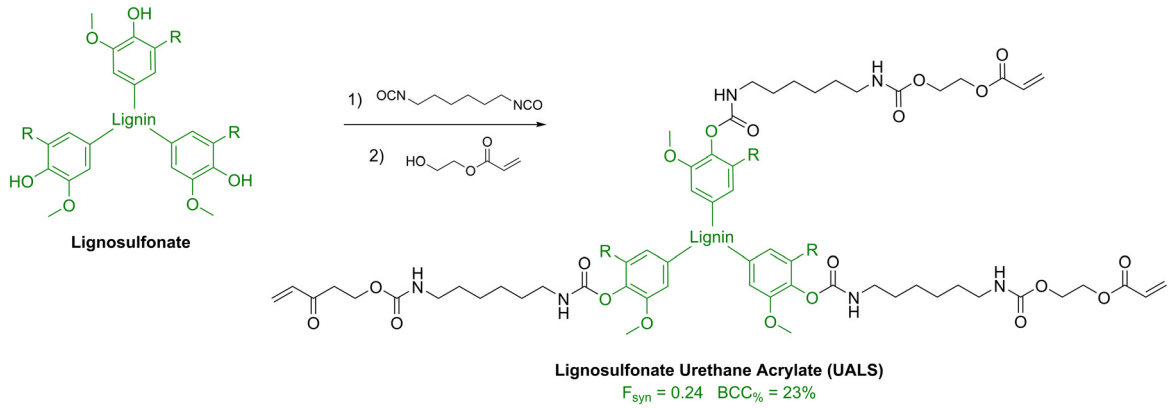

Scheme 14 Acrylation of lignosulfonate through intermediate formation of urethane linkages. The bioderived portion of each structure is depicted in green. Re-drawn from ref. 208.

sizing green metrics such as biobased carbon content (BCC%) and the Sustainable Formulation Score (SFS) to quantify the environmental impact of photocurable formulations. While these approaches improve the renewable content of photopolymers, they often face limitations in mechanical performance and process efficiency that challenge their broader applicability. In contrast, a new paradigm is emerging in which the design of recyclable systems is prioritized as a key sustainability parameter.[209–211] These innovative formulations are engineered to achieve superior overall sustainability by incorporating dynamic covalent bonding, reversible crosslinking, and self-healing functionalities, although sometimes they feature lower bioderived content,. Such approaches enable closed-loop processing and end-of-life reprocessing, thereby reducing waste and facilitating material recovery. In this section, we focus on the development of these recyclable systems, critically examining how they reconcile lower biobased contents with enhanced environmental performance and how they pave the way toward a circular economy in additive manufacturing.

Nonetheless, this section will focus only on recyclable systems that are at least partially biobased, in line with the scope of the review. As a result, formulations with BCC% = 0, and thus SFS = 0 according to eqn (4), are not considered, regardless of their recyclability or reprocessability.

Reprocessability by inclusion of transesterification catalysts. The incorporation of transesterification catalysts into photocurable resin formulations offers a promising approach to introduce reprocessability through dynamic covalent chemistry. These catalysts promote transesterification reactions, the exchange of ester bonds, within the polymer network when the material is subjected to elevated temperatures. As a result, the covalent bonds in the crosslinked network can rearrange without leading to a loss of overall network connectivity. This bond exchange mechanism enables the material to soften, flow, and be reshaped, while still maintaining its structural integrity once cooled, thus allowing for recycling or repair of crosslinked thermoset materials.[212–214] This vitrimer-like behavior not only enables stress relaxation and reprocessing but also helps maintain the material's mechanical integrity over multiple recycling cycles. By strategically integrating these catalysts, researchers have demonstrated that it is possible to create closed-loop systems where 3D printed objects can be efficiently remolded or repaired, thereby significantly reducing material waste and enhancing the overall sustainability of the process. A summary of the formulations presented in this section, together with their sustainability indexes and mechanical properties before and after reprocessing is provided in Table 12.

A particularly popular approach for the inclusion of transesterification catalysts involves the use of Miramer A99, a bifunctional PEG chain with a methacrylic acid residue on one side and a phosphoric acid group on the other. Phosphoric acids are known for their ability to activate esters towards their transesterification by reducing the electron density on the carboxylic carbon, especially at high temperatures and pressures, and its covalent binding to the photopolymer ensured by the presence of the methacrylate group prevent its leaking after 3D printing.[215] This approach was used by a series of works published since 2022, where methacrylated phosphate esters were formulated in concentrations ranging from 5 to 15 wt% with partially biobased photocurable hydroxylated building blocks, including acrylated epoxidized lineseed oil (AELO), AESO, HEMA, tetrahydrofurfuryl methacrylate (THFMA), glycerol 1,3-diglycerolate diacrylate (GDGDA), malic acid bis(glyceryl methacrylate) (MAMA), and dihydroxypropyl methacrylate (DHPMA), and VP 3D printed into thermally healable thermosets.[216–221] In all the reported works, upon treating a broken piece of 3D printed material with temperatures in the range of 140–200 °C for several hours, transesterification reaction between free OH groups in the monomers and methacrylate esters could take place, thus forming new covalent interactions throughout the broken interface, leading to healed materials without significant losses in mechanical properties. For what concerns the sustainability of the formulations, it must be pointed out that even though the thermal treatment required for triggering the self-repair process is sometimes

Table 12 Sustainability indexes and mechanical properties of reprocessable 3D printed photocurable formulations including transesterification catalysts

Formulation (wt%)	Catalyst (wt%)	Reprocessing conditions	BCC%	SFS		Elastic modulus (MPa)	Elongation at break (%)	Tensile strength (MPa)	Tensile strength recovery (%)	Ref.
AELO 70% EGMP 20%	DMEP 8%	180 °C 4 h	60.3%	32.7		—	19	0.58	100%	216
THFMA 40% HPPA 50%	Miramer A99 5%	200 °C 3 bar 1 h	22.1%	12.8		—	31.7	0.5	340%	217
GDGDA 54% THFMA 36%	Miramer A99 5%	180 °C 5 h	48.5%	30.1		—	38	5	500%	218
MAMA 70% HEMA 15%	Miramer A99 15%	200 °C 40 kN 1 h	43.2%	32.3		3710 ± 67	3.14 ± 0.78	65.9 ± 6.2	35%	221
DHPMA 68% GDGDA 16%	Miramer A99 15%	140 °C 8 h	37.7%	22.3		—	6.3	56	95%	220
PHI 83.5% BA 15%	$ZnCl_2$ 2%	230 °C 20 MPa 1 h	97.8%	52.5		—	6.5	43	53%	222
VGEA 68% DGEVDA 25%	$Zn(acac)_2$ 5%	140 °C 1500 psi 4 h	49.3%	4.0		322.2	5.5	22.1	93%[a]	223
VGEA 68% DGEVDA 25%			49.3%	3.5		322.2	5.5	22.1	93%[a]	
GuGEA 66% DGEVDA 27%			46.8%	3.1		301.8	7.6	12.5	—	

[a] Percentage of recovery of compressive strength.

accompanied by a significant improvement in the materials' mechanical performances, the high temperatures and prolonged times needed may limit the overall energetic benefit granted by the reprocessability. This is particularly true for the formulations reported to this day, which are characterized by significantly low $BCC_{\%}$. Nonetheless, the extended lifespan of the 3D printed materials, taken into account in the evaluation of the end-of-life factor F_{EoL}, has led in some cases to SFSs that are comparable to those of previously discussed biobased formulations (in the 15–30 range) but with significantly lower BCC%, (in the 20–60% range) suggesting how the translation of this approach to formulations that possesses inherently higher biobased content might lead to 3D printed materials with outstanding sustainability.

This was in fact the strategy of Huang *et al.*, who recently reported the VP of reprocessable resins composed poly(hexanediyl itaconate) (PHI) and butyl acetate (BA), using this time $ZnCl_2$ as the transesterification catalyst.[222] The 3D printed material was efficiently reprocessed after grinding into fine powder by hot press moulding, leading to partial loss in mechanical properties but still presenting good tensile strength. Furthermore, by using a fully biobased itaconic acid polyester as the main component of their formulations, the authors of this work reached biobased carbon contents as high as 97.8% and sustainability scores surpassing 52, the highest reported in this review so far.

A further approach involving zinc-based transesterification catalysis has been described by Cortes-Guzman *et al.*, who included 5 mol% of zinc acetylacetonate ($Zn(acac)_2$) in formulations based on vanillin, eugenol and guaiacol-derived acrylates.[223] In order for the reactive diluents to display the free OH group required for self-healing *via* transesterification, vanillin, eugenol and guaiacol were separately reacted with epichlorohydrin to produce the corresponding glycidyl ether, followed by opening the oxirane ring using acrylic acid (Scheme 15). Analogously, a bifunctional crosslinker was also prepared, by firstly reducing vanillin into the corresponding diol and then performing the analogous attack with ECH followed by acrylation. As it could be expected, the use of hazardous epichlorohydrin and of a large excess of reagents (especially acrylic acid) during the synthetic steps had a huge impact of the F_{syn} of the acrylated components (which was as low as 0.06 in all case) leading to very low sustainability scores (around 3–4).

Nonetheless, the inclusion of the transesterification catalyst allowed to reprocess ground 3D printed objects by hot press moulding, with no significant losses of material performances after reforming.

Monomer upcycling. An additional strategy to enhance the sustainability of photocurable resins involves the upcycling of specific building blocks within the resin network. The objective is to recover part of the original chemical constituents used during resin synthesis, which can then be reused to produce new resin formulations or other products. Given that most of the resins discussed thus far are based on poly(meth) acrylate esters, this strategy leverages their known susceptibility to alkaline hydrolysis or alcoholysis. Under alkaline conditions in aqueous or alcoholic media (typically methanol), the ester bonds in poly(meth)acrylates can be cleaved, effectively replacing the alcohol moiety originally linked to the (meth)acrylic acid unit with either a water molecule or an alcohol molecule from the reaction medium. This controlled bond cleavage enables the selective recovery of monomers or oligomers, facilitating material circularity. Nonetheless, even though this approach is virtually compatible with any poly (meth)acrylate thermoset network, its use is not widespread,

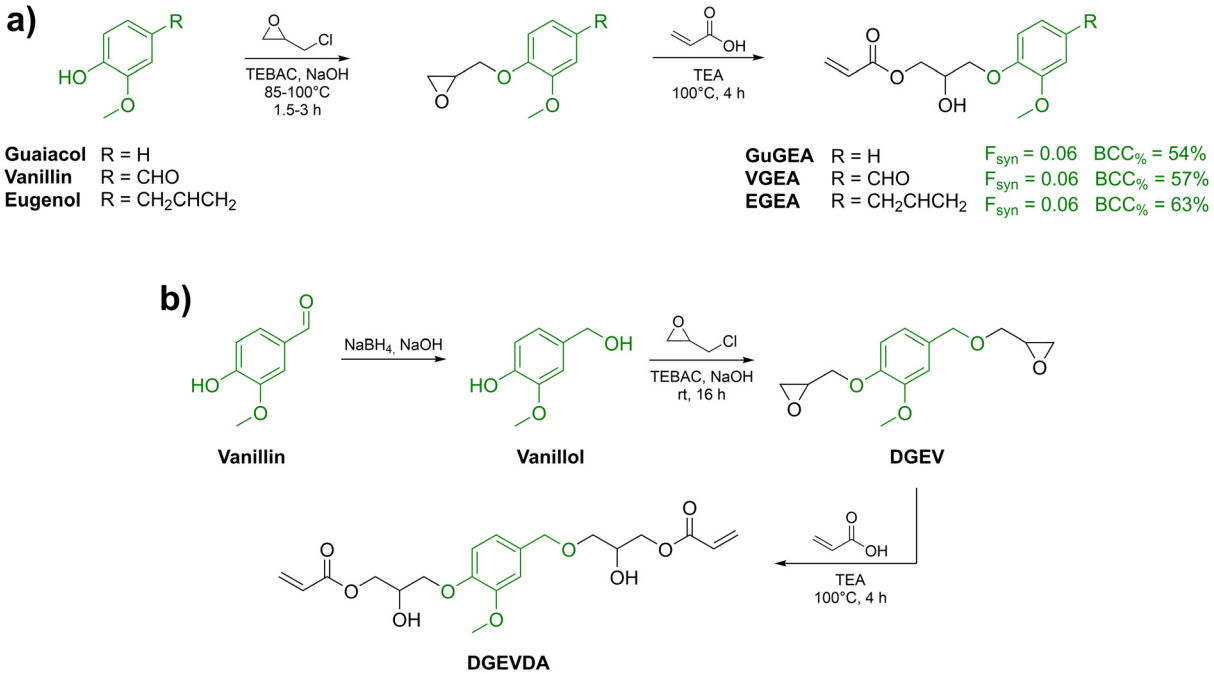

Scheme 15 Synthesis of (a) eugenol, guaiacol and vanillin-based reactive diluents (GuGEA, VGEA and EGEA) and (b) difunctional crosslinker (DGEVDA) for healable resins containing Zn-based transesterification catalyst. The bioderived portion of each structure is depicted in green. Redrawn from ref. 223.

since it requires plenty of heat and harsh alkali conditions to recover only a small fraction of the components of the photocurable resins. Furthermore, the recovered alcohols, are usually the least concerning component of the formulation, from a sustainability perspective, as they would need to be (meth)acrylated again with impactful processes before being 3D printed one more time.

An exception is represented by the work of Yue *et al.*, who recently described the formulation of poly(δ-valerolactone) acrylate with 30 wt% ACMO, to achieve a 3D printed polyester-based network that could be thermally decomposed into δ-valerolactone upon heating at 200 °C for 4 h under high vacuum.[224] However, the high amount of energy required for the upcycling of δ-valerolactone almost fully compensates for the sustainability advantages introduced by the recovery of a fraction of the 3D printed photopolymer mass.

Reprocessability *via* dynamic or reversible covalent bonds. Integrating dynamic or reversible covalent bonds into photopolymer networks offers an innovative approach to recycling, as these bonds can undergo reversible reactions in response to external stimuli such as heat, light, or chemical triggers. By designing polymer structures that incorporate reversible chemistries, the material can be depolymerized or reconfigured under controlled conditions, facilitating repair, reshaping, or complete recycling of the 3D printed object. This strategy preserves the integrity of the polymer network during reprocessing, enabling multiple recycling cycles without a significant loss in mechanical performance. Moreover, the dynamic behaviour of these bonds contributes to self-healing capabilities, further extending the lifespan of the materials. Ultimately, leveraging dynamic covalent bonds supports the development of a circular economy in additive manufacturing by reducing waste and promoting resource-efficient material recovery. A summary of the formulations presented in this section, together with their sustainability indexes and mechanical properties before and after reprocessing is provided in Table 13.

For example, imine bonds, also known as Schiff bases, are dynamic covalent bonds formed by the reaction of a primary amine with an aldehyde or ketone. Their reversible nature allows for bond dissociation and reformation under mild conditions, making them highly suitable for self-healing materials.[225–227] The ability of imine bonds to break and reform in response to environmental stimuli such as temperature, humidity, pH, or solvent exposure enables autonomous or stimuli-responsive self-healing.

As anticipated in a previous section of this review, the aldehyde functionality of biobased vanillin is perfectly suited for this purpose, as its reaction with amines leads to imines with good efficiency and in mild conditions. This approach was exploited by Cortes-Guzman *et al.* in 2022, who developed multifunctional vanillin methacrylate imines by reacting vanillin methacrylate with Jeffamine, composed of linear and star-shaped amine-terminating poly(propyleneglycol)s (Scheme 16).[228] These were formulated with vanillin acrylate (VA) and VP 3D printed into healable solid objects. Analogously to what reported for the use of transesterification catalysts, upon the application of heat and pressure, damaged

Table 13 Sustainability indexes and mechanical properties of reprocessable 3D printed photocurable formulations including dynamic or reversible covalent bonds

Formulations	Dynamic bond	Recycling conditions	BCC%	SFS		Elastic modulus (MPa)	Elongation at break (%)	Tensile strength (MPa)	Tensile strength recovery (%)	Ref.
VA 44% JT403-MA-VA 54%	Imine	140 °C	52.6%	14.4		7.2[a]	48.7[a]	155.6[a]	122%	228
VA 20% JT3000-MA-VA 78%			24.0%	6.7		0.07[a]	61.6[a]	13.5[a]	69%	
VA 50% JD400-MA-VA 48%		1500 psi	52.7%	13.5		1.9[a]	57.6[a]	125.2[a]	112%	
VA 26% JD2000-MA-VA 72%		3 h	27.6%	7.4		0.05[a]	68.7[a]	18.1[a]	92%	
VA 36% JED900-MA-VA 62%			37.5%	9.9		0.11[a]	75.7[a]	231.6[a]	94%	
BDG 79% IBOMA 20%		150 °C	78.5%	22.3		1300	8.5	25	100%	228
CROSS 5%			77.1%	21.9		1380	5	27.5	90%	
BDG 74% IBOMA 20%		40 kN 5 min								
CROSS 10%			75.7%	21.5		1450	3	34	74%	
BDG 69% IBOMA 20%										
POPIT 49% IBOA 49%	Urea	400 wt% TBEM	53.6%	32.6		466 ± 30	10.28 ± 0.81	48.2 ± 0.61	98%	233
COIT 98%		90 °C 4 h	45.3%	21.2		441 ± 1 6	90 ± 2.1	14.7 ± 0.53	95%	234
ACMO 40% NVP 10% TA 50%	Disulfide	90 °C 10 min or solvent casting or monomer-added reprinting	43.1%	84.6		0.7	574	0.5	96%	238
DIS-Lip$_2$ 90% nBA 10%		0.05 M DBU in DCM	74.2%	37.2		7	16	1.1	82%	239
IsoLp2 70% MenLp1 30%		Thiophenol (P_1-t-Bu) 80 °C 15 min	97.3%	148		—	25	3	83%	240
Citric acid 36% Glycerol 13% Acrylamide 13% Dimethylacrylamide 37%	H-bonding	Monomer-added reprinting	38.0%	119		144.35 ± 8	212 ± 7	37.2 ± 0.8	100%	247

[a] Determined by compressive testing.

3D printed materials were able to fully recover their original mechanical properties thanks to the reorganization of imine bonds at the broken interface, expanding the lifespan of 3D printed objects. Nonetheless, the use of high molecular weight non-biobased cores in the photocurable imines, together with the use of high amounts of VA, severely impacted on the sustainability of the formulations, that reached a maximum SFS of 14.4 and a maximum BCC$_{\%}$ of 53%. However, this worked proved the potential of vanillin imines for the manufacturing of healable materials, but the use of biobased amines and/or more sustainable reactive diluents could greatly improve the sustainability of the overall approach. This was in fact the path followed the following year by Stouten *et al.*, who produced a photocurable vanillin imine using Priamine 1075 as the amine.[229] Priamine 1075 is an aliphatic fatty acid derived diamine, which is certified to be composed of 100° renewable carbon. The obtained diamine, named BDG, was formulated with a less sustainable trifunctional vanillin imine analogue (CROSS) and IBOMA, to achieve VP 3D printable resins with higher sustainability scores. When ground in fine powder and subjected to elevated temperature and pressures, the 3D printed material was able to regenerate most of its original mechanical properties, with no significant differences detected after up to three reprocessing cycles. Nonetheless, the harsh experimental conditions used to synthetized BDG and CROSS heavily affect their synthetic factor F_{syn} to below 0.2, thus leading to SFSs around 24 regardless of the high biobased carbon contents, in the 75–80% range. This once again demonstrates the importance of considering green metrics related to the experimental conditions required for the synthesis of bioderived resin components, since the only evaluation of the BCC$_{\%}$ might be misleading. In addition to imines, urea bonds have attracted significant interest in the development of self-healing materials due to their ability to enable reversible bonding and restore material properties after damage. These bonds are based on hydrogen bonding interactions between the urea group (–NH–CO–NH–) and other functional groups, such as carbonyl or amine groups. The dynamic nature of urea bonds, as part of dynamic covalent chemistry, allows them to break and re-form under certain

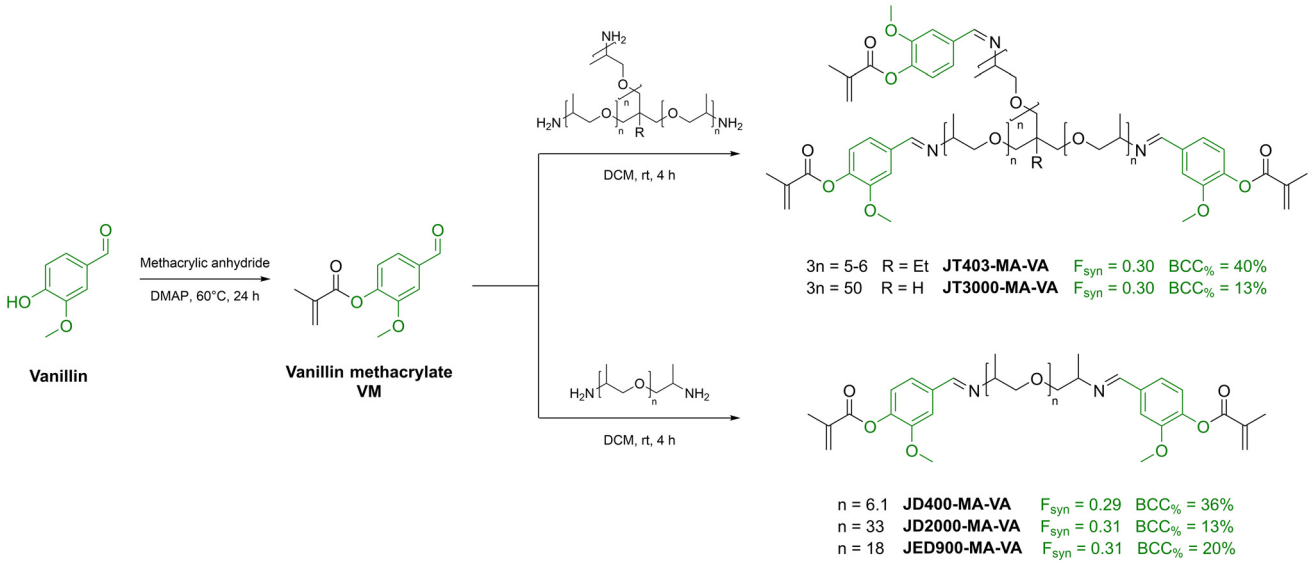

Scheme 16 Synthesis of vanillin methacrylate-functionalized linear and star-shaped amine-terminating poly(propyleneglycol) imines. The bioderived portion of each structure is depicted in green. Re-drawn from ref. 228.

conditions, such as exposure to heat or solvents. This reversible bonding is crucial for self-healing, as it enables the material to repair itself upon mechanical stress or damage, restoring its original structure and functionality.[230–232]

These properties of urea linkages have been recently exploited by Zhu *et al.* in two similar works, where the authors described the development of urea-functionalized plant oil derivatives which were efficiently 3D printed and then depolymerized to achieve a recycled liquid resin that could be once again printed by means of VP.[233,234] In particular, OH-rich plant oils such as castor oil (CO) or thiol–ene adducts of plant oils and 2-mercaptoethanol (POPs) were firstly functionalized with isophorone diisocyanate (IPDI), followed by functionalization of the free isocyanate pending group with 2-(*tert*-butylamino) ethyl methacrylate (TBEM), which led to the formation of sterically hindered urea linkages (Scheme 17). The steric hindrance on one side of the urea linkage made it susceptible to nucleophilic substitution in the presence of an excess of free amine: in fact, when the 3D printed materials were ground into fine powder and placed in the presence of an excess of TBEM at 90 °C the solution became clear, and after the addition of some fresh co-monomers and photoinitiators the mixture could be 3D printed without loss of mechanical performance or print resolution. However, it must be considered that this approach led to the accumulation of linear poly(TBEM) during recycling, which limit the amount of waste material that can be included into the recycled resins due to viscosity constraints.

Furthermore, the use of isocyanates such as IPDI heavily affects the sustainability of the formulations, strongly compensating for the increase in sustainability related to the improved end-of-life of the material. In fact, regardless for the high value of F_{EoI} (1.5) the formulations were associated to SFSs of around 22.

Disulfide bonds (S–S) play a crucial role in self-healing materials due to their dynamic and reversible nature. These covalent bonds can undergo exchange reactions under specific conditions, such as the presence of a catalyst, changes in pH, or exposure to light or heat. The reversibility of disulfide bonds allows the material to break and reform its network, enabling the restoration of mechanical integrity after damage.[235–237] This property is particularly useful in polymeric materials, where disulfide linkages facilitate self-healing without the need for external additives. In addition to their use in autonomous self-healing systems, disulfide bonds contribute to material recyclability, as they allow for reprocessing and reshaping under controlled conditions. The disulfide that has been employed in most cases for this purpose is α-lipoic acid (ALA), a biobased derivative of caproic acid bearing a 1,2-dithiolane pending group at its end.

A first example of ALA-containing resins has been reported by Zhu *et al.* in 2024, who prepared photocurable mixtures of ACMO and *N*-vinyl pyrrolidone (NVP) containing up to 50 wt% of free lipoic acid.[238] Upon exposure to UV light, ACMO and NVP were able to polymerize into stiff non-crosslinked thermoplastic poly(ACMO-*co*-NVP), but when VP 3D printed materials were subjected to a thermal treatment at 90 °C for 10 min, free ALA polymerized into the corresponding polydisulfide, leading to the formation of a soft double thermoplastic polymer network, thus achieving tuneable mechanical properties ranging from a few tenths to thousands of MPa. The uncrosslinked double polymer network was found: (i) to be soluble in organic solvents, which allowed for reprocessing by solvent casting, (ii) to show self-healing properties, due to the thermally driven reorganization of dynamic disulfide bond at the interface between two broken pieces, (iii) to allow for full reprinting, by dissolving the 3D printed materials in a monomer mixture, and (iv) to optimize a protocol for the separation of

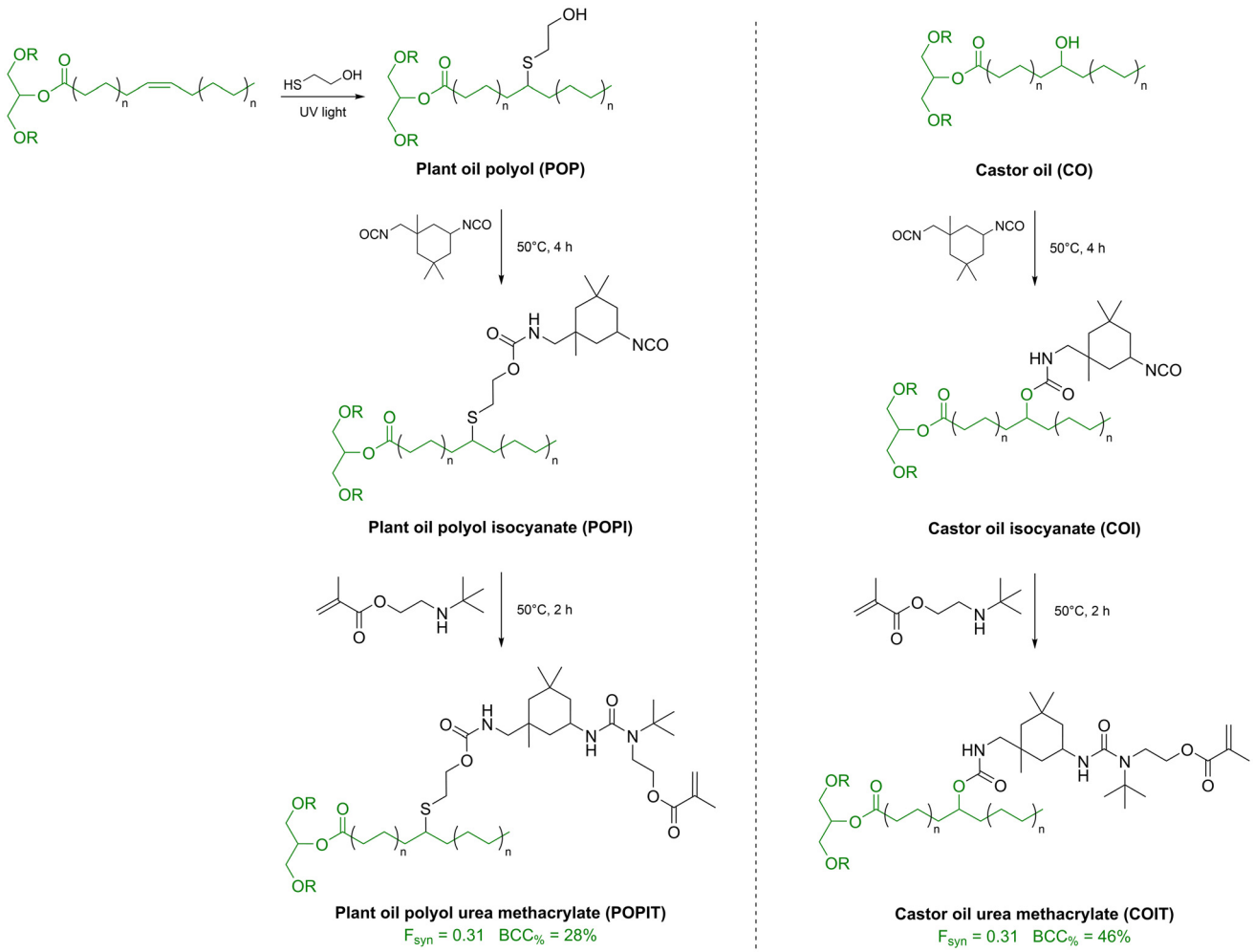

Scheme 17 Synthesis of plant oil-derived photocurable urethanes bearing a pendant labile urea linkage. The bioderived portion of each structure is depicted in green. Re-drawn from ref. 233 and 234.

the polydisulfide thermoplastic and its depolymerization, to achieve close-loop recycling of lipoic acid. This quadruple reprocessability opportunity, together with the high concentration of biobased and unmodified lipoic acid, have granted this approach a sustainability score of 85, even if the BCC is as low as 43%. A similar strategy was reported the same year by Han *et al.*, who employed *n*-butyl acrylate (*n*BA) as the photocurable component and the diester of 2-hydroxyethyldisulfide with lipoic acid (DIS-Lip$_2$) as the source of disulfides.[239] Analogously, materials able to self-heal, to dissolve in organic solvents, and to be reprinted after the base-catalysed dissolution of 3D printed objects in solutions containing fresh monomers were successfully obtained. However, with respect to the work from Zhu *et al.* of the same year, the authors of this work achieved lower SFS due to impactful chemical modification process for synthesis of DIS-Lip$_2$ (SFS = 37) even though their formulation was characterized by significantly higher BCC$_{\%}$ (74%). A further and most significant advancement in this field has been published the same year by Machado *et al.*, who successfully formulated, and VP 3D printed, a (meth)acrylate resin purely based on lipoic acid esters of biobased diols. Amongst many tested formulations, one stands out specifically, composed of isosorbide bis(lipoate) (IsoLp$_2$) and menthol lipoate (MenLp$_1$) in 7 : 3 weight ratio and no additional reactive diluent or crosslinker.[240] Furthermore, a sustainable bulk esterification approach has been optimized to produce in a single step the mixture of IsoLp2 and MenLp2 with the exact weight ratio used for 3D printing, which only required the addition of 1 wt% photoinitiator. In these conditions, the disulfide bonds of lipoic acid were able to generate thiyl radical upon light exposure, leading to the formation of polydisulfide networks which can be fully depolymerized into a reprintable photocurable liquid mixture, upon treatment with thiophenol and *tert*-butyliminotri(pyrrolidino)phosphorane (P$_1$-*t*-Bu) at 80 °C for 15 min in MeTHF, as it has been previously described. In this work, sustainability was maximized in all the aspects of the VP process, from the composition of the photocurable mixture to the

possibility of closed-loop recycling of the printed resins, which were finally characterized by an SFS of 148 and BCC% of 97%, the highest values reported in this review.

In addition to imines, ureas and disulfides, thiourethane bonds, formed through the photoradical reaction of thiols with isocyanates, have emerged as a key component in self-healing materials due to their dynamic and reversible nature.[241,242]

Compared to conventional urethanes, thiourethanes exhibit stronger hydrogen bonding and enhanced chemical resistance, which contribute to improved mechanical properties and durability. Their self-healing capability arises from the reversibility of the thiourethane bond exchange under thermal or chemical stimuli, allowing for network reformation after damage. This was applied to VP by Lopez de Pariza *et al.* in 2023, who developed a photocurable isocyanate-thiol mixture for 3D printing and chemical recycling of the resin, but since no sustainable monomer was employed in the synthesis, the sustainability of the resin, as defined in this review, is as low as zero.[243] Furthermore, isocyanate-based resins are extremely toxic, and particular care must be taken when handling them, since they can give rise to severe respiratory issues and persistent skin sensitization.[244]

Finally, self-healing and reprocessability of 3D printed materials can be ensured by the presence of extensive H-bonding.[245,246] This phenomenon has been exploited by Liu *et al.* in 2023 who reported the preparation of a photocurable deep eutectic solvent (PDES) composed of acrylamide, *N*,*N*-dimethylacrylamide, citric acid and glycerol, where the non-reactive sustainable additives were able to crosslink the poly(acrylamide) linear chains through hydrogen bonding.[247] After 3D printing, the material exhibited self-healing behaviour, thanks to the reorganization of H-bonding between the broken interfaces placed in contact upon heating. Furthermore, the material was fully recyclable upon treatment at 90 °C with the correct amount of fresh monomers and H-bonding crosslinkers, which were able to dissolve the poly(acrylamide) chains and to reform the PDES, which could be effectively reprinted with no detected loss in mechanical properties. Due to the absence of any synthetic step in the preparation of the photocurable mixture, as well as due to the high concentration of natural products in the formulations and the closed-loop recyclability of the proposed resin, the described approach was associated with a very high sustainability score (SFS = 119) even though the total biobased carbon content was not very high (BCC% = 38%).

Photoinitiators, photoabsorbers and radical inhibitors

Photoinitiators are central to the success of VP, as they serve to convert light energy into the reactive species necessary to initiate polymer network formation. The analysis of the composition of the formulations presented in this review (detailed in the ESI†) revealed that the vast majority of the photocurable formulations employ acylphosphine oxides, in their lipophilic versions (diphenyl (2,4,6−trimethylbenzoyl)phosphine oxide, MAPO, phenyl bis(2,4,6−trimethylbenzoyl)phosphine oxide, BAPO and ethyl phenyl(2,4,6-trimethylbenzoyl)phosphinate, Et-APO) or in their water-soluble analogues (lithium phenyl-2,4,6-trimethylbenzoylphosphinate, LAP, or bismesitoylphosphinic acid, BAPO-OH) depending on the physical–chemical nature of the resin being developed (Scheme 18).[248] The development of new sustainable photoinitiators has received less attention compared to the development of biobased monomers, partly because photoinitiators typically constitute a minor fraction of resin formulations (generally less than 3 wt%). Although conventional photoinitiators—often synthesized from petrochemical sources—are highly effective in initiating polymerization under UV or visible light, they can pose environmental concerns due to their toxicity and the generation of hazardous byproducts upon photolysis. In recent years, growing interest in sustainable manufacturing has stimulated research into photoinitiators based on green chemistry principles, including the use of naturally occurring chromophores such as flavonoids, coumarins, and lignin derivatives. However, since the focus of this review is on the sustainability of resin components, the development of sustainable photoinitiators is considered outside the scope of this work. Readers are referred to several recent reviews that comprehensively address this topic.[249–253]

In addition to photoinitiators, photoabsorbers and radical inhibitors, though present in minor amounts, play crucial

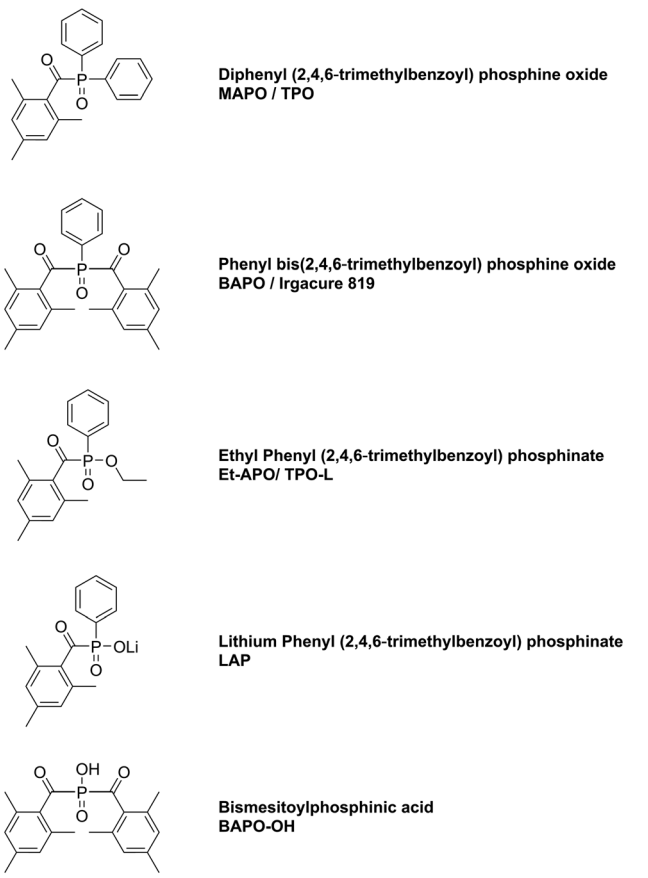

Scheme 18 Chemical structure of the most common photoinitiators employed in photocurable formulations for VP.

roles in regulating the performance and stability of photocurable formulations used in VP. Photoabsorbers are commonly incorporated to limit light penetration depth and enhance spatial resolution during layer-by-layer curing. Traditional photoabsorbers, such as Sudan dyes and anthraquinone derivatives, are derived from petrochemical sources and raise concerns due to their toxicity, persistence, and potential environmental impact.[254,255] In light of this, the development of biobased alternatives has emerged as a promising yet underexplored strategy to enhance the sustainability of VP resin formulations. Naturally occurring chromophores, including flavonoids (*e.g.*, quercetin[256]), diarylheptanoids (*e.g.*, curcumin[257]), and betalain pigments (*e.g.* betanin[258]), have demonstrated significant potential as biobased photoabsorbers (Scheme 19). These molecules exhibit strong absorption in the UV-visible spectrum and are derived from renewable sources such as fruits, vegetables, and medicinal plants. Nevertheless, challenges persist with regard to their solubility in hydrophobic resins, photostability under prolonged exposure, and reactivity under curing conditions.

Radical inhibitors, typically added at concentrations below 0.5 wt%, increase the printing resolution by preventing the polymerization front to diffuse outside of the irradiated area during 3D printing. Widely used stabilisers such as methylhydroquinone (MHQ), butylated hydroxytoluene (BHT), are effective but are derived from non-renewable feedstocks and may leach from cured networks under physiological or environmental conditions. This has spurred investigations into naturally derived radical scavengers as more benign alternatives. Polyphenolic compounds such as tannic acid, gallic acid, and rosmarinic acid, rich in phenolic hydroxyl groups, have shown promising radical-inhibiting properties owing to their electron-donating capabilities and resonance-stabilised radical forms (Scheme 20).[259] However, their incorporation requires careful formulation optimisation, as excessive radical inhibition can suppress polymer conversion and compromise mechanical performance.

Overall, while the contribution of photoabsorbers and inhibitors to resin mass is minor, their impact on formulation behaviour and environmental compatibility is substantial. The development and incorporation of biobased analogues for these additives are key to advancing fully sustainable photopolymer systems and should be pursued in parallel with efforts on green monomers and oligomers.

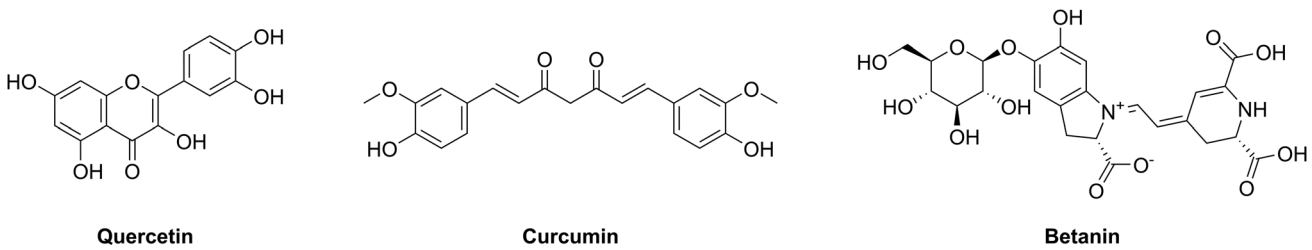

Scheme 19 Chemical structure of emerging sustainable photoabsorbers for VP formulations.

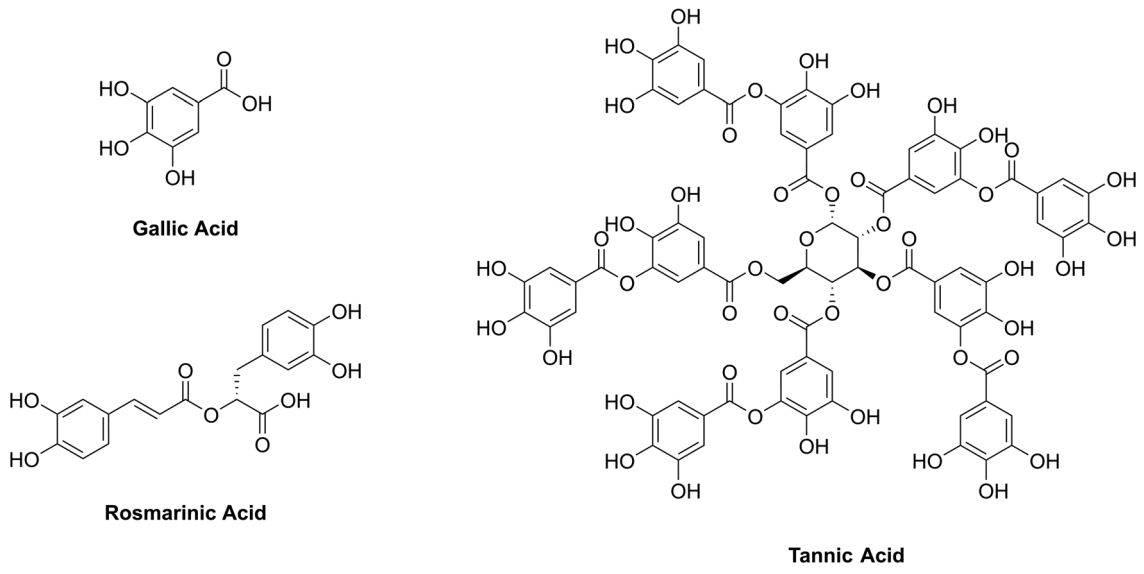

Scheme 20 Chemical structure of emerging sustainable radical inhibitors for VP formulations.

Conclusions

This review has critically examined the progress and challenges in developing sustainable photopolymer resins for vat photopolymerization (VP) 3D printing. The field of sustainability in VP formulations has seen a growing emphasis on alternative resin formulations, incorporating biobased and non-toxic components to reduce environmental impact while maintaining mechanical integrity comparable to conventional SLA/DLP resins. Various strategies have been explored, including vegetable oil derivatives, biobased molecules, non-isocyanate urethanes, and thiol–ene systems. Each of these approaches presents unique advantages in terms of sustainability, mechanical properties, and processability, yet no single formulation has emerged as a definitive solution. Instead, the choice of material depends on balancing renewable content with performance and manufacturing feasibility.

A key challenge in assessing the sustainability of these resins is the reliance on conventional green metrics. While these parameters provide valuable insights into the proportion of renewable raw materials in a formulation, they fail to account for the broader environmental implications of resin synthesis and end-of-life behaviour. A resin with a high BCC% may still involve energy-intensive processing steps or generate hazardous by-products, offsetting its presumed sustainability benefits. Additionally, these traditional metrics do not adequately capture factors such as recyclability, degradation behaviour, or the potential toxicity of breakdown products. To address these gaps, the Sustainable Formulation Score (SFS) has been proposed as a more comprehensive metric that integrates multiple sustainability parameters, including atom economy (AE), synthesis efficiency, and end-of-life considerations. This approach allows for a more holistic assessment, ensuring that sustainability claims extend beyond raw material selection to encompass the entire lifecycle of the resin.

Despite these advancements, several challenges remain in improving the synthesis and processing of sustainable photopolymer resins. Many promising biobased or degradable resins require multi-step chemical modifications, some of which involve hazardous reagents or high-energy reactions that diminish their overall environmental benefits. Furthermore, the functionalization of bio-based monomers to enhance photopolymerization may introduce structural modifications that negatively impact their biodegradability or recyclability. The development of new synthetic strategies that minimize the use of toxic solvents, toxic catalysts, and energy-intensive reaction conditions is essential for making truly sustainable resins viable at an industrial scale. Techniques such as enzymatic polymerization, solvent-free synthesis, and the incorporation of dynamic covalent chemistry hold potential for improving both sustainability and performance.

Looking ahead, optimizing the synthesis routes of biobased resins will be a crucial step toward enhancing both their environmental and mechanical properties. This includes exploring milder reaction conditions, identifying alternative reagents with lower toxicity, and designing formulations that maintain their structural integrity without relying on petrochemical-based stabilizers. Additionally, the field would benefit from the development of new or refined sustainability metrics that provide a more nuanced evaluation of resin performance, considering aspects such as material circularity, long-term durability, and compatibility with industrial-scale VP processes.

Another key area of future research involves integrating these sustainable resins into large-scale manufacturing. Many biobased photopolymers still face limitations in terms of printability, curing efficiency, and mechanical stability when compared to their petrochemical-based counterparts. Addressing these challenges will require a combination of material innovation and process optimization, including tailored photoinitiator systems, improved crosslinking strategies, and the incorporation of reinforcing additives that enhance mechanical robustness while maintaining biocompatibility. Scaling up these technologies while ensuring cost-effectiveness and consistency in performance remains a priority for widespread adoption in industries such as healthcare, automotive, and consumer goods.

Ultimately, the future of photopolymer resin design will be shaped by the ability to balance sustainability with performance. The shift towards fully biobased reactive diluents, novel polymerization mechanisms, and scalable green-compatible formulations represents a promising direction for research and development. By leveraging interdisciplinary approaches that combine chemistry, materials science, and engineering, the next generation of photopolymer resins can be tailored to meet both functional and environmental requirements. As regulatory pressures and consumer demand for eco-friendly materials continue to grow, adopting sustainable strategies in photopolymer resin development will be essential for ensuring that VP-based 3D printing remains a viable and responsible manufacturing technology.

Author contributions

The manuscript was written through contributions of all authors. All authors have given approval to the final version of the manuscript.

Conflicts of interest

There are no conflicts to declare.

Data availability

All data supporting this article are provided in the ESI,† including detailed resin formulations, sustainable formulation score (SFS) calculations, and referenced mechanical property datasets.

Acknowledgements

M. M. acknowledges the University of Cádiz for his postdoctoral fellowship (2025-042/PU/POSTDOC-R3/CD). This work was funded by the Spanish Ministry of Science, Innovation, and Universities MICIU/AEI/10.13039/501100011033 (Project PID2023-151632OB-C22) and by FEDER, EU. We also acknowledge support to TEP-946 research group from UCA.

References

1 J. D. Prince, *J. Electron. Resour. Med. Libr.*, 2014, **11**, 39–45.
2 C. Schubert, M. C. van Langeveld and L. A. Donoso, *Br. J. Ophthalmol.*, 2014, **98**, 159–161.
3 T. Campbell, C. Williams, O. Ivanova and B. Garrett, *Could 3D Printing Change the World? Technologies, Potential, and Implications of Additive Manufacturing*, Strategic Foresight Initiative, Atlantic Council, 2011.
4 M. Attaran, *Bus. Horiz.*, 2017, **60**, 677–688.
5 C. Schmidleithner and D. M. Kalaskar, Stereolithography, 3D Printing, IntechOpen, 2018, DOI: 10.5772/INTECHOPEN.78147.
6 J. Huang, Q. Qin and J. Wang, *Processes*, 2020, **8**, 1138.
7 L. Andjela, V. M. Abdurahmanovich, S. N. Vladimirovna, G. I. Mikhailovna, D. D. Yurievich and M. Y. Alekseevna, *Dent. Mater.*, 2022, **38**, e284–e296.
8 X. Xu, A. Awad, P. Robles-Martinez, S. Gaisford, A. Goyanes and A. W. Basit, *J. Controlled Release*, 2021, **329**, 743–757.
9 D. Chekkaramkodi, L. Jacob, C. M. Shebeeb, R. Umer and H. Butt, *Addit. Manuf.*, 2024, **86**, 104189.
10 M. Pagac, J. Hajnys, Q.-P. Ma, L. Jancar, J. Jansa, P. Stefek and J. Mesicek, *Polymers*, 2021, **13**, 598.
11 G. Chen, Y. Song, H. Zhang, Y. Sun, D. Zeng, Z. Cheng and B. Yan, *Waste Manage.*, 2024, **187**, 61–69.
12 D. B. Short, D. Volk, P. D. Badger, J. Melzer, P. Salerno and A. Sirinterlikci, *3D Print. Addit. Manuf.*, 2014, **1**, 24–33.
13 E. M. Maines, M. K. Porwal, C. J. Ellison and T. M. Reineke, *Green Chem.*, 2021, **23**, 6863–6897.
14 H. Lai, J. Zhang and P. Xiao, *ACS Sustainable Chem. Eng.*, 2023, **11**, 16365–16406.
15 V. S. D. Voet, J. Guit and K. Loos, *Macromol. Rapid Commun.*, 2021, **42**, 2000475.
16 M. Weiss, J. Haufe, M. Carus, M. Brandão, S. Bringezu, B. Hermann and M. K. Patel, *J. Ind. Ecol.*, 2012, **16**, DOI: 10.1111/j.1530-9290.2012.00468.x.
17 J. Ruf, A. Emberger-Klein and K. Menrad, *Sustain. Prod. Consum.*, 2022, **34**, 353–370.
18 M. Maturi, C. Spanu, E. Locatelli, L. Sambri and M. Comes Franchini, *Addit. Manuf.*, 2024, **92**, 104360.
19 M. Maturi, C. Spanu, E. Maccaferri, E. Locatelli, T. Benelli, L. Mazzocchetti, L. Sambri, L. Giorgini and M. Comes Franchini, *ACS Sustainable Chem. Eng.*, 2023, **11**, 17285–17298.
20 R. Carmenini, C. Spanu, E. Locatelli, L. Sambri, M. Comes Franchini and M. Maturi, *Prog. Addit. Manuf.*, 2024, **9**, 2499–2510.
21 L. Dai, Y. Zhang, F. Ma, T. Ji, L. Zhang and B. Lyu, *ACS Appl. Polym. Mater.*, 2025, **7**, 1062–1073.
22 ASTM D6866, 2022.
23 G. A. Norton and S. L. Devlin, *Bioresour. Technol.*, 2006, **97**, 2084–2090.
24 G. Quarta, L. Calcagnile, M. Giffoni, E. Braione and M. D'Elia, *Radiocarbon*, 2013, **55**, 1834–1844.
25 M. R. Haverly, S. R. Fenwick, F. P. K. Patterson and D. A. Slade, *Fuel*, 2019, **237**, 1108–1111.
26 B. M. Trost, *Angew. Chem., Int. Ed. Engl.*, 1995, **34**, 259–281.
27 B. Trost, *Science*, 1991, **254**, 1471–1477.
28 R. A. Sheldon, *Green Chem.*, 2023, **25**, 1704–1728.
29 R. A. Sheldon, *Green Chem.*, 2007, **9**, 1273.
30 F. Tieves, F. Tonin, E. Fernández-Fueyo, J. M. Robbins, B. Bommarius, A. S. Bommarius, M. Alcalde and F. Hollmann, *Tetrahedron*, 2019, **75**, 1311–1314.
31 C. Jimenez-Gonzalez, C. S. Ponder, Q. B. Broxterman and J. B. Manley, *Org. Process Res. Dev.*, 2011, **15**, 912–917.
32 K. Budzinski, M. Blewis, P. Dahlin, D. D'Aquila, J. Esparza, J. Gavin, S. V. Ho, C. Hutchens, D. Kahn, S. G. Koenig, R. Kottmeier, J. Millard, M. Snyder, B. Stanard and L. Sun, *Nat. Biotechnol.*, 2019, **49**, 37–42.
33 F. G. Calvo-Flores, *ChemSusChem*, 2009, **2**, 905–919.
34 G. Stone, J. H. Barnes and C. Montgomery, *Psychol. Mark.*, 1995, **12**, 595–612.
35 K. Van Aken, L. Strekowski and L. Patiny, *Beilstein J. Org. Chem.*, 2006, **2**, DOI: 10.1186/1860-5397-2-3.
36 R. A. Sheldon, *ACS Sustainable Chem. Eng.*, 2018, **6**, 32–48.
37 C. Winder, R. Azzi and D. Wagner, *J. Hazard. Mater.*, 2005, **125**, 29–44.
38 D. Prat, A. Wells, J. Hayler, H. Sneddon, C. R. McElroy, S. Abou-Shehada and P. J. Dunn, *Green Chem.*, 2016, **18**, 288–296.
39 Huizhou Changrunfa Coating, CO, CN106699553A, 2017.
40 Dow Chemical Co, US2917538A, 1959.
41 M. Melchiorre, M. E. Cucciolito, R. Esposito, S. Silvestro and F. Ruffo, *Molecules*, 2024, **29**, 918.
42 Mitsubishi Rayon Co, US9303003B2, 2017.
43 J. Herzberger, K. Niederer, H. Pohlit, J. Seiwert, M. Worm, F. R. Wurm and H. Frey, *Chem. Rev.*, 2016, **116**, 2170–2243.
44 E. Takács and L. Wojnárovits, *Radiat. Phys. Chem.*, 1995, **46**, 1007–1010.
45 E. Yoshii, *J. Biomed. Mater. Res.*, 1997, **37**, 517–524.
46 L. S. Andrews and J. J. Clary, *J. Toxicol. Environ. Health*, 1986, **19**, 149–164.
47 T. Hideji and H. Kazuo, *Toxicol. Lett.*, 1982, **11**, 125–129.
48 M. Rafiq, Y. Z. Lv, Y. Zhou, K. B. Ma, W. Wang, C. R. Li and Q. Wang, *Renewable Sustainable Energy Rev.*, 2015, **52**, 308–324.
49 C. Lu, J. A. Napier, T. E. Clemente and E. B. Cahoon, *Curr. Opin. Biotechnol.*, 2011, **22**, 252–259.

50 M. N. Belgacem and A. Gandini, *Monomers, Polymers and Composites from Renewable Resources*, Elsevier, 2008, pp. 39–66.
51 J. Thomas and R. Patil, *Ind. Eng. Chem. Res.*, 2023, **62**, 1725–1735.
52 S. M. Danov, O. A. Kazantsev, A. L. Esipovich, A. S. Belousov, A. E. Rogozhin and E. A. Kanakov, *Catal. Sci. Technol.*, 2017, **7**, 3659–3675.
53 W. Wikström, A. Freites Aguilera, P. Tolvanen, R. Lassfolk, A. Medina, K. Eränen and T. Salmi, *Ind. Eng. Chem. Res.*, 2023, **62**, 9169–9187.
54 E. Milchert, K. Malarczyk and M. Kłos, *Molecules*, 2015, **20**, 21481–21493.
55 R. Mungroo, N. C. Pradhan, V. V. Goud and A. K. Dalai, *J. Am. Oil Chem. Soc.*, 2008, **85**, 887–896.
56 H. Hosney, B. Nadiem, I. Ashour, I. Mustafa and A. El-Shibiny, *J. Appl. Polym. Sci.*, 2018, **135**, DOI: **10.1002/app.46270**.
57 C.-D. Varganici, L. Rosu, D. Rosu, F. Mustata and T. Rusu, *Environ. Chem. Lett.*, 2021, **19**, 307–328.
58 S. Ammar, A. W. M. Iling, K. Ramesh and S. Ramesh, *Renewable Sustainable Energy Rev.*, 2020, **140**, 105523.
59 A. Li and K. Li, *ACS Sustainable Chem. Eng.*, 2014, **2**, 2090–2096.
60 Z. Liu, S. Z. Erhan, D. E. Akin and F. E. Barton, *J. Agric. Food Chem.*, 2006, **54**, 2134–2137.
61 Y. H. Ho, A. Parthiban, M. C. Thian, Z. H. Ban and P. Siwayanan, *Int. J. Polym. Sci.*, 2022, **2022**, 1–12.
62 A. Gandini, *Macromolecules*, 2008, **41**, 9491–9504.
63 P. Zhang and J. Zhang, *Green Chem.*, 2013, **15**, 641.
64 P. Zhang, J. Xin and J. Zhang, *ACS Sustainable Chem. Eng.*, 2014, **2**, 181–187.
65 C. Mendes-Felipe, I. Isusi, O. Gómez-Jiménez-Aberasturi, S. Prieto-Fernandez, L. Ruiz-Rubio, M. Sangermano and J. L. Vilas-Vilela, *Polymers*, 2023, **15**, DOI: **10.3390/polym15143136**.
66 C. Vazquez-Martel, L. Becker, W. V. Liebig, P. Elsner and E. Blasco, *ACS Sustainable Chem. Eng.*, 2021, **9**, 16840–16848.
67 B. Wu, A. Sufi, R. Ghosh Biswas, A. Hisatsune, V. Moxley-Paquette, P. Ning, R. Soong, A. P. Dicks and A. J. Simpson, *ACS Sustainable Chem. Eng.*, 2020, **8**, 1171–1177.
68 B. Perez, N. Blanco, H. Villaverde, O. Echeverria, O. Gomez de Miranda and R. Rodriguez, *Polymers*, 2024, **16**, 2355.
69 S. Miao, W. Zhu, N. J. Castro, M. Nowicki, X. Zhou, H. Cui, J. P. Fisher and L. G. Zhang, *Sci. Rep.*, 2016, **6**, 1–10.
70 A. Barkane, O. Platnieks, M. Jurinovs and S. Gaidukovs, *Polym. Degrad. Stab.*, 2020, **181**, 109347.
71 D. Mondal, Z. Haghpanah, C. J. Huxman, S. Tanter, D. Sun, M. Gorbet and T. L. Willett, *Mater. Sci. Eng., C*, 2021, **130**, 112456.
72 M. Lebedevaite, V. Talacka and J. Ostrauskaite, *J. Appl. Polym. Sci.*, 2021, **138**, 1–13.
73 L. Pezzana, R. Wolff, J. Stampfl, R. Liska and M. Sangermano, *Addit. Manuf.*, 2024, **79**, 103929.
74 A. Barkane, O. Platnieks, M. Jurinovs, S. Kasetaite, J. Ostrauskaite, S. Gaidukovs and Y. Habibi, *Polymers*, 2021, **13**, 1–16.
75 D. Lublin, T. Hao, R. Malyala and D. Kisailus, *RSC Adv.*, 2024, **14**, 10422–10430.
76 M. Bergoglio, Z. Najmi, A. Cochis, M. Miola, E. Vernè and M. Sangermano, *Polymers*, 2023, **15**, 4089.
77 M. Bergoglio, Z. Najmi, A. Cochis, M. Miola, E. Vernè and M. Sangermano, *Mater. Today Chem.*, 2025, **44**, 102559.
78 M. Bodor, A. Lasagabáster-Latorre, G. Arias-Ferreiro, M. S. Dopico-García and M. J. Abad, *Polymers*, 2024, **16**, DOI: **10.3390/polym16070977**.
79 M. Porcarello, C. Mendes-Felipe, S. Lanceros-Mendez and M. Sangermano, *Sustainable Mater. Technol.*, 2024, **40**, e00927.
80 M. Jurinovs, A. Barkane, O. Platnieks, S. Beluns, L. Grase, R. Dieden, M. Staropoli, D. F. Schmidt and S. Gaidukovs, *ACS Appl. Polym. Mater.*, 2023, **5**, 3104–3118.
81 J. Guit, M. B. L. Tavares, J. Hul, C. Ye, K. Loos, J. Jager, R. Folkersma and V. S. D. Voet, *ACS Appl. Polym. Mater.*, 2020, **2**, 949–957.
82 G. Zhu, J. Zhang, J. Huang, X. Yu, J. Cheng, Q. Shang, Y. Hu, C. Liu, L. Hu and Y. Zhou, *Green Chem.*, 2021, **23**, 5911–5923.
83 X. Wang, X. Cai, J. Hu, J. Li, R. Zhou and S. Lin, *Addit. Manuf.*, 2024, **95**, 104543.
84 C. Bodhak, T. Patel, P. Sahu and R. K. Gupta, *ACS Appl. Polym. Mater.*, 2024, **6**, 12886–12896.
85 S. D. Silbert, P. Simpson, R. Setien, M. Holthaus, J. La Scala, C. A. Ulven and D. C. Webster, *ACS Appl. Polym. Mater.*, 2020, **2**, 2910–2918.
86 S. Ghasemi, M. P. Sibi, C. A. Ulven, D. C. Webster and G. Pourhashem, *Molecules*, 2020, **25**, 2797.
87 S. Briede, A. Barkane, M. Jurinovs, V. K. Thakur and S. Gaidukovs, *Curr. Opin. Green Sustainable Chem.*, 2022, **35**, 100626.
88 R. Morales-Cerrada, S. Molina-Gutierrez, P. Lacroix-Desmazes and S. Caillol, *Biomacromolecules*, 2021, **22**, 3625–3648.
89 S. Caillol, B. Boutevin and R. Auvergne, *Polymer*, 2021, **223**, 123663.
90 L. Liu, H. Yun, X. Chen, Y. Duan, Z. Ji, S. Lv and Y. Zhang, *ACS Sustainable Chem. Eng.*, 2024, **12**, 2739–2750.
91 A. L. Holmberg, K. H. Reno, N. A. Nguyen, R. P. Wool and T. H. Epps, *ACS Macro Lett.*, 2016, **5**, 574–578.
92 J. Xu, X. Liu and S. Fu, *J. Mater. Sci.*, 2022, **57**, 9493–9507.
93 C. Aouf, H. Nouailhas, M. Fache, S. Caillol, B. Boutevin and H. Fulcrand, *Eur. Polym. J.*, 2013, **49**, 1185–1195.
94 M. Fache, B. Boutevin and S. Caillol, *ACS Sustainable Chem. Eng.*, 2016, **4**, 35–46.
95 M. M. Kumar, V. S. Prabhudesai and R. Vinu, *Mol. Catal.*, 2023, **549**, 113474.
96 A. Llevot, E. Grau, S. Carlotti, S. Grelier and H. Cramail, *Macromol. Rapid Commun.*, 2016, **37**, 9–28.
97 L. Martínková, M. Grulich, M. Pátek, B. Křístková and M. Winkler, *Biomolecules*, 2023, **13**, 717.
98 K. C. H. Chin, J. Cui, R. M. O'Dea, T. H. Epps and A. J. Boydston, *ACS Sustainable Chem. Eng.*, 2023, **11**, 1867–1874.

99 Y. Zhou, G. Wei, Z. Wu, R. Liu and J. T. Miao, *Eur. Polym. J.*, 2024, **217**, 113317.
100 R. Sesia, M. Porcarello, M. Hakkarainen, S. Ferraris, S. Spriano and M. Sangermano, *Macromol. Chem. Phys.*, 2024, **1–9**, 2400181.
101 H. Fouilloux and C. M. Thomas, *Macromol. Rapid Commun.*, 2021, **42**, DOI: **10.1002/marc.202000530**.
102 M. Fache, E. Darroman, V. Besse, R. Auvergne, S. Caillol and B. Boutevin, *Green Chem.*, 2014, **16**, 1987–1998.
103 Y. Xu, K. Odelius and M. Hakkarainen, *ACS Sustainable Chem. Eng.*, 2020, **8**, 17272–17279.
104 E. D. Hernandez, A. W. Bassett, J. M. Sadler, J. J. La Scala and J. F. Stanzione, *ACS Sustainable Chem. Eng.*, 2016, **4**, 4328–4339.
105 R. Ding, Y. Du, R. B. Goncalves, L. F. Francis and T. M. Reineke, *Polym. Chem.*, 2019, **10**, 1067–1077.
106 A. W. Bassett, A. E. Honnig, C. M. Breyta, I. C. Dunn, J. J. La Scala and J. F. Stanzione, *ACS Sustainable Chem. Eng.*, 2020, **8**, 5626–5635.
107 A. Almena and M. Martín, *Ind. Eng. Chem. Res.*, 2016, **55**, 3226–3238.
108 G. M. Lari, G. Pastore, C. Mondelli and J. Pérez-Ramírez, *Green Chem.*, 2018, **20**, 148–159.
109 J. T. Miao, S. Peng, M. Ge, Y. Li, J. Zhong, Z. Weng, L. Wu and L. Zheng, *ACS Sustainable Chem. Eng.*, 2020, **8**, 9415–9424.
110 Ľ. Hodásová, I. Isarn, F. Bravo, C. Alemán, N. Borràs, G. Fargas and E. Armelin, *RSC Appl. Polym.*, 2024, **2**, 284–295.
111 B. A. Basilia, A. J. C. Boniel, G. S. B. Borilla III and P. A. N. de Yro, *Adv. Sci. Technol.*, 2024, **155**, 59–64.
112 H. Bakhshi, G. Kuang, F. Wieland and W. Meyer, *Polymers*, 2022, **14**, 2974.
113 A. Pongwisuthiruchte, C. Aumnate and P. Potiyaraj, *ACS Omega*, 2024, **9**, 2884–2895.
114 M. Sáenz-Pérez, E. Lizundia, J. M. Laza, J. García-Barrasa, J. L. Vilas and L. M. León, *RSC Adv.*, 2016, **6**, 69094–69102.
115 D. Rother and U. Schlüter, *Ann. Work Exposures Health*, 2021, **65**, 893–907.
116 D. Bello, C. A. Herrick, T. J. Smith, S. R. Woskie, R. P. Streicher, M. R. Cullen, Y. Liu and C. A. Redlich, *Environ. Health Perspect.*, 2007, **115**, 328–335.
117 A. R. Mahendran, N. Aust, G. Wuzella, U. Müller and A. Kandelbauer, *J. Polym. Environ.*, 2012, **20**, 926–931.
118 E. Delebecq, J.-P. Pascault, B. Boutevin and F. Ganachaud, *Chem. Rev.*, 2013, **113**, 80–118.
119 L. Meng, X. Wang, M. Ocepek and M. D. Soucek, *Polymer*, 2017, **109**, 146–159.
120 V. Schimpf, A. Asmacher, A. Fuchs, B. Bruchmann and R. Mülhaupt, *Macromolecules*, 2019, **52**, 3288–3297.
121 V. Gosu, S. Arora, V. Subbaramaiah, V. C. Srivastava and R. B. Gupta, *ACS Sustainable Resour. Manage.*, 2024, **1**, 816–841.
122 J. Becker, A. Lange, J. Fabarius and C. Wittmann, *Curr. Opin. Biotechnol.*, 2015, **36**, 168–175.
123 S. Kumar, S. Krishnan, S. K. Samal, S. Mohanty and S. K. Nayak, *Polym. Int.*, 2017, **66**, 1349–1363.
124 T. Werpy and G. Petersen, Us Nrel, 2004, Medium: ED; Size: 76 pages.
125 T. Klement and J. Büchs, *Bioresour. Technol.*, 2013, **135**, 422–431.
126 T. O. Machado, C. Sayer and P. H. H. Araujo, *Eur. Polym. J.*, 2017, **86**, 200–215.
127 N. B. Cramer and C. N. Bowman, *J. Polym. Sci., Part A: Polym. Chem.*, 2001, **39**, 3311–3319.
128 N. B. Cramer, S. K. Reddy, A. K. O'Brien and C. N. Bowman, *Macromolecules*, 2003, **36**, 7964–7969.
129 N. B. Cramer, T. Davies, A. K. O'Brien and C. N. Bowman, *Macromolecules*, 2003, **36**, 4631–4636.
130 Q. Li, H. Zhou and C. E. Hoyle, *Polymer*, 2009, **50**, 2237–2245.
131 H. Liu and H. Chung, *ACS Sustainable Chem. Eng.*, 2017, **5**, 9160–9168.
132 M. Jawerth, M. Johansson, S. Lundmark, C. Gioia and M. Lawoko, *ACS Sustainable Chem. Eng.*, 2017, **5**, 10918–10925.
133 M. R. Thomsett, T. E. Storr, O. R. Monaghan, R. A. Stockman and S. M. Howdle, *Green Mater.*, 2016, **4**, 115–134.
134 F. Della Monica and A. W. Kleij, *Polym. Chem.*, 2020, **11**, 5109–5127.
135 M. Winnacker and B. Rieger, *ChemSusChem*, 2015, **8**, 2455–2471.
136 A. J. D. Silvestre and A. Gandini, *Monomers, Polymers and Composites from Renewable Resources*, Elsevier, 2008, pp. 17–38.
137 W. Schwab, C. Fuchs and F. Huang, *Eur. J. Lipid Sci. Technol.*, 2013, **115**, 3–8.
138 A. C. Weems, K. R. Delle Chiaie, J. C. Worch, C. J. Stubbs and A. P. Dove, *Polym. Chem.*, 2019, **10**, 5959–5966.
139 J. Hartung, T. Gottwald and K. Špehar, *Synthesis*, 2002, 1469–1498.
140 A. C. Weems, K. R. Delle Chiaie, R. Yee and A. P. Dove, *Biomacromolecules*, 2020, **21**, 163–170.
141 E. Constant, O. King and A. C. Weems, *Biomacromolecules*, 2022, **23**, 2342–2352.
142 D. Merckle, E. Constant and A. C. Weems, *ACS Sustainable Chem. Eng.*, 2021, **9**, 12213–12222.
143 V. Chiaradia, E. Pensa, T. O. Machado and A. P. Dove, *ACS Sustainable Chem. Eng.*, 2024, **12**, 6904–6912.
144 Y. Tian, Q. Wang, J. Cheng and J. Zhang, *Green Chem.*, 2020, **22**, 921–932.
145 M. K. Porwal, M. M. Hausladen, C. J. Ellison and T. M. Reineke, *Green Chem.*, 2023, **25**, 1488–1502.
146 L. Pezzana, S. Fadlallah, G. Giri, C. Archimbaud, I. Roppolo, F. Allais and M. Sangermano, *ChemSusChem*, 2024, **17**, DOI: **10.1002/cssc.202301828**.
147 V. Sereikaite, A. Navaruckiene, J. Jaras, E. Skliutas, D. Ladika, D. Gray, M. Malinauskas, V. Talacka and J. Ostrauskaite, *Polymers*, 2022, **14**, DOI: **10.3390/polym14245361**.
148 S. Pal and S. K. Asha, *Eur. Polym. J.*, 2024, **205**, 112761.

149 S.-S. Kim, H. Ha and C. J. Ellison, *ACS Sustainable Chem. Eng.*, 2018, **6**, 8364–8373.
150 X. Wang, H. Liang, J. Jiang, Q. Wang, Y. Luo, P. Feng and C. Zhang, *Green Chem.*, 2020, **22**, 5722–5729.
151 Y. Nakada, S. Iioka, K. Sugane and M. Shibata, *Eur. Polym. J.*, 2024, **212**, 113072.
152 Z. Weng, X. Huang, S. Peng, L. Zheng and L. Wu, *Nat. Commun.*, 2023, **14**, 4303.
153 A. Al Rashid, W. Ahmed, M. Y. Khalid and M. Koç, *Addit. Manuf.*, 2021, **47**, 102279.
154 G. Taormina, C. Sciancalepore, M. Messori and F. Bondioli, *J. Appl. Biomater. Funct. Mater.*, 2018, **16**, 151–160.
155 M. Maturi, C. Pulignani, E. Locatelli, V. Vetri Buratti, S. Tortorella, L. Sambri and M. Comes Franchini, *Green Chem.*, 2020, **22**, 6212–6224.
156 V. Vetri Buratti, A. Sanz de Leon, M. Maturi, L. Sambri, S. I. Molina and M. Comes Franchini, *Macromolecules*, 2022, **55**, 3087–3095.
157 L. Papadopoulos, N. M. Malitowski, D. Bikiaris and T. Robert, *Eur. Polym. J.*, 2023, **186**, 111872.
158 L. Papadopoulos, L. Pezzana, N. M. Malitowski, M. Sangermano, D. N. Bikiaris and T. Robert, *ACS Omega*, 2023, **8**, 31009–31020.
159 L. Papadopoulos, L. Pezzana, N. Malitowski, M. Sangermano, D. N. Bikiaris and T. Robert, *Discover Appl. Sci.*, 2024, **6**, 290.
160 N. M. Schulz, L. Papadopoulos, L. Hagenlocher, A. Gohla, D. N. Bikiaris and T. Robert, *React. Funct. Polym.*, 2025, **208**, 106161.
161 C. M. Barker, G. Nayyar, T. P. Chase and T. E. Long, *MRS Commun.*, 2023, **13**, 841–847.
162 J. Jansen, G. Mihov, J. Feijen and D. W. Grijpma, *Macromol. Biosci.*, 2012, **12**, 692–702.
163 R. Magri, C. Gaglieri, R. T. Alarcon, G. I. dos Santos and G. Bannach, *J. Polym. Res.*, 2023, **30**, 236.
164 H. Wei, T. Y. Lee, W. Miao, R. Fortenberry, D. H. Magers, S. Hait, A. C. Guymon, S. E. Jönsson and C. E. Hoyle, *Macromolecules*, 2007, **40**, 6172–6180.
165 M. Maturi, S. Maturi, A. Sanz de León, L. Migliorini, M. de la Mata, T. Benelli, L. Giorgini, P. Milani, M. Comes Franchini and S. I. Molina, *ACS Appl. Polym. Mater.*, 2025, **7**, 4371–4382.
166 T. K. Dash and V. B. Konkimalla, *J. Controlled Release*, 2012, **158**, 15–33.
167 E. Archer, M. Torretti and S. Madbouly, *Phys. Sci. Rev.*, 2023, **8**, 4391–4414.
168 E. Malikmammadov, T. E. Tanir, A. Kiziltay, V. Hasirci and N. Hasirci, *J. Biomater. Sci., Polym. Ed.*, 2018, **29**, 863–893.
169 L. M. Bernhard and H. Gröger, *ChemSusChem*, 2024, **17**, DOI: **10.1002/cssc.202400073**.
170 M. Das, B. Mandal and V. Katiyar, in *Advances in Sustainable Polymers*, 2020, pp. 21–33.
171 L. Elomaa, S. Teixeira, R. Hakala, H. Korhonen, D. W. Grijpma and J. V. Seppälä, *Acta Biomater.*, 2011, **7**, 3850–3856.
172 L. Elomaa, Y. Kang, J. V. Seppälä and Y. Yang, *J. Polym. Sci., Part A: Polym. Chem.*, 2014, **52**, 3307–3315.
173 M. Zarek, M. Layani, I. Cooperstein, E. Sachyani, D. Cohn and S. Magdassi, *Adv. Mater.*, 2016, **28**, 4449–4454.
174 A. Quaak, Q. Thijssen and S. Van Vlierberghe, *Polym. Chem.*, 2023, **14**, 3392–3403.
175 Q. Thijssen, A. Quaak, J. Toombs, E. De Vlieghere, L. Parmentier, H. Taylor and S. Van Vlierberghe, *Adv. Mater.*, 2023, **35**, 1–16.
176 C. Spanu, E. Locatelli, L. Sambri, M. Comes Franchini and M. Maturi, *ACS Appl. Polym. Mater.*, 2024, **6**, 2417–2424.
177 T. Kuhnt, R. Marroquín García, S. Camarero-Espinosa, A. Dias, A. T. Ten Cate, C. A. Van Blitterswijk, L. Moroni and M. B. Baker, *Biomater. Sci.*, 2019, **7**, 4984–4989.
178 D. J. Darensbourg, A. Horn Jr and A. I. Moncada, *Green Chem.*, 2010, **12**, 1376.
179 J. Huang, J. De Winter, A. P. Dove and O. Coulembier, *Green Chem.*, 2019, **21**, 472–477.
180 S. Figalla, V. Jašek, J. Fučík, P. Menčík and R. Přikryl, *Biomacromolecules*, 2024, **25**, 6645–6655.
181 K. C. Poon, M. Segal, A. J. Bahnick, Y. M. Chan, C. Gao, M. L. Becker and C. K. Williams, *Angew. Chem., Int. Ed.*, 2024, **63**, DOI: **10.1002/anie.202407794**.
182 A. C. Q. Silva, A. J. D. Silvestre, C. Vilela and C. S. R. Freire, *Molecules*, 2021, **27**, 94.
183 K. Müller, C. Zollfrank and M. Schmid, *Macromol. Mater. Eng.*, 2019, **304**, DOI: **10.1002/mame.201800760**.
184 K. Van de Velde and P. Kiekens, *Polym. Test.*, 2002, **21**, 433–442.
185 V. G. Muir and J. A. Burdick, *Chem. Rev.*, 2021, **121**, 10908–10949.
186 M. K. Thakur, A. K. Rana, Y. Liping, A. S. Singha and V. K. Thakur, *Surface Modification of Biopolymers*, Wiley, 2015, pp. 1–19.
187 V. C. F. Li, X. Kuang, A. Mulyadi, C. M. Hamel, Y. Deng and H. J. Qi, *Cellulose*, 2019, **26**, 3973–3985.
188 S. U. Bae and B. J. Kim, *Appl. Sci.*, 2021, **11**, 6835.
189 M. Maturi, C. Spanu, N. Fernández-Delgado, S. I. Molina, M. Comes Franchini, E. Locatelli and A. Sanz de León, *Addit. Manuf.*, 2023, **61**, 103342.
190 N. B. Palaganas, J. D. Mangadlao, A. C. C. de Leon, J. O. Palaganas, K. D. Pangilinan, Y. J. Lee and R. C. Advincula, *ACS Appl. Mater. Interfaces*, 2017, **9**, 34314–34324.
191 A. R. Parikh, K. P. Cortés-Guzmán, N. Bian, R. M. Johnson, R. A. Smaldone, H. Lu and W. E. Voit, *J. Polym. Sci.*, 2024, **62**, 2692–2703.
192 L. Cellante, R. Costa, I. Monaco, G. Cenacchi and E. Locatelli, *New J. Chem.*, 2018, **42**, 5237–5242.
193 S. Tortorella, M. Maturi, F. Dapporto, C. Spanu, L. Sambri, M. Comes Franchini, M. Chiariello and E. Locatelli, *Cellulose*, 2020, **27**, 8503–8511.
194 M. Maturi, C. Spanu, A. Baschieri, M. Comes Franchini, E. Locatelli and L. Sambri, *Biomolecules*, 2022, **12**, DOI: **10.3390/biom12091165**.

195 D. Cafiso, A. A. Septevani, C. Noè, T. Schiller, C. F. Pirri, I. Roppolo and A. Chiappone, *Sustainable Mater. Technol.*, 2022, **32**, e00444.
196 M. Zanon, R. Cue-López, E. Martínez-Campos, P. Bosch, D.-L. Versace, H. Hayek, N. Garino, C. F. Pirri, M. Sangermano and A. Chiappone, *Addit. Manuf.*, 2023, **69**, 103553.
197 Z. Feng, J. Li, D. Zhou, H. Song, J. Lv and W. Bai, *Int. J. Bioprint.*, 2022, **9**, 104–117.
198 J. H. Galarraga, A. P. Dhand, B. P. Enzmann and J. A. Burdick, *Biomacromolecules*, 2023, **24**, 413–425.
199 M. Zanon, L. Montalvillo-Jiménez, R. Cue-López, E. Martínez-Campos, M. Sangermano, A. Chiappone and P. Bosch, *Polym. Chem.*, 2023, **14**, 4856–4868.
200 L. Wang, Q. Wang, A. Slita, O. Backman, Z. Gounani, E. Rosqvist, J. Peltonen, S. Willför, C. Xu, J. M. Rosenholm and X. Wang, *Green Chem.*, 2022, **24**, 2129–2145.
201 S. H. Kim, Y. K. Yeon, J. M. Lee, J. R. Chao, Y. J. Lee, Y. B. Seo, M. T. Sultan, O. J. Lee, J. S. Lee, S. Yoon, I.-S. Hong, G. Khang, S. J. Lee, J. J. Yoo and C. H. Park, *Nat. Commun.*, 2018, **9**, 1620.
202 H. Hong, Y. B. Seo, D. Y. Kim, J. S. Lee, Y. J. Lee, H. Lee, O. Ajiteru, M. T. Sultan, O. J. Lee, S. H. Kim and C. H. Park, *Biomaterials*, 2020, **232**, 119679.
203 P. T. Smith, B. Narupai, J. H. Tsui, S. C. Millik, R. T. Shafranek, D. H. Kim and A. Nelson, *Biomacromolecules*, 2020, **21**, 484–492.
204 V. T. Duong and C. C. Lin, *Macromol. Biosci.*, 2023, **23**, 1–12.
205 A. García, M. González Alriols, G. Spigno and J. Labidi, *Biochem. Eng. J.*, 2012, **67**, 173–185.
206 T. Dizhbite, G. Telysheva, V. Jurkjane and U. Viesturs, *Bioresour. Technol.*, 2004, **95**, 309–317.
207 J. T. Sutton, K. Rajan, D. P. Harper and S. C. Chmely, *ACS Appl. Mater. Interfaces*, 2018, **10**, 36456–36463.
208 J. Yang, X. An, L. Yin, B. Lu, X. Lyu, Z. Cheng, G. Pan, H. Liu and Y. Ni, *Addit. Manuf.*, 2024, **95**, 104519.
209 Z. Chen, M. Yang, M. Ji, X. Kuang, H. J. Qi and T. Wang, *Mater. Des.*, 2021, **197**, 109189.
210 A. S. Kuenstler, J. J. Hernandez, M. Trujillo-Lemon, A. Osterbaan and C. N. Bowman, *ACS Appl. Mater. Interfaces*, 2023, **15**, 11111–11121.
211 J. Cui, F. Liu, Z. Lu, S. Feng, C. Liang, Y. Sun, J. Cui and B. Zhang, *Adv. Mater.*, 2023, **35**, DOI: **10.1002/adma.202211417**.
212 E. Manarin, F. Da Via, B. Rigatelli, S. Turri and G. Griffini, *ACS Appl. Polym. Mater.*, 2023, **5**, 828–838.
213 M. Capelot, D. Montarnal, F. Tournilhac and L. Leibler, *J. Am. Chem. Soc.*, 2012, **134**, 7664–7667.
214 H. Liang, W. Tian, H. Xu, Y. Ge, Y. Yang, E. He, Z. Yang, Y. Wang, S. Zhang, G. Wang, Q. Chen, Y. Wei and Y. Ji, *Polymers*, 2024, **16**, 3216.
215 F. Bazi, H. El Badaoui, S. Tamani, S. Sokori, L. Oubella, M. Hamza, S. Boulaajaj and S. Sebti, *J. Mol. Catal. A: Chem.*, 2006, **256**, 43–47.
216 U. Shaukat, B. Sölle, E. Rossegger, S. Rana and S. Schlögl, *Polymers*, 2022, **14**, 5377.
217 S. Grauzeliene, A. S. Schuller, C. Delaite and J. Ostrauskaite, *Eur. Polym. J.*, 2023, **198**, 112424.
218 S. Grauzeliene, A. S. Schuller, C. Delaite and J. Ostrauskaite, *ACS Appl. Polym. Mater.*, 2023, **5**, 6958–6965.
219 I. Cazin, E. Rossegger, I. Roppolo, M. Sangermano, P. Granitzer, K. Rumpf and S. Schlögl, *RSC Adv.*, 2023, **13**, 17536–17544.
220 C. Ye, K. Janssen, G. H. M. Schnelting, V. S. D. Voet, R. Folkersma and K. Loos, *Polymer*, 2025, **319**, 127997.
221 K. Janssen, G. H. M. Schnelting, M. Waterink, J. Guit, J. Hul, C. Ye, K. Loos and V. S. D. Voet, *Macromol. Mater. Eng.*, 2024, **309**, 1–9.
222 W. Huang, Z. Zu, Y. Huang, H. Xiang and X. Liu, *Addit. Manuf.*, 2024, **91**, 104352.
223 K. P. Cortés-Guzmán, A. R. Parikh, M. L. Sparacin, R. M. Johnson, L. Adegoke, M. Ecker, W. E. Voit and R. A. Smaldone, *Polym. Chem.*, 2023, **14**, 2697–2707.
224 L. Yue, Y. L. Su, M. Li, L. Yu, X. Sun, J. Cho, B. Brettmann, W. R. Gutekunst, R. Ramprasad and H. J. Qi, *Adv. Mater.*, 2024, **36**, 1–8.
225 J. Hu, R. Mo, X. Sheng and X. Zhang, *Polym. Chem.*, 2020, **11**, 2585–2594.
226 A. Chao, I. Negulescu and D. Zhang, *Macromolecules*, 2016, **49**, 6277–6284.
227 X. Liu, E. Zhang, J. Liu, J. Qin, M. Wu, C. Yang and L. Liang, *Chem. Eng. J.*, 2023, **454**, 139992.
228 K. P. Cortés-Guzmán, A. R. Parikh, M. L. Sparacin, A. K. Remy, L. Adegoke, C. Chitrakar, M. Ecker, W. E. Voit and R. A. Smaldone, *ACS Sustainable Chem. Eng.*, 2022, **10**, 13091–13099.
229 J. Stouten, G. H. M. Schnelting, J. Hul, N. Sijstermans, K. Janssen, T. Darikwa, C. Ye, K. Loos, V. S. D. Voet and K. V. Bernaerts, *ACS Appl. Mater. Interfaces*, 2023, **15**, 27110–27119.
230 H. Ying, Y. Zhang and J. Cheng, *Nat. Commun.*, 2014, **5**, 3218.
231 Z. Wang, S. Gangarapu, J. Escorihuela, G. Fei, H. Zuilhof and H. Xia, *J. Mater. Chem. A*, 2019, **7**, 15933–15943.
232 Z. Zhou, S. Chen, X. Xu, Y. Chen, L. Xu, Y. Zeng and F. Zhang, *Prog. Org. Coat.*, 2021, **154**, 106213.
233 G. Zhu, M. Liu, Z. Kou, G. Zhang, C. Bo, L. Hu, Y. Hu and Y. Zhou, *Chem. Eng. J.*, 2023, **475**, 146080.
234 G. Zhu, J. Zhang, J. Huang, Y. Qiu, M. Liu, J. Yu, C. Liu, Q. Shang, Y. Hu, L. Hu and Y. Zhou, *Chem. Eng. J.*, 2023, **452**, 139401.
235 S. Nevejans, N. Ballard, J. I. Miranda, B. Reck and J. M. Asua, *Phys. Chem. Chem. Phys.*, 2016, **18**, 27577–27583.
236 J. M. Matxain, J. M. Asua and F. Ruipérez, *Phys. Chem. Chem. Phys.*, 2016, **18**, 1758–1770.
237 J. Canadell, H. Goossens and B. Klumperman, *Macromolecules*, 2011, **44**, 2536–2541.
238 G. Zhu, N. von Coelln, Y. Hou, C. Vazquez-Martel, C. A. Spiegel, P. Tegeder and E. Blasco, *Adv. Mater.*, 2024, **36**, 1–13.

239 S. Han, V. A. Bobrin, M. Michelas, C. J. Hawker and C. Boyer, *ACS Macro Lett.*, 2024, 1495–1502.
240 T. O. Machado, C. J. Stubbs, V. Chiaradia, M. A. Alraddadi, A. Brandolese, J. C. Worch and A. P. Dove, *Nature*, 2024, **629**, 1069–1074.
241 W. Wang, Y. Zhang, Y. Gao, J. Nie and F. Sun, *Eur. Polym. J.*, 2024, **208**, 112874.
242 Y. Qian, F. Dong, L. Guo, S. Lu, X. Xu and H. Liu, *Biomacromolecules*, 2023, **24**, 1184–1193.
243 X. Lopez de Pariza, O. Varela, S. O. Catt, T. E. Long, E. Blasco and H. Sardon, *Nat. Commun.*, 2023, **14**, 1–11.
244 K. Nakashima, T. Takeshita and K. Morimoto, *Environ. Health Prev. Med.*, 2002, **7**, 1–6.
245 X. Yu, C. Li, C. Gao, X. Zhang, G. Zhang and D. Zhang, *SmartMat*, 2021, **2**, 347–366.
246 L. Chen, J. Xu, M. Zhu, Z. Zeng, Y. Song, Y. Zhang, X. Zhang, Y. Deng, R. Xiong and C. Huang, *Mater. Horiz.*, 2023, **10**, 4000–4032.
247 M. Liu, G. Zhang, Y. Hu, C. Bo, Y. Dai, L. Hu, G. Zhu and Y. Zhou, *Green Chem.*, 2023, 10441–10455.
248 Y. Bao, *Macromol. Rapid Commun.*, 2022, **43**, DOI: **10.1002/marc.202200202**.
249 H. Chen, D. Zhu, T. Kavalli, P. Xiao, M. Schmitt and J. Lalevée, *Polym. Chem.*, 2023, **14**, 3543–3568.
250 J. Zhao, J. Lalevée, H. Lu, R. MacQueen, S. H. Kable, T. W. Schmidt, M. H. Stenzel and P. Xiao, *Polym. Chem.*, 2015, **6**, 5053–5061.
251 T. Borjigin, J. Feng, M. Schmitt, D. Zhu, F. Morlet-Savary, P. Xiao and J. Lalevée, *Green Chem.*, 2023, **26**, 277–286.
252 C. Vazquez-Martel, P. Mainik and E. Blasco, *Org. Mater.*, 2022, **4**, 281–291.
253 A. Enayati-Gerdroodbar, A. Khayati, M. Ahmadi, B. Pourabbas, M. Ali Aboudzadeh and M. Salami-Kalajahi, *Eur. Polym. J.*, 2024, **221**, 113552.
254 T. M. Fonovich, *Drug Chem. Toxicol.*, 2013, **36**, 343–352.
255 L. E. Sendelbach, *Toxicology*, 1989, **57**, 227–240.
256 X. He, J. Cheng, Z. Sun, H. Ye, Q. Liu, B. Zhang and Q. Ge, *Soft Matter*, 2023, **19**, 3700–3710.
257 P. K. Sharma, D. Choudhury, T. Karanwad, P. Mohapatra, U. S. Murty and S. Banerjee, *Biomater. Adv.*, 2023, **153**, 213527.
258 J. W. Seo, G. M. Kim, Y. Choi, J. M. Cha and H. Bae, *Int. J. Mol. Sci.*, 2022, **23**, 5428.
259 W. S. de Almeida, J. D. Marinho Filho, A. J. Araújo, A. B. Barros and D. A. da Silva, *Mater. Today Commun.*, 2022, **33**, 104611.